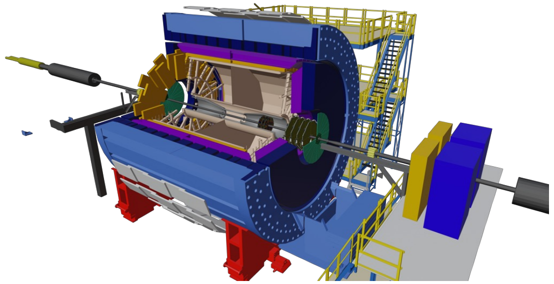

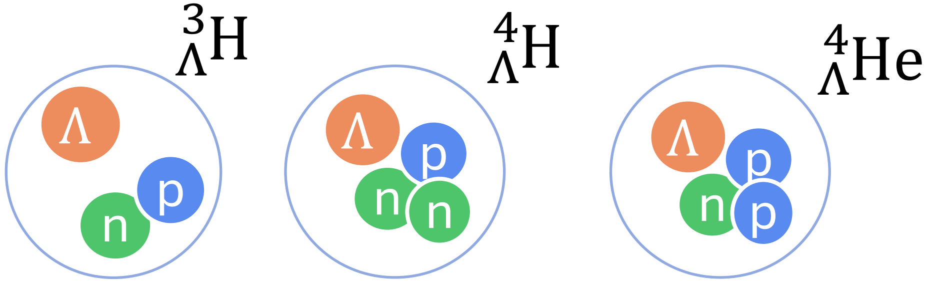

Recent Measurements of Hypernuclei Properties and Production from STAR BES II

Yuanjing Ji (纪媛婧)
GSI

Jan 3rd, 2024, UCAS

What are Hypernuclei?

Hypernucleus: A bound system of nucleons with ≥ 1 hyperon.

Hyperon: A baryon with ≥ 1 strange quark (e.g. Λ, Ξ, Ω etc).

Additional dimension in chart of nuclides

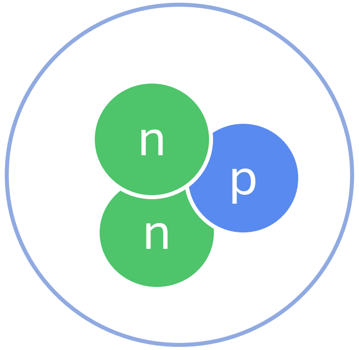

$^3H(t)$

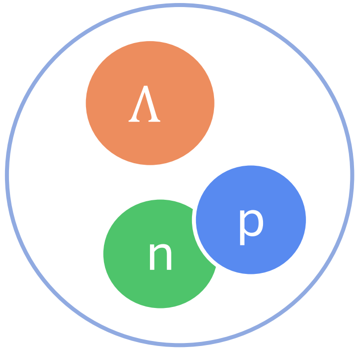

$^3_\Lambda H$

lightest hypernucleus

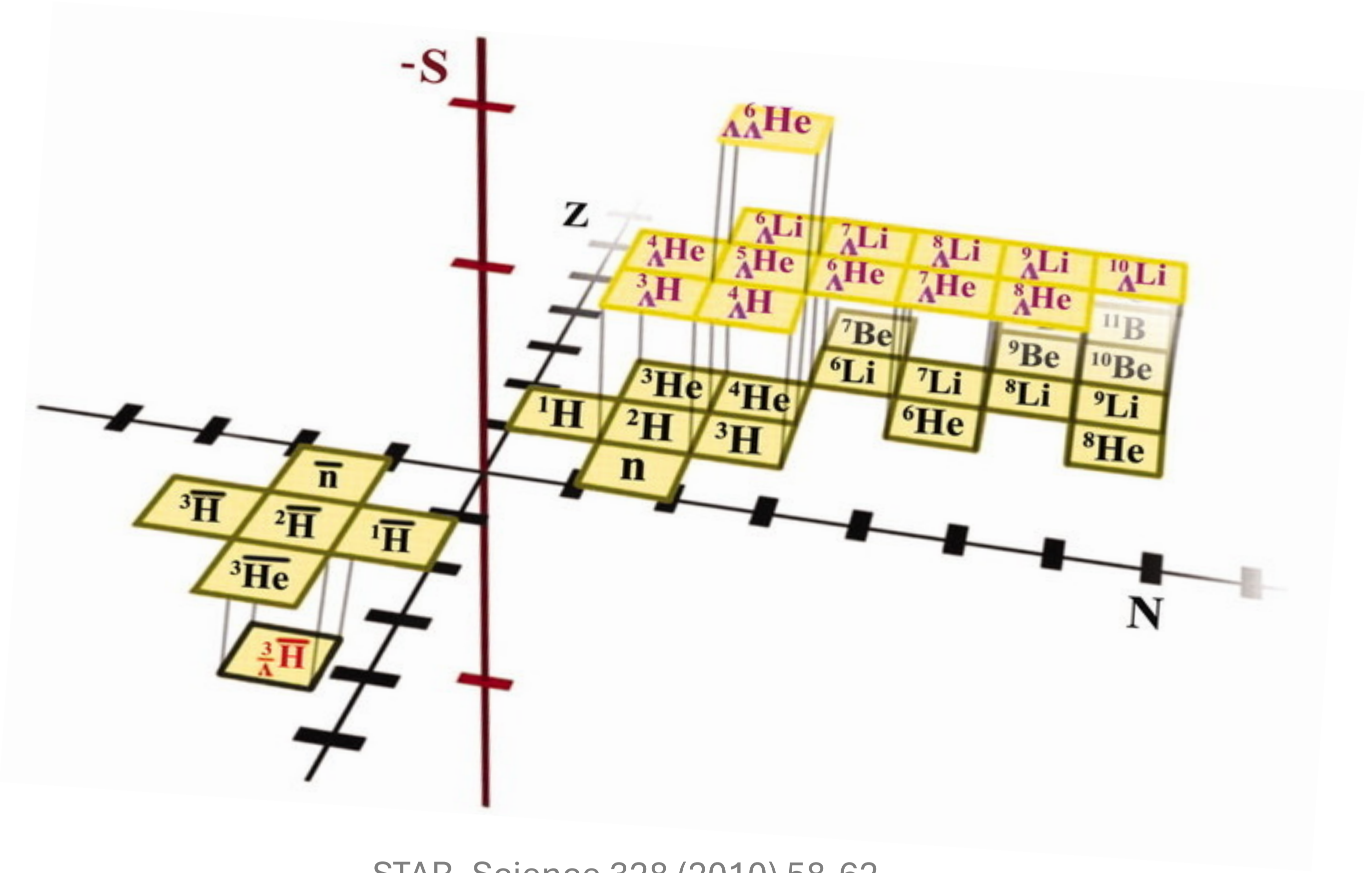

STAR, Science 328 (2010) 58-62

Hypernuclei and Hyperon-Nucleon (Y-N) Interaction

Hypernuclei -> probe to Y-N (Y-N-N) interaction

- Inner structure governed by interactions between nucleons (and hyperons)

Hypertriton ($^{3}_{\Lambda}\mathrm{H}$)

A=3:

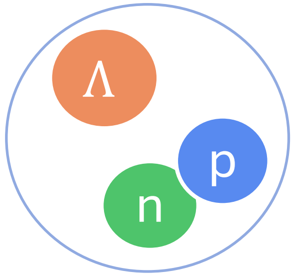

Hyperhydrogen-4 ($^{4}_{\Lambda}\mathrm{H}$)

Hyperhelium-4 ($^{4}_{\Lambda}\mathrm{He}$)

A=4:

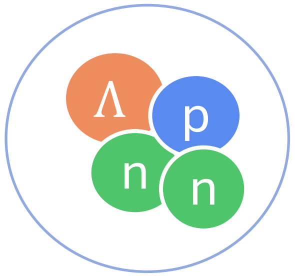

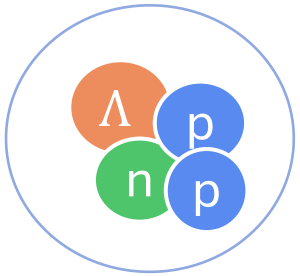

Observables in heavy ion collisions

Intrinsic Properties

- How tight they bind together
- Internal spin structure
- How they decay: lifetime, branching ratio

Production mechanism

- How they form in heavy ion collisions
  - Collectivity, production yields

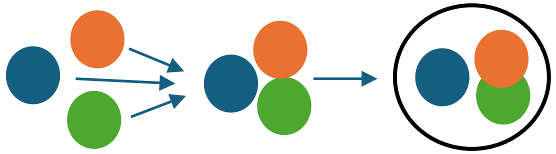

Y-N Interaction, EoS and Astrophysics

- **Equation of State (EoS) in dense nuclear matter**
  - The strangeness degree of freedom in EoS at high baryon density region
- High baryon density nuclear matter
  - e.g. low energy HIC, neutron stars

Compact star

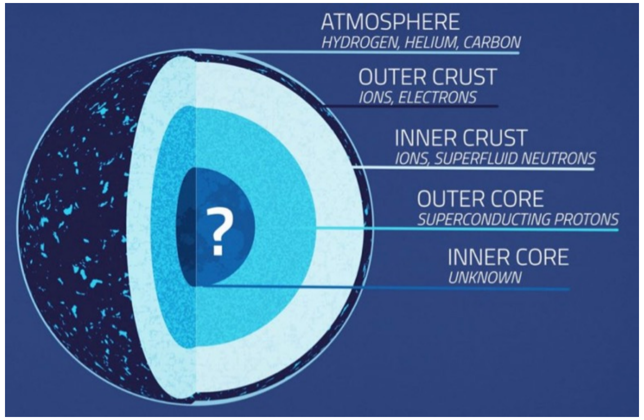

"Hyperon puzzle"

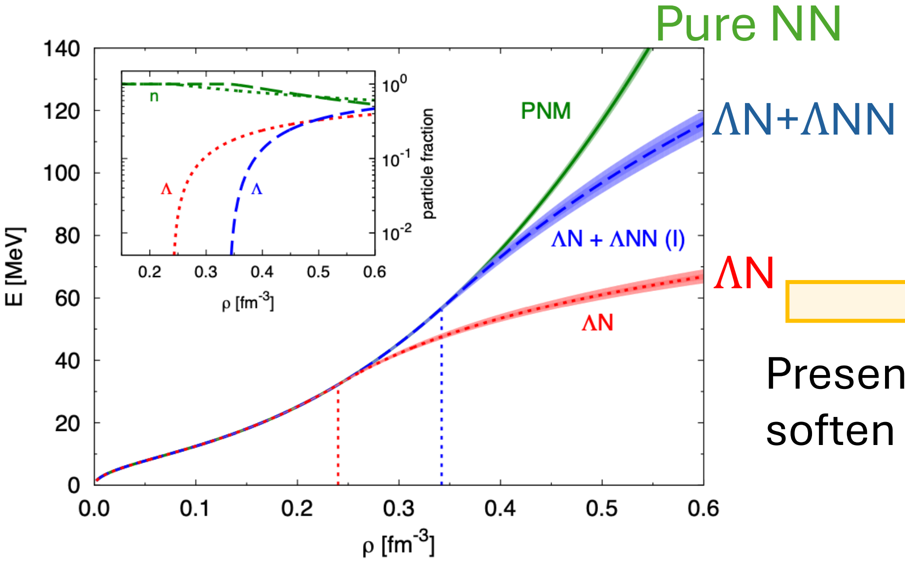

Presence of hyperon soften EoS

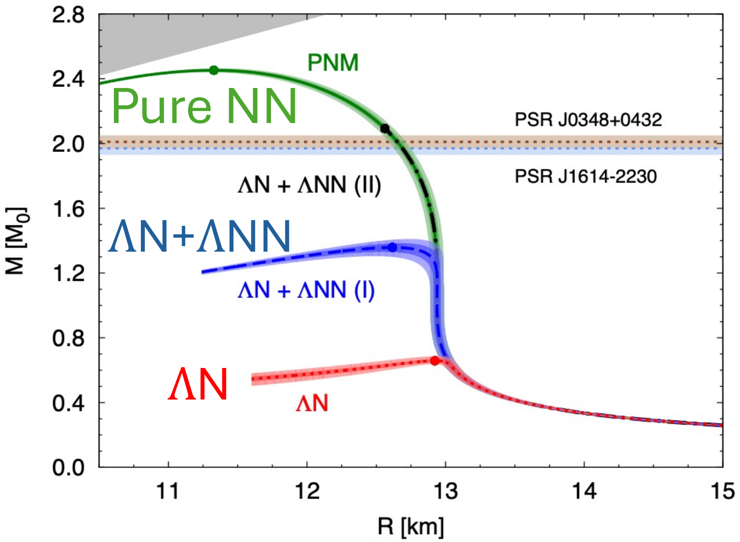

Observed heavy neutron stars

Nuclear matter EoS

D. Lonardoni, et al. PRL 114, 092301 (2015)

Mass vs R

RHIC and The STAR Detector

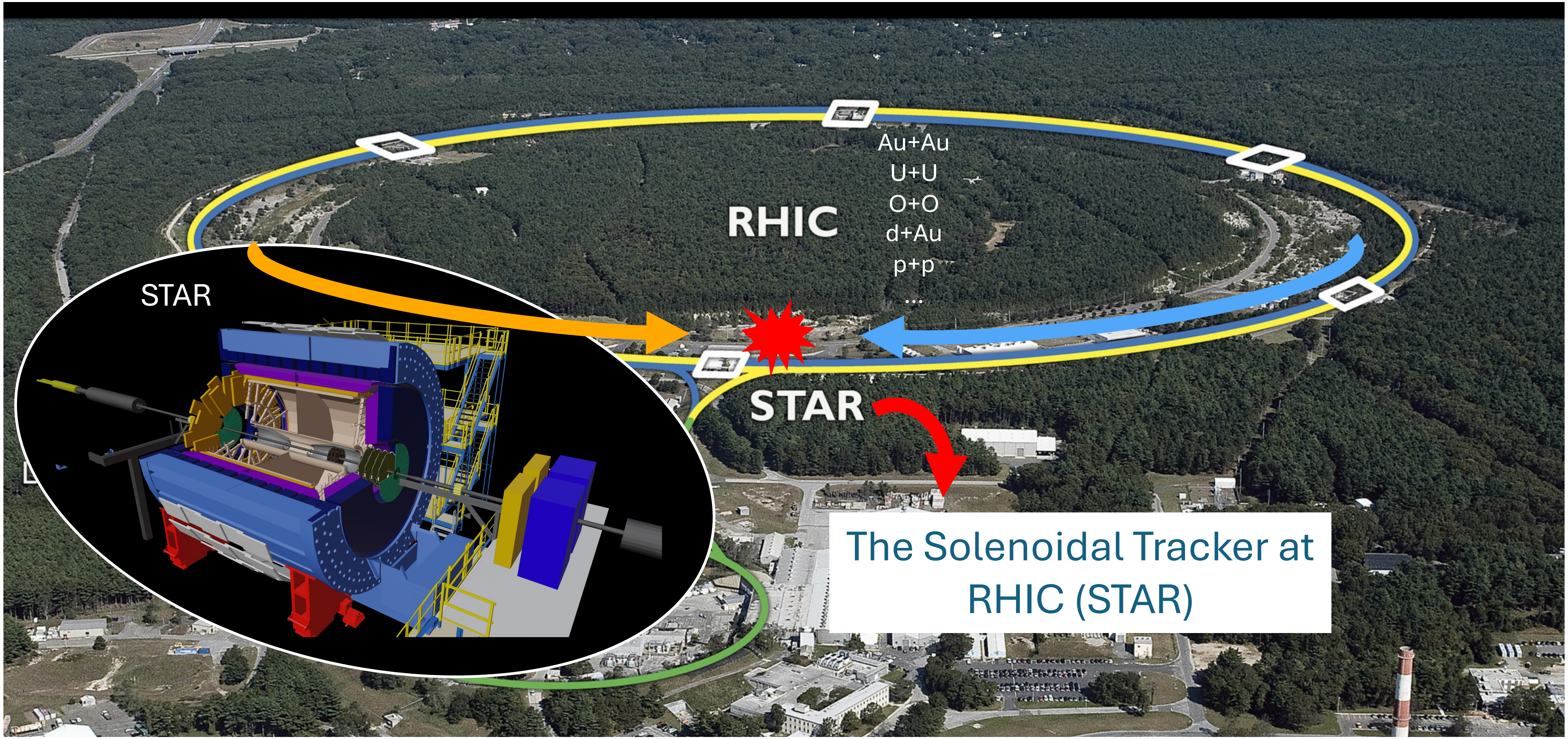

Previous Hypernuclei Measurements at STAR

- STAR observed ${}^{3}_{\Lambda}\overline{\mathrm{H}}$ in 2010
  - Starting of hypernuclei measurements at STAR

2010

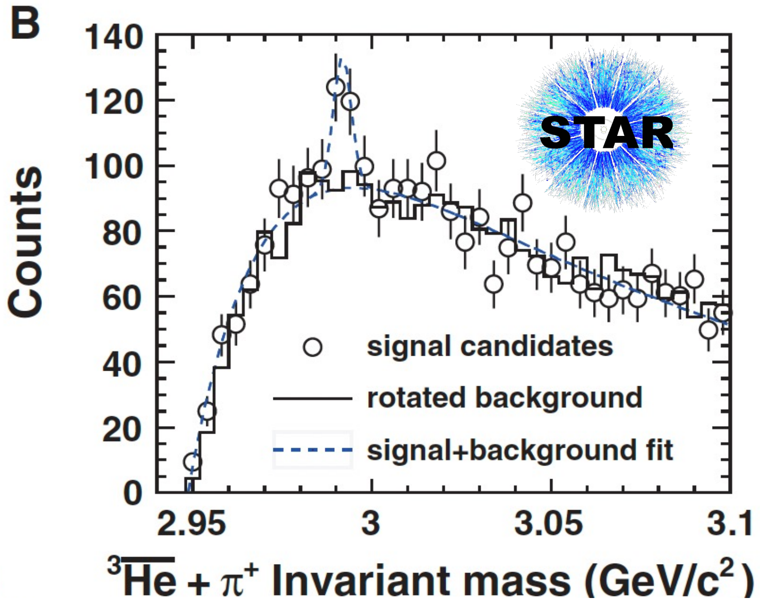

$${}^{3}_{\Lambda}\overline{\mathrm{H}} \rightarrow {}^{3}\overline{\mathrm{He}} + \pi^{+}$$

Science 328 (2010) 58-62

2024

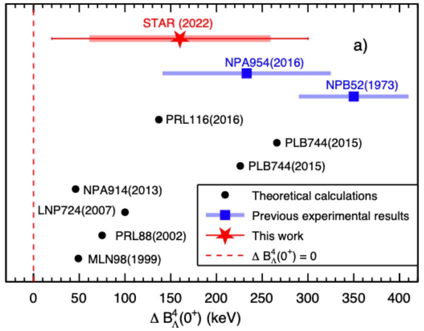

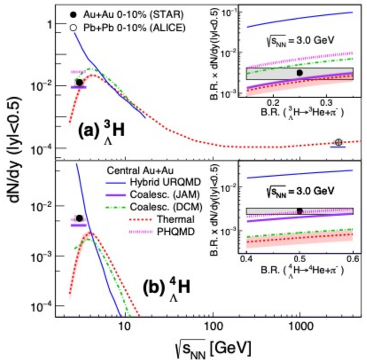

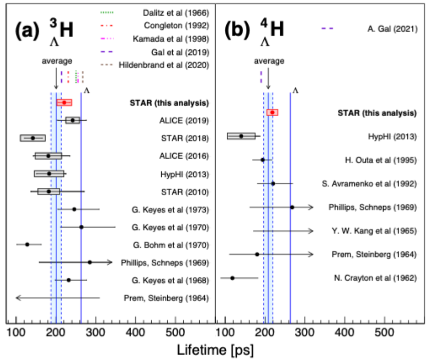

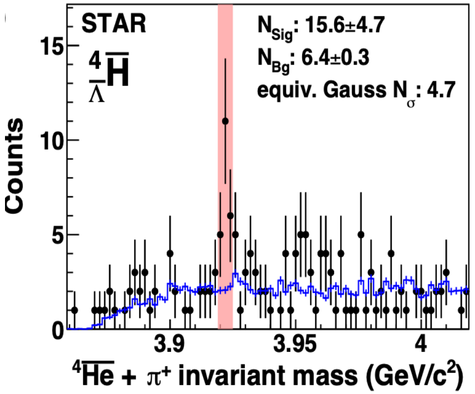

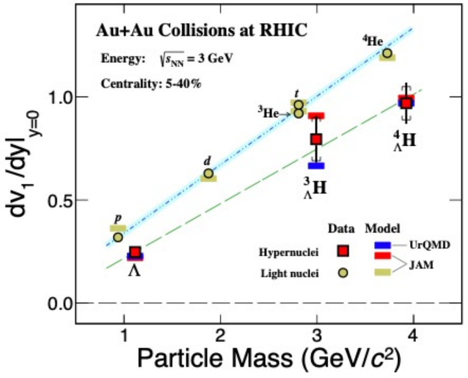

……

Today's talk would focus on hypernuclei production yields measurements.

STAR Beam Energy Scan II (BES II)

- Mapping the QCD diagram in the region of $200 < \mu_B \leq \sim 750$ MeV
  - Collisions species: Au+Au
  - Collider mode: $\sqrt{s_{NN}}$ = 7.7 - 27 GeV
  - Fixed-Target mode: $\sqrt{s_{NN}}$ = 3.0 – 7.7 GeV

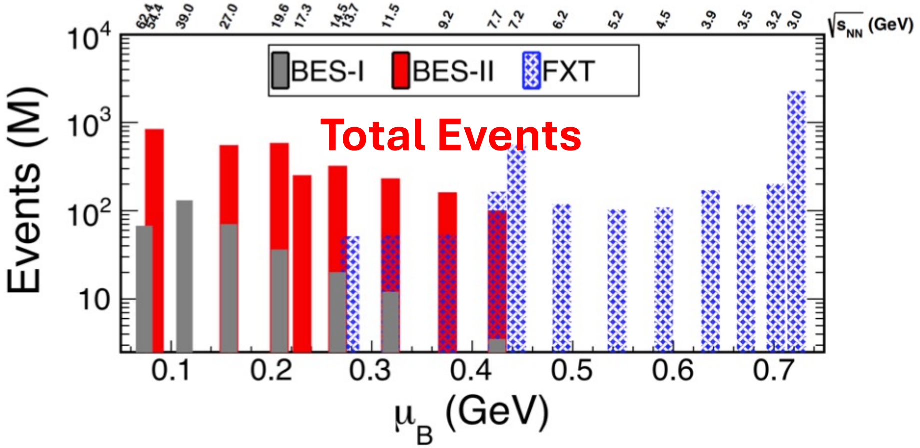

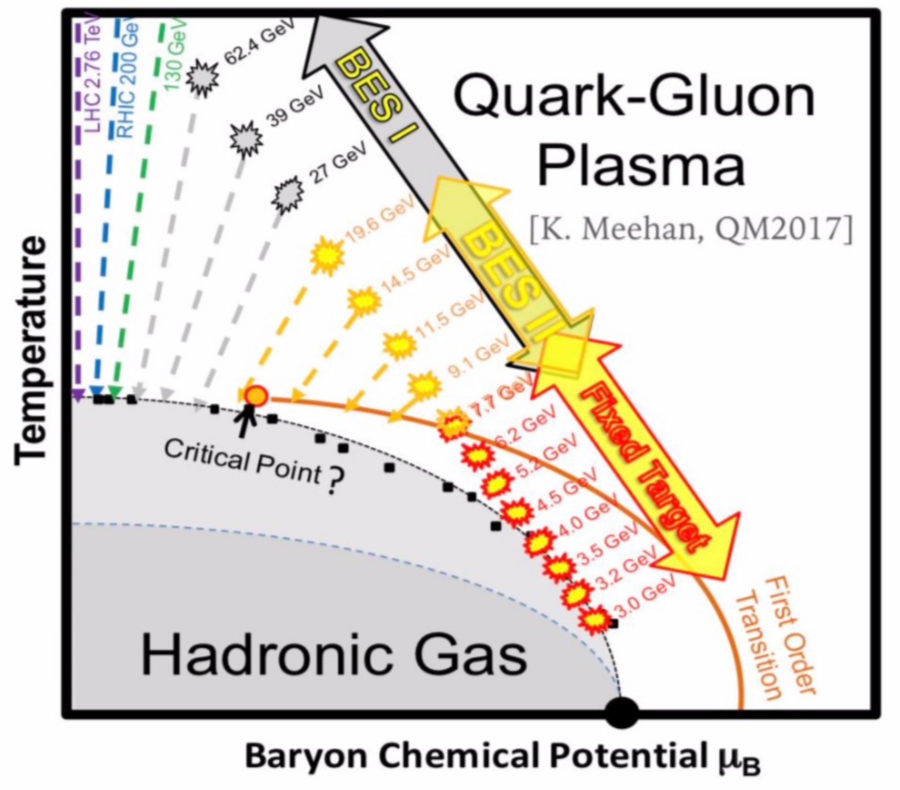

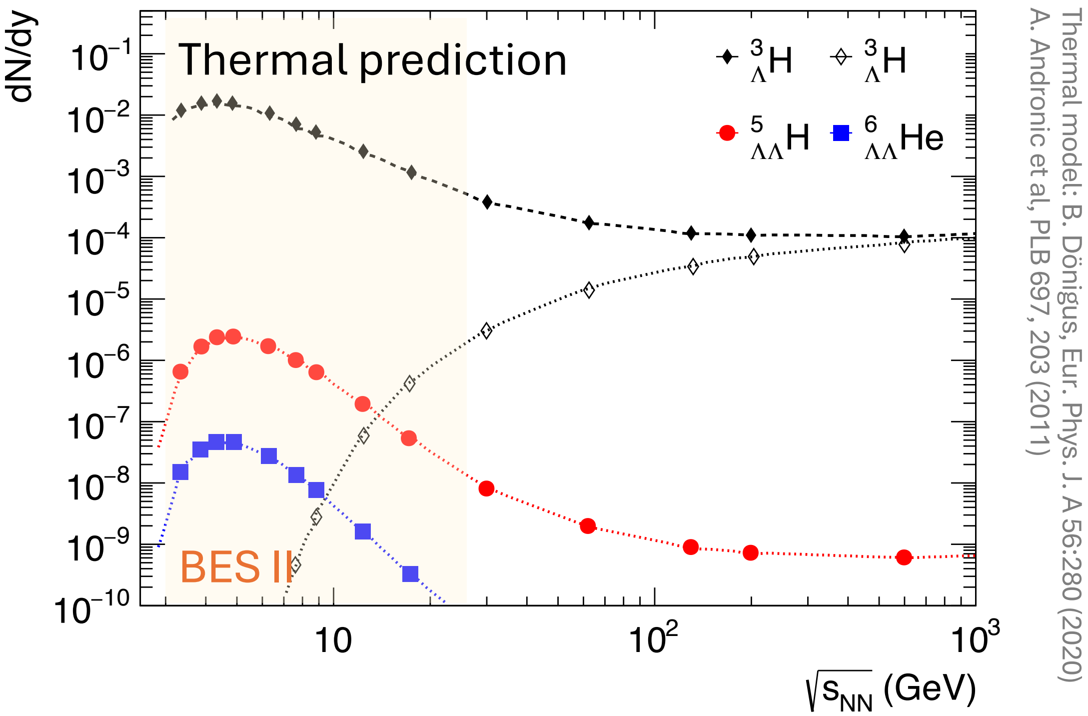

Fixed-Target Setup at STAR

Gold foil,
250 μm thick

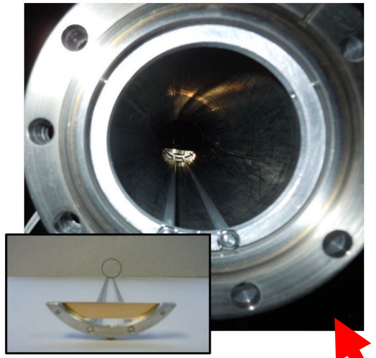

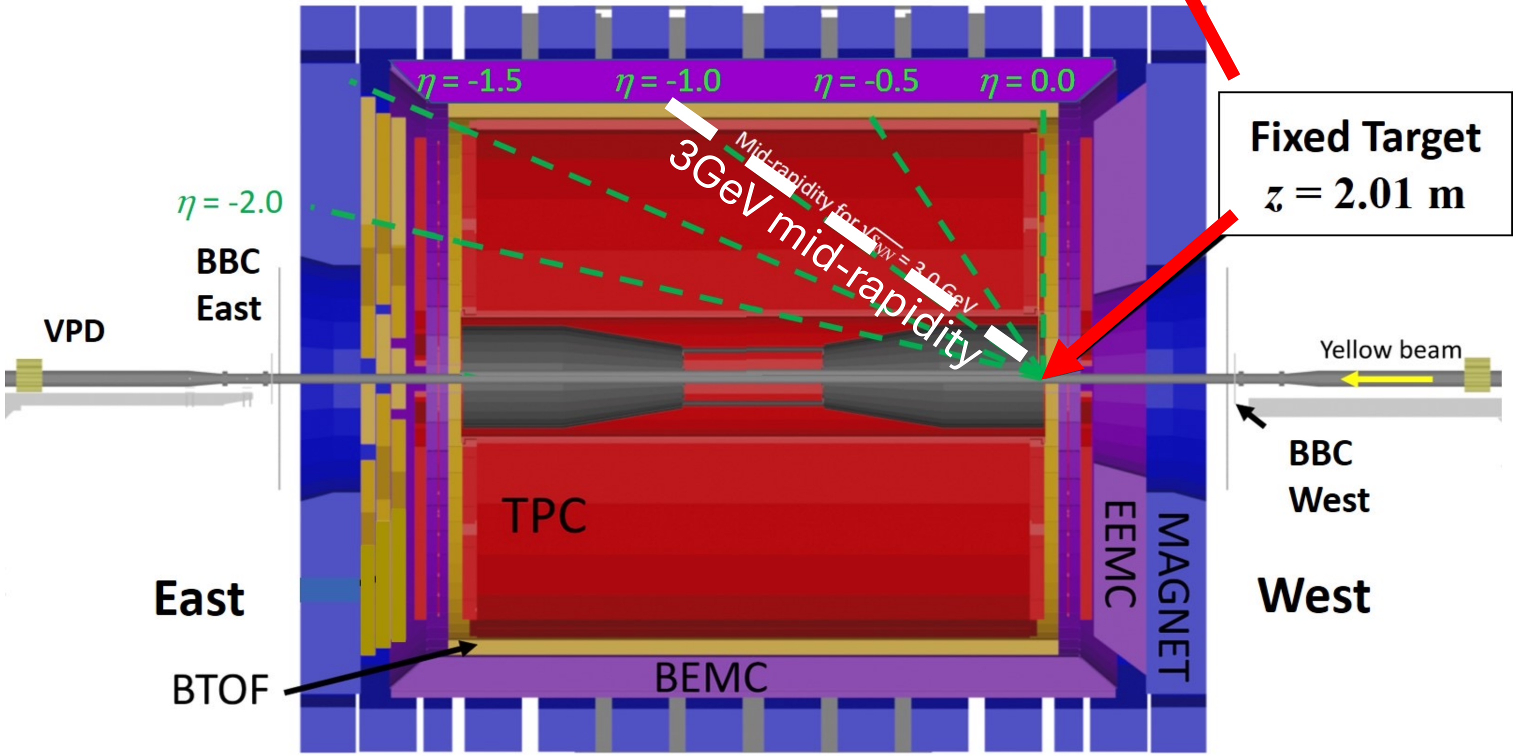

Fixed Target
$z = 2.01$ **m**

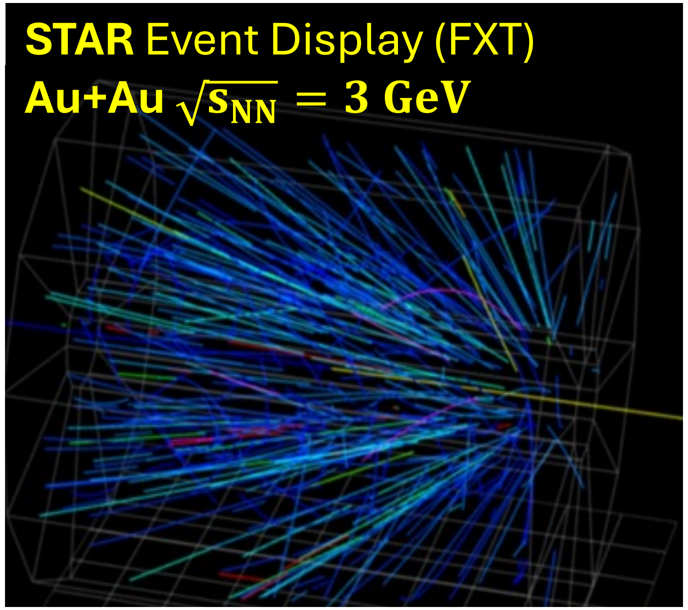

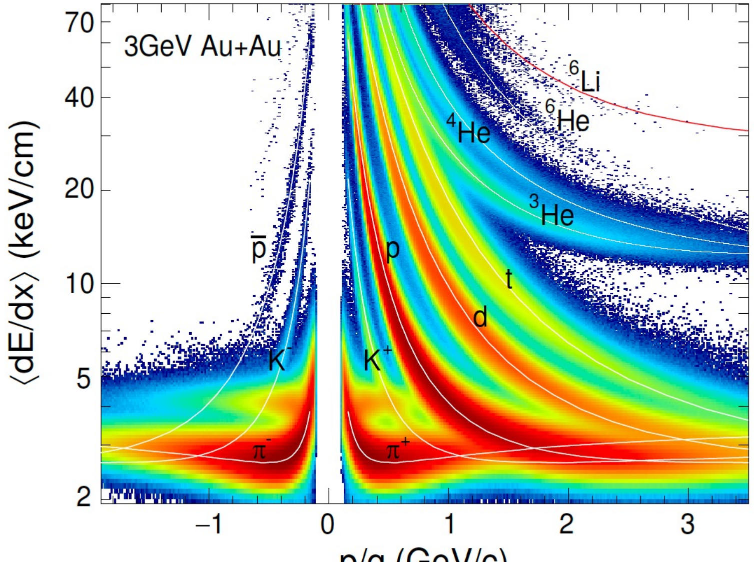

Hypernuclei reconstruction at STAR

- Signals are reconstructed by KFParticle package. X. Ju et al. Nucl. Sci. Tech. 34, 10, 158 (2023)
  - Combinatorial backgrounds reconstructed by rotation of $^{3(4)}\mathrm{He}$ tracks.

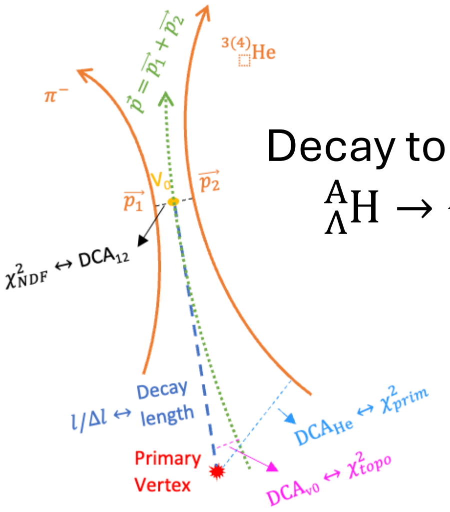

Decay topology of $^{A}_{\Lambda}\mathrm{H} \rightarrow {}^{A}\mathrm{He}\,\pi^-$

$^{3}_{\Lambda}\mathrm{H} \rightarrow {}^{3}\mathrm{He}\,\pi^-$

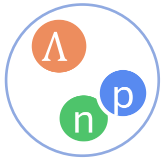

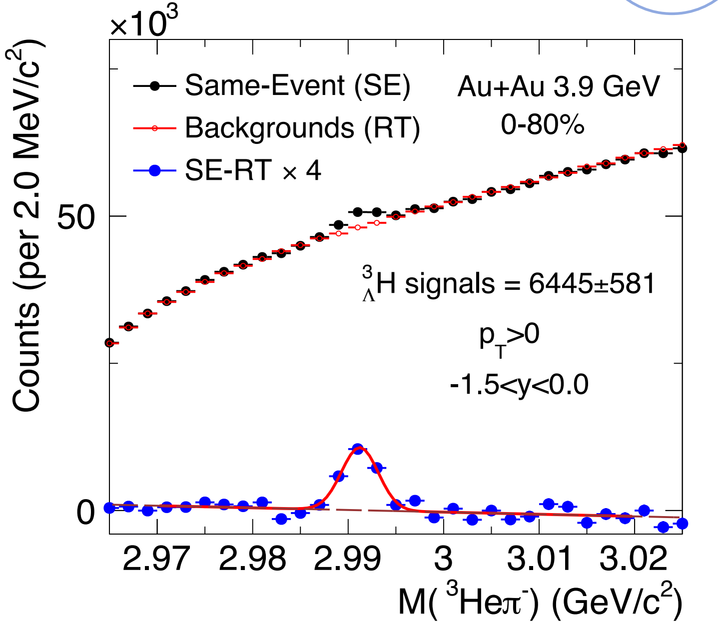

$^{4}_{\Lambda}\mathrm{H} \rightarrow {}^{4}\mathrm{He}\,\pi^-$

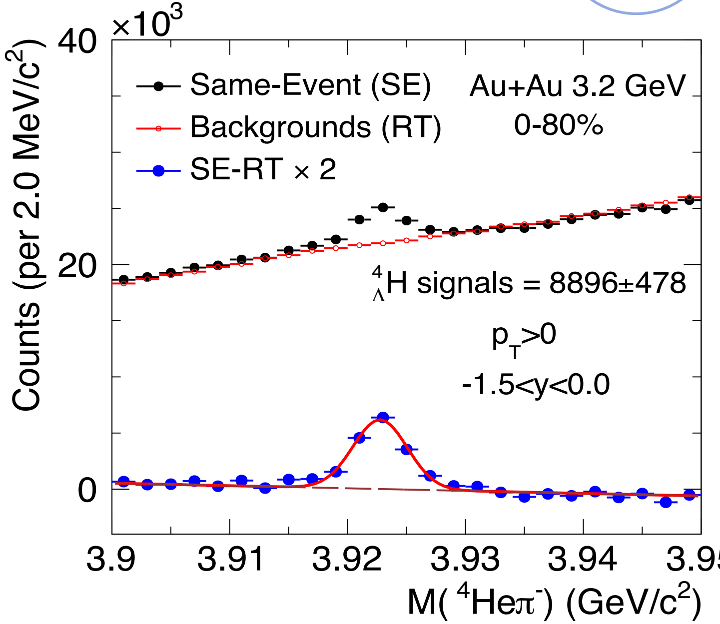

$^{4}_{\Lambda}\mathrm{He} \rightarrow {}^{3}\mathrm{He}\,p\pi^-$

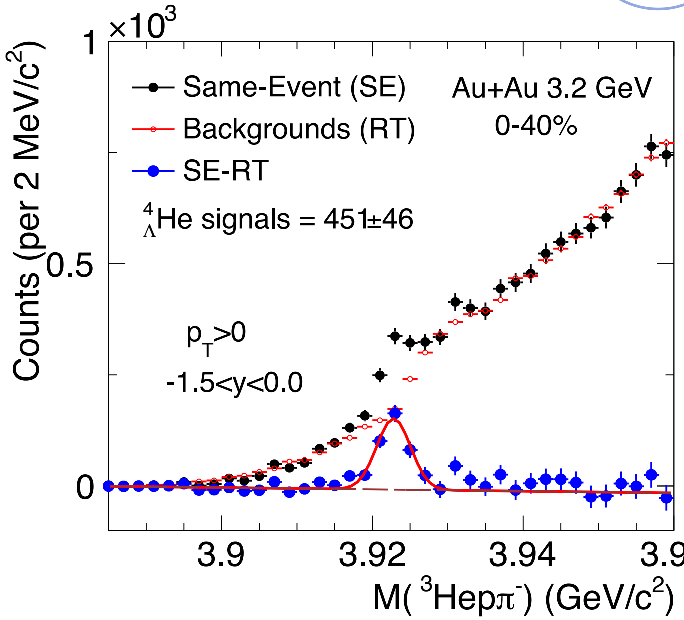

${}^{3}_{\Lambda}$H reconstruction via 3-body channel

${}^{3}_{\Lambda}\mathrm{H} \rightarrow \mathrm{d}p\pi^{-}$, B.R. ~ 40-50%
${}^{3}_{\Lambda}\mathrm{H} \rightarrow {}^{3}\mathrm{He}\,\pi^{-}$, B.R. ~15-25%

- ${}^{3}_{\Lambda}$H: Simplest hypernuclei system
- ${}^{3}_{\Lambda}$H decay topological distribution very similar as Λ+d

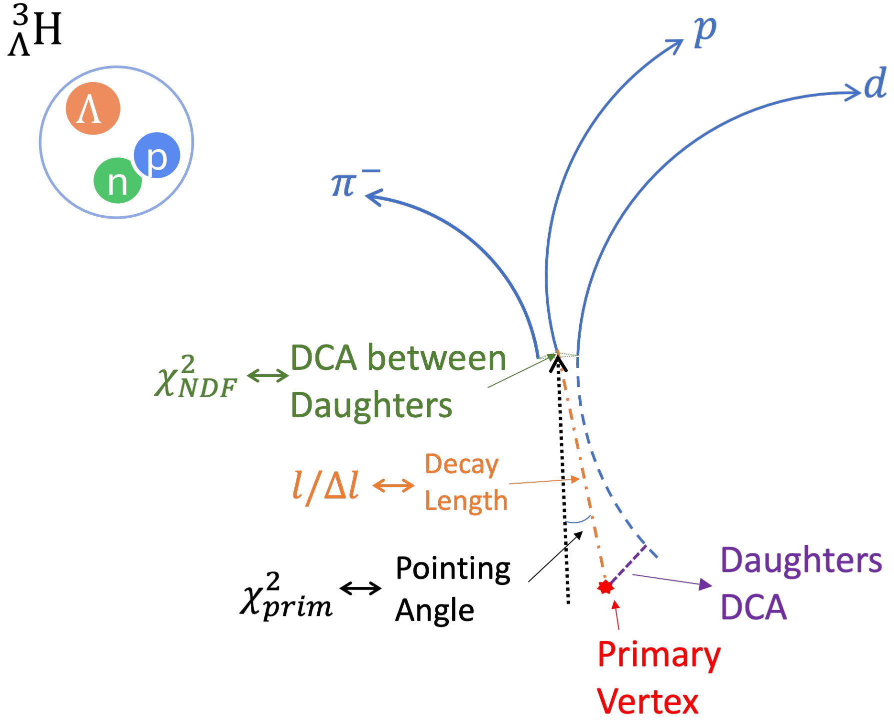

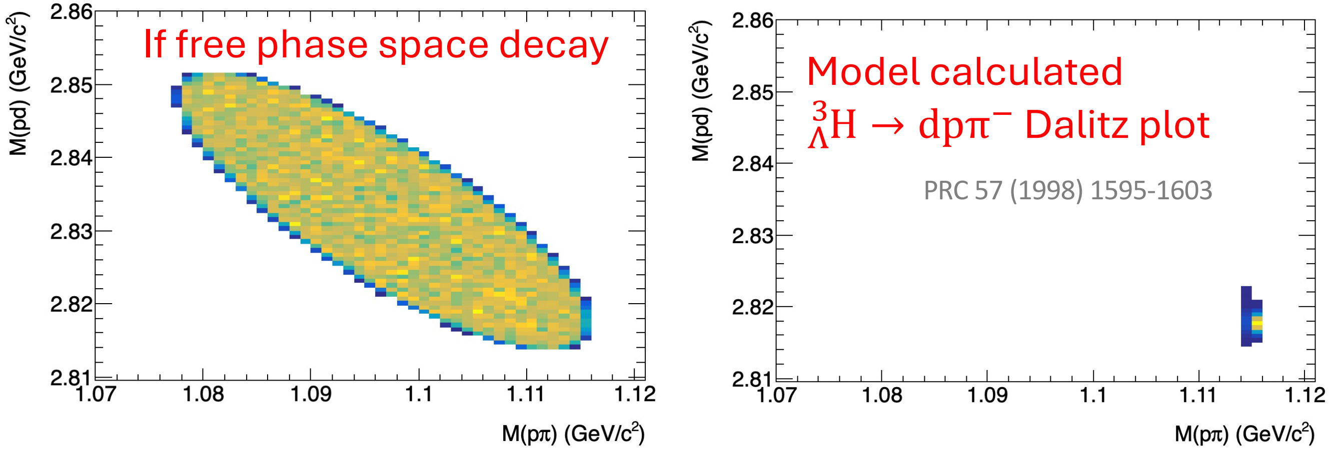

Real Λ and ($p\pi$) from ${}^{3}_{\Lambda}$H decay

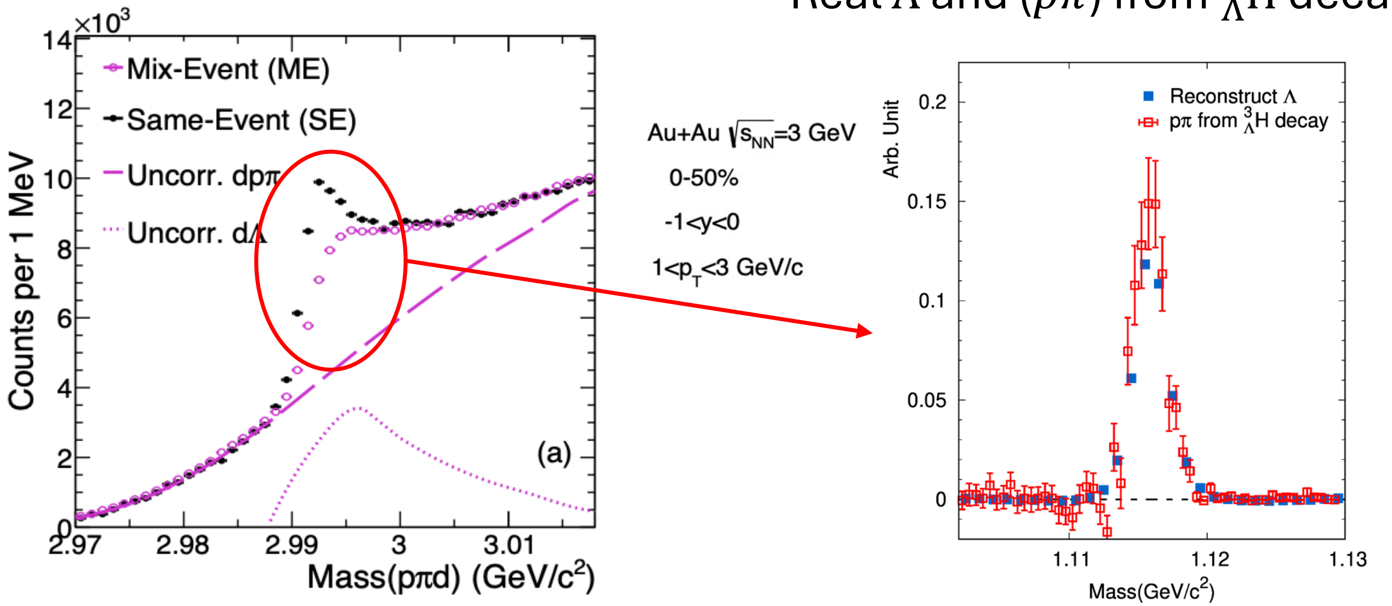

Correlated Λd contamination in ${}^{3}_{\Lambda}\mathrm{H} \rightarrow \mathrm{dp}\pi^{-}$ signal

- Λd may have kinematic correlations according to theory calculation.

C(k*)=$\frac{P(\Lambda d)}{P(\Lambda)P(d)}$, p is the possibility of finding particle
No correlation -> C(k*)=1.
k* -> relative momentum between Λ and d.

When k*=0, in Λ and d pair CMS framework:

$$p_\Lambda = -p_d = 0$$

$\mathrm{P}(\Lambda)$: (p_Λ, E_Λ) = (0, m_Λ)

$\mathrm{P}(\mathrm{d})$: (p_d, E_d) = (0, m_d)

-> $\mathrm{P}(\Lambda d)$: ($p_\Lambda + p_d$, $E_\Lambda + E_d$) = (0, $m_\Lambda + m_d$)

PRC 102, 034001 (2020)

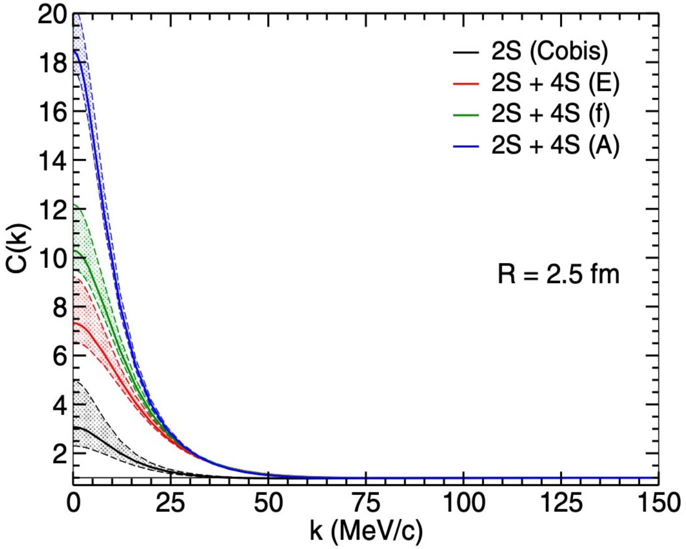

Model predicts peak structure in C(k*) at k*->0.

Set C(k*) weight on uncorrected Λ and d

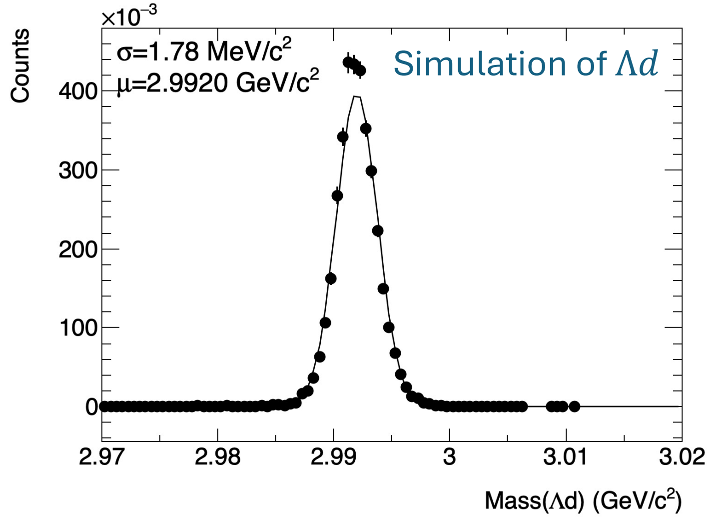

- Correlated Λd could form a peak near M(${}^{3}_{\Lambda}\mathrm{H}$) even after subtracting combinatorial background.
  - $M(\Lambda) + M(d)$ ~2.9913 GeV/c^2, M(${}^{3}_{\Lambda}\mathrm{H}$)~2.991 GeV/c^2.

${}^{3}_{\Lambda}H$ reconstruction via 3-body channel

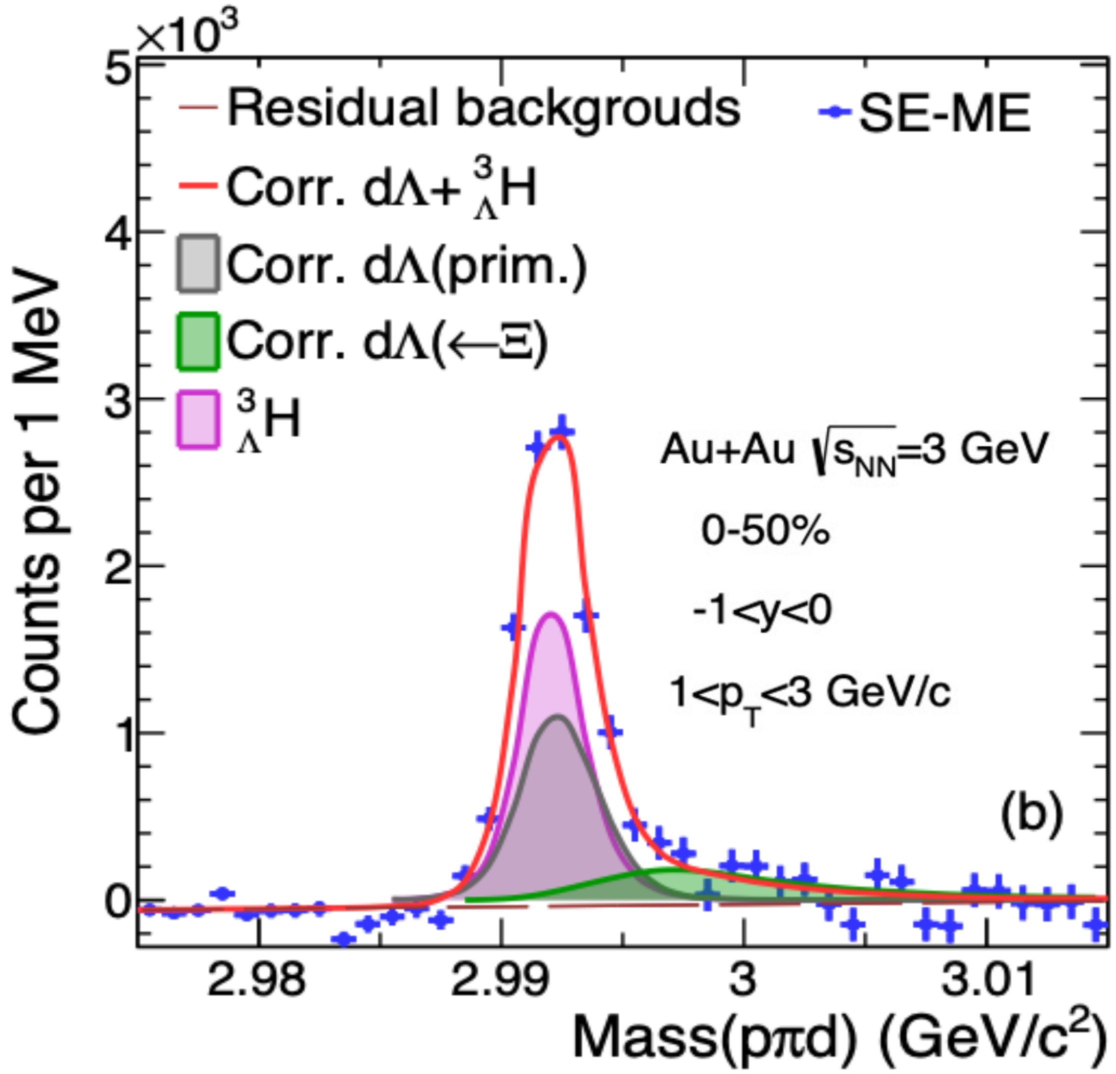

- Template fit method to estimate ${}^{3}_{\Lambda}H$ purity statistically.
  - $\chi^2_{NDF\,\Lambda d}, \chi^2_{NDF\,{}^{3}_{\Lambda}H}$ template estimated from simulations.

$$\chi^2_{NDF\,Data} = p_0 \cdot (\chi^2_{NDF\,\Lambda d} + p_1 \cdot \chi^2_{NDF\,{}^{3}_{\Lambda}H})$$

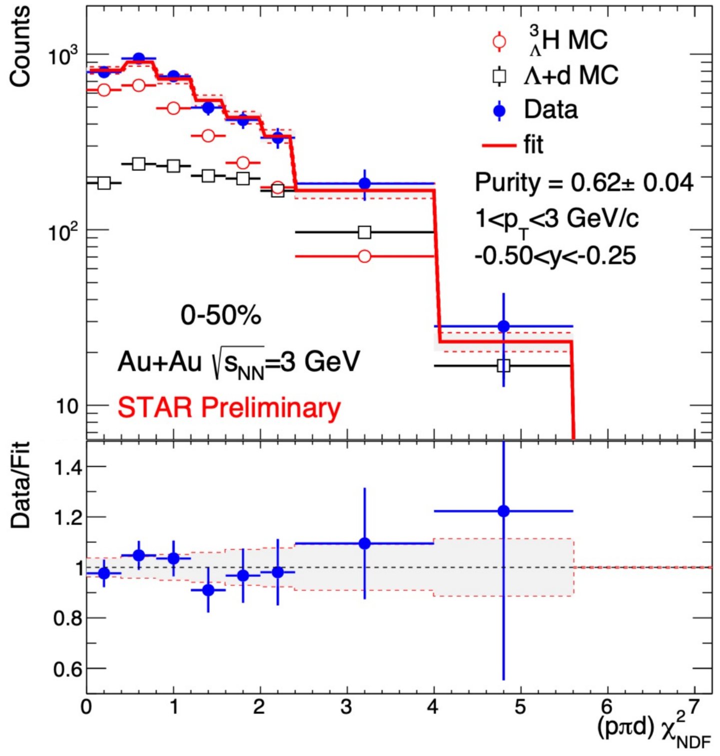

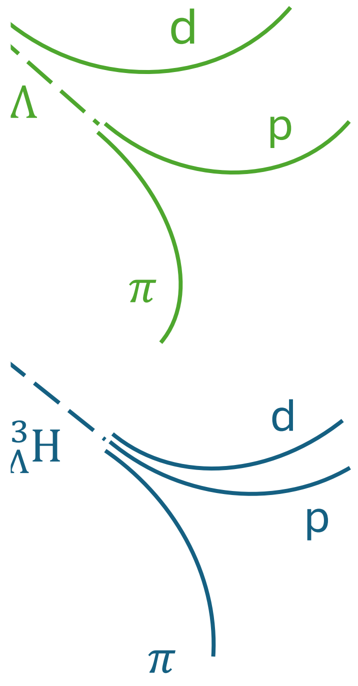

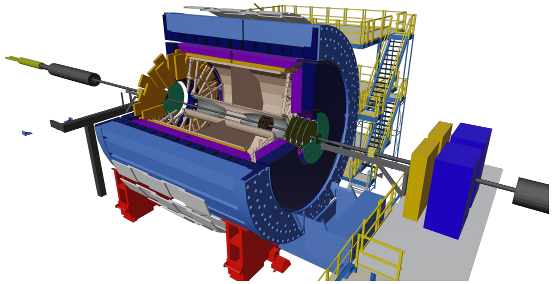

Measurements on Hypernuclei
Branching ratio

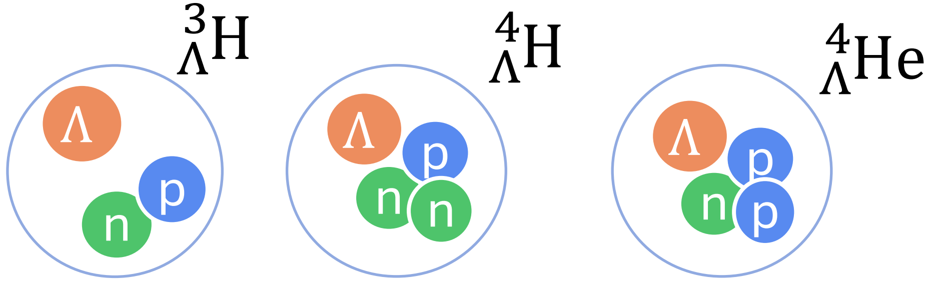

${}^{3}_{\Lambda}$H Branching Ratio R_3

- Calculations propose that ${}^{3}_{\Lambda}\mathrm{H}$ R_3 may be sensitive to Λ separation energy B_Λ
  - ${}^{3}_{\Lambda}\mathrm{H}\ B_\Lambda = \mathrm{M}(d) + \mathrm{M}(\Lambda) - \mathrm{M}({}^{3}_{\Lambda}\mathrm{H})$
- Sensitive to ${}^{3}_{\Lambda}\mathrm{H}$ spin states
- Global uncertainty for yields measurements

$$R_3 = \frac{\mathrm{B.R.}({}^{3}_{\Lambda}\mathrm{H} \to 3\mathrm{He}\pi^-)}{\mathrm{B.R.}({}^{3}_{\Lambda}\mathrm{H} \to \mathrm{pd}\pi^-) + \mathrm{B.R.}({}^{3}_{\Lambda}\mathrm{H} \to {}^{3}\mathrm{He}\pi^-)}$$

F. Hildenbrand et al, PRC 102, 064002 (2020)

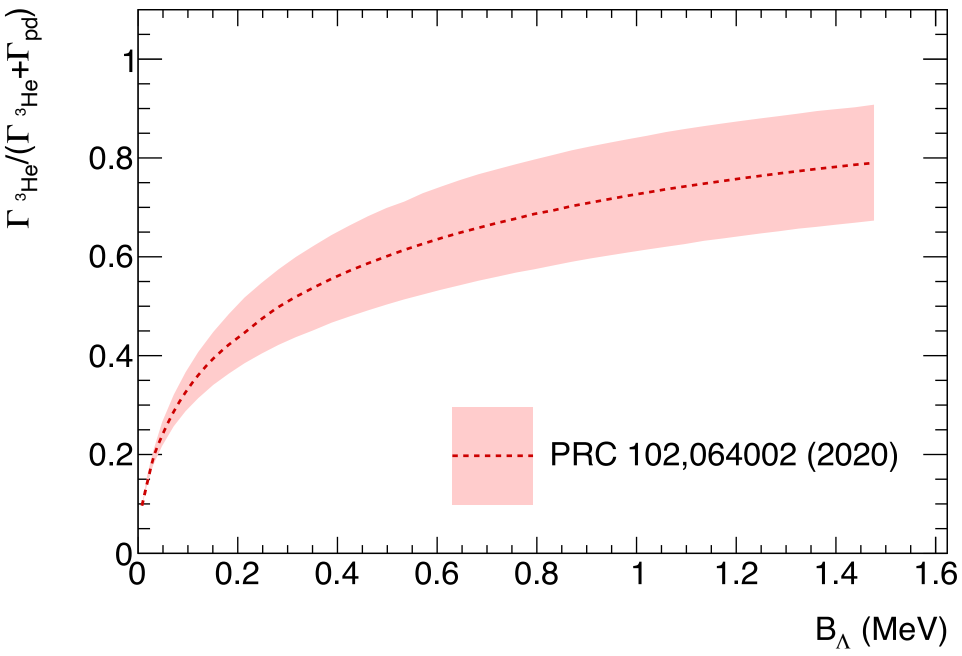

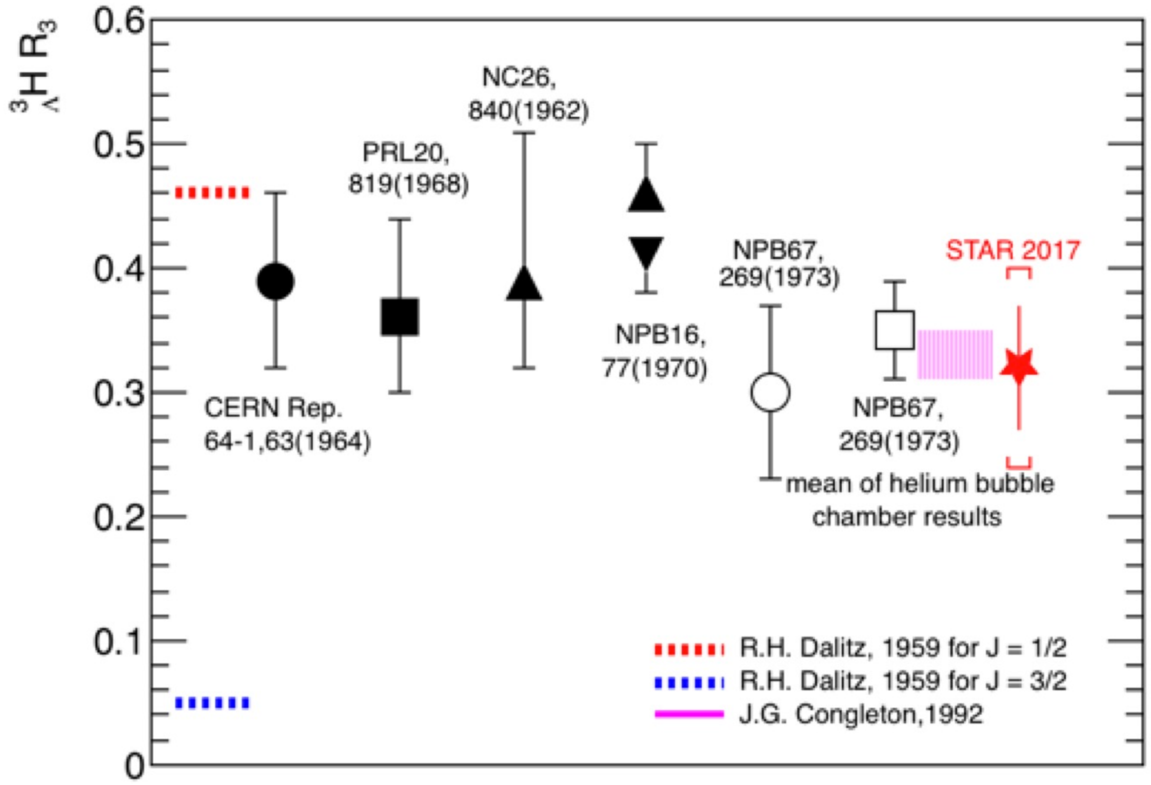

${}^{3}_{\Lambda}\mathrm{H}$ Branching Ratio R_3

$$R_3 = \frac{\mathrm{B.R.}\,({}^{3}_{\Lambda}\mathrm{H} \rightarrow 3\mathrm{He}\pi^-)}{\mathrm{B.R.}\,({}^{3}_{\Lambda}\mathrm{H} \rightarrow \mathrm{pd}\pi^-) + \mathrm{B.R.}\,({}^{3}_{\Lambda}\mathrm{H} \rightarrow {}^{3}\mathrm{He}\pi^-)}$$

STAR: $R_3 = 0.272 \pm 0.030 \pm 0.042$

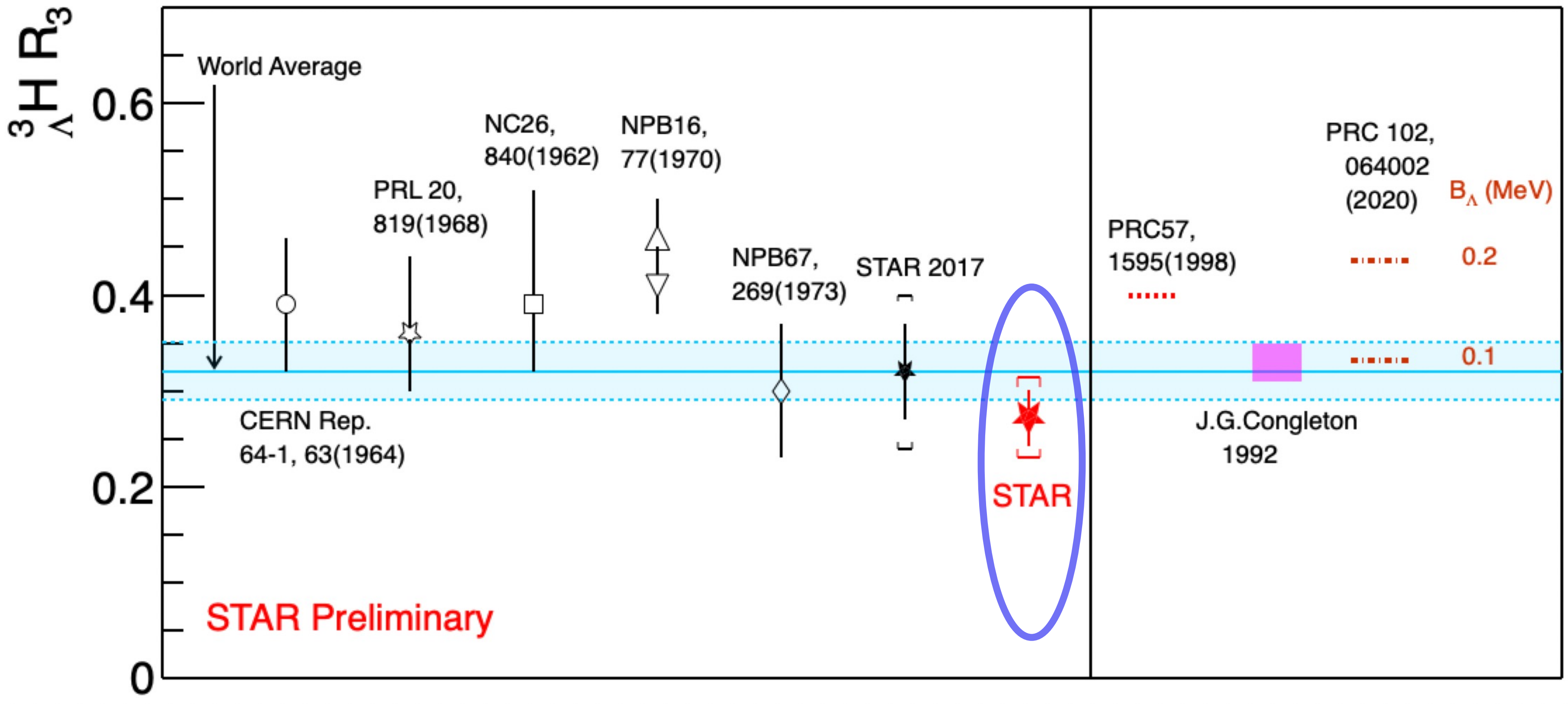

- STAR new R_3 data favors small binding energy of hypertriton.

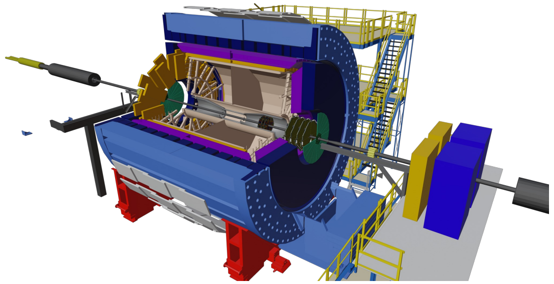

Measurements on Hypernuclei Production at STAR

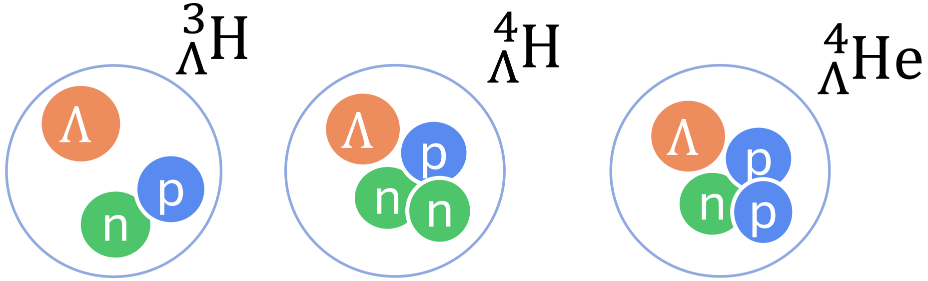

Hypernuclei Production in HIC

Models at mid-rapidity

Thermal model

- Hadron chemical freeze out T_{ch} and μ_B
  - $\frac{dN}{d^3\,\mathrm{p}} \sim \exp(-\frac{E-\mu_B}{T})$
- Assuming the conserved baryon entropy after hadron chemical freeze-out

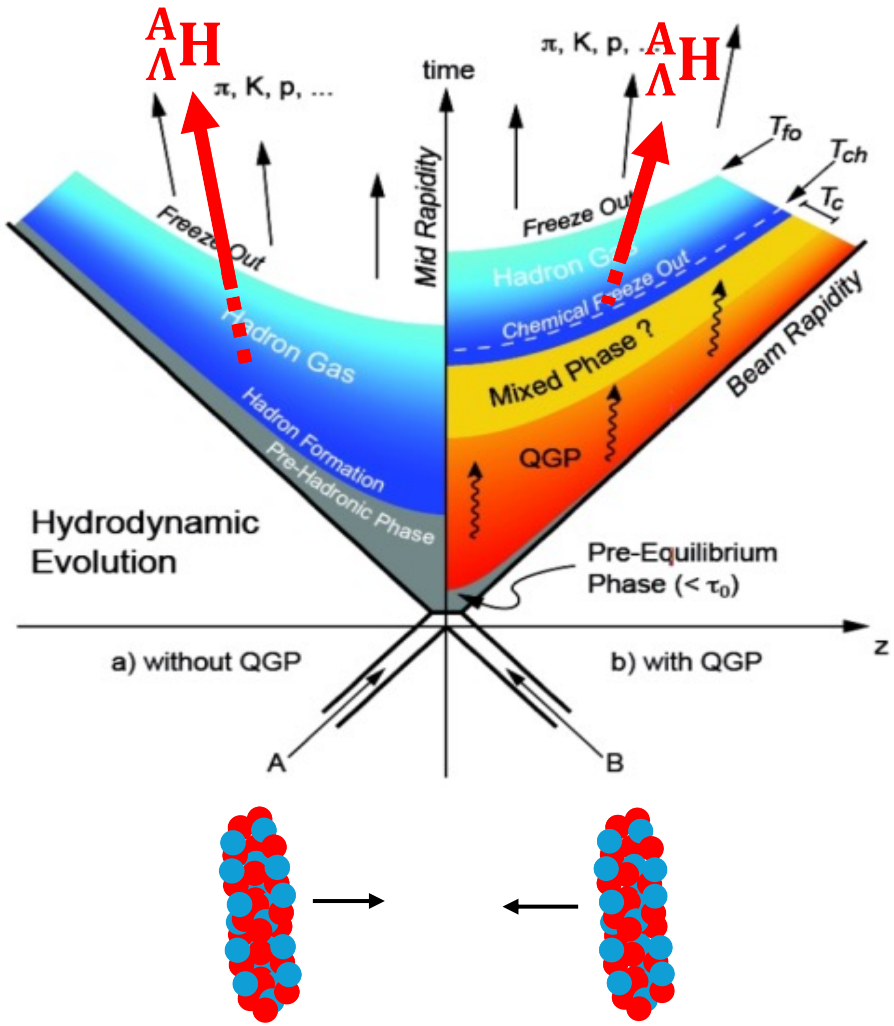

Coalescence formation

- Baryons / nuclei very close in phase space $(\vec{p}, \vec{r})$.
  - Any experimental evidence?
  - The role of *Y-N* interaction?

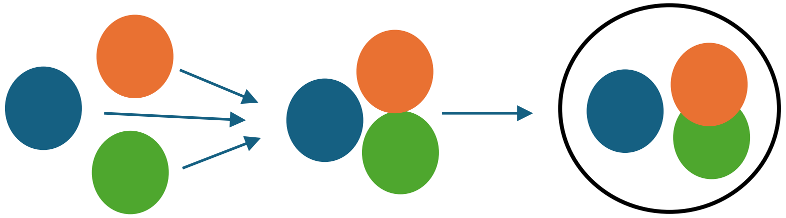

Fruitful Results from STAR BES II

- Utilizing BES II datasets, we measure:
  - ${}^{3}_{\Lambda}\mathrm{H}$ p_T spectra, dN/dy, $\langle p_T \rangle$ in Au+Au collisions at $\sqrt{s_{NN}}$ = 3-27 GeV
  - ${}^{4}_{\Lambda}\mathrm{H}$, ${}^{4}_{\Lambda}\mathrm{He}$ p_T spectra, dN/dy, $\langle p_T \rangle$ in Au+Au collisions at $\sqrt{s_{NN}}$ =3-3.5 GeV

A=3: ${}^{3}_{\Lambda}\mathrm{H}$ (Au+Au $\sqrt{s_{NN}}$ =3-27 GeV)

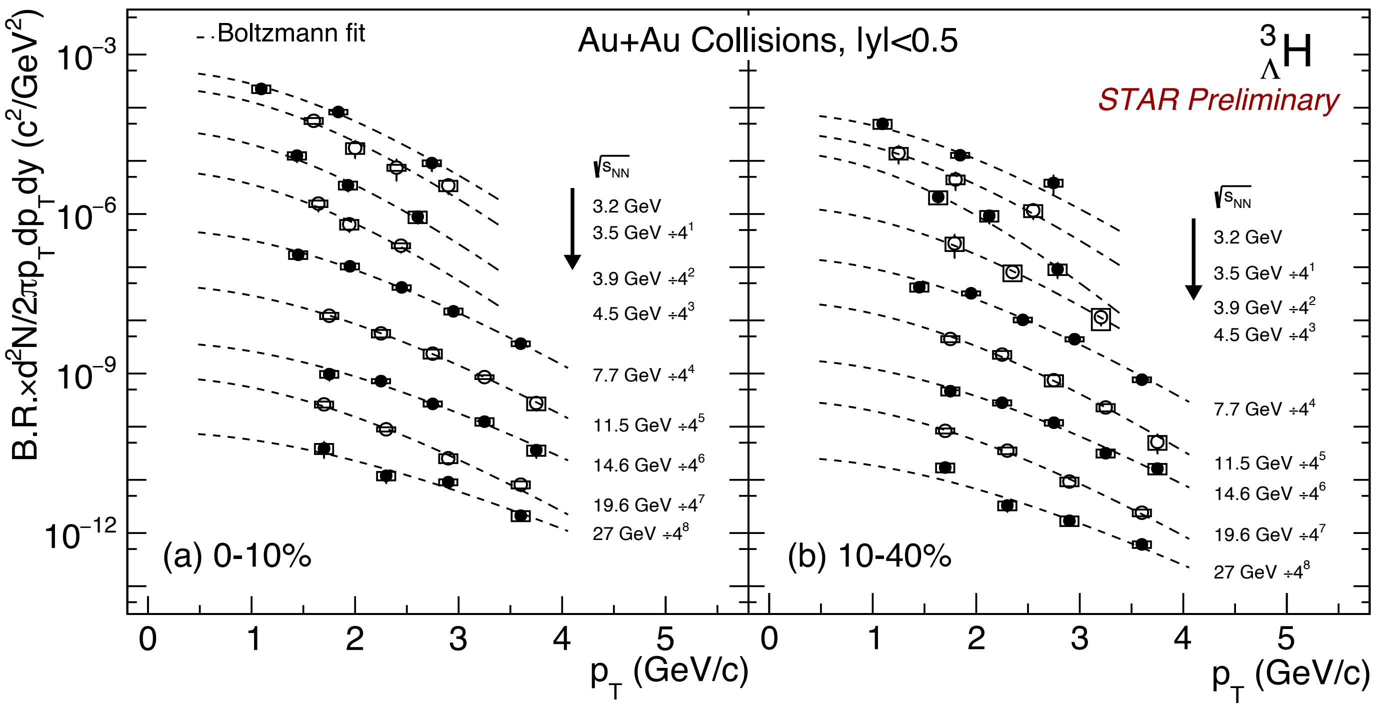

A=4: ${}^{4}_{\Lambda}\mathrm{H}$, ${}^{4}_{\Lambda}\mathrm{He}$ (Au+Au $\sqrt{s_{NN}}$ =3-3.5 GeV)

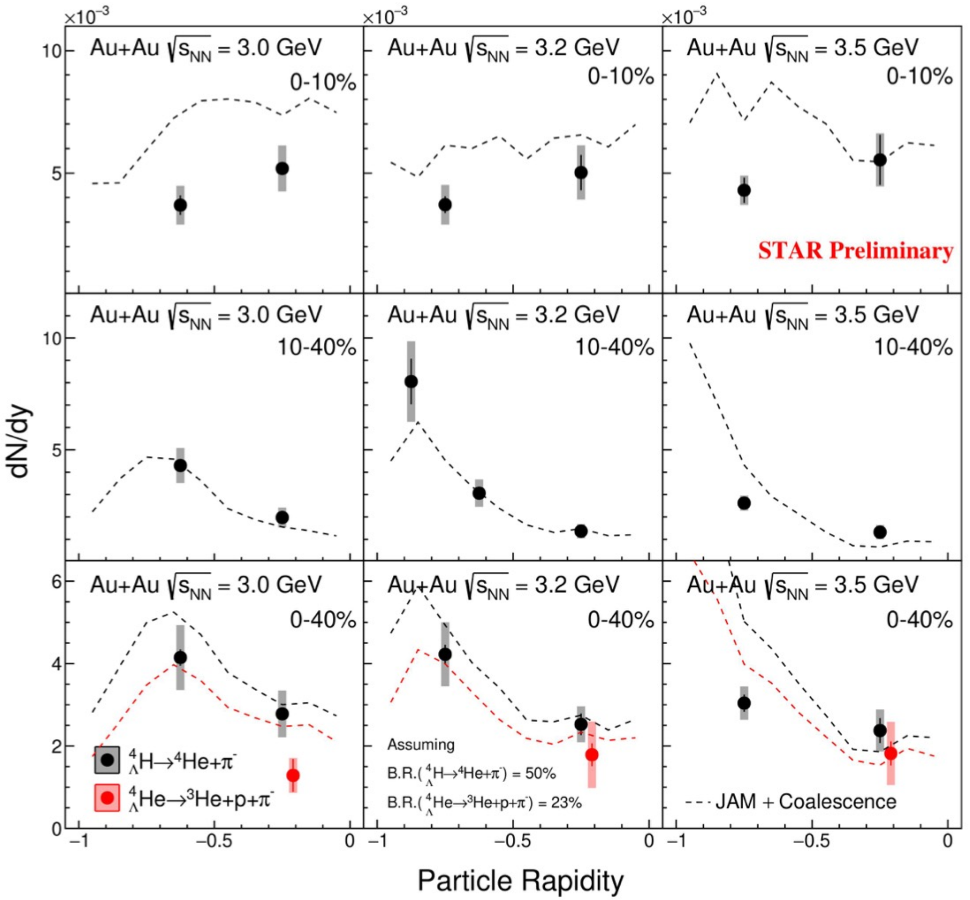

${}^{3}_{\Lambda}H$ and ${}^{4}_{\Lambda}H$ dN/dy in Au+Au collisions at 3 GeV

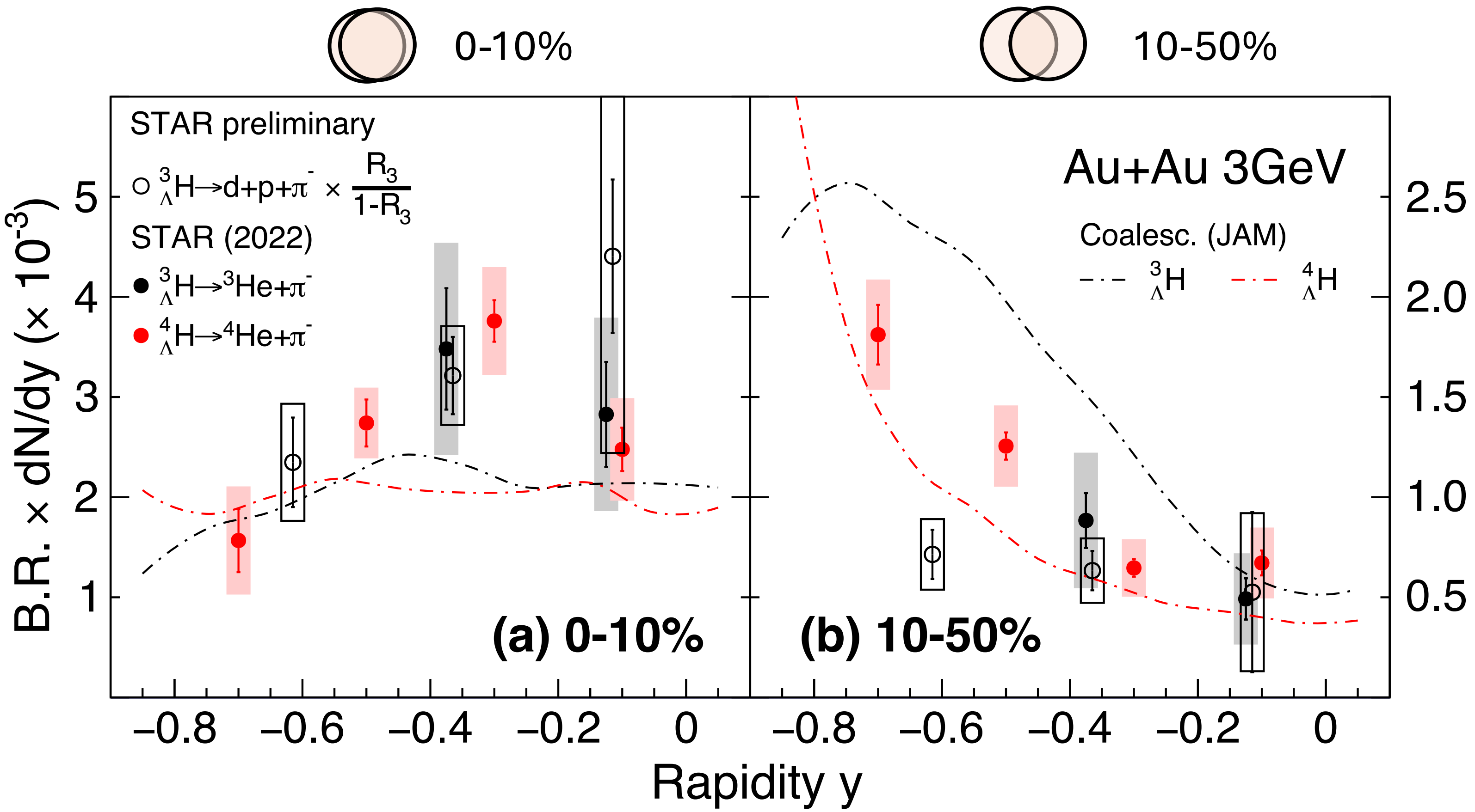

JAM+Coal.

- Tuned to match proton and Λ spectra from data;
- Instant coalescence after kinetic freeze-out
- Two body coalescence: d/t+Λ

3 GeV ${}^{3(4)}_{\Lambda}H \rightarrow {}^{3(4)}He + \pi^{-}$:
PRL 128, 202301 (2022)

- Coalescence models with tuned parameters:
  - Qualitatively describe the trend of ${}^{4}_{\Lambda}H$ yields versus rapidity.
  - Fail to describe the ${}^{3}_{\Lambda}H$ tendency in 10-50% centralities.

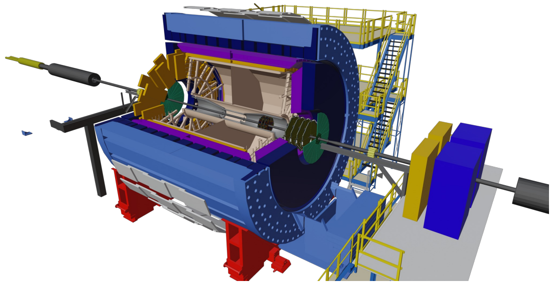

Energy Dependence of Hypernuclei Production

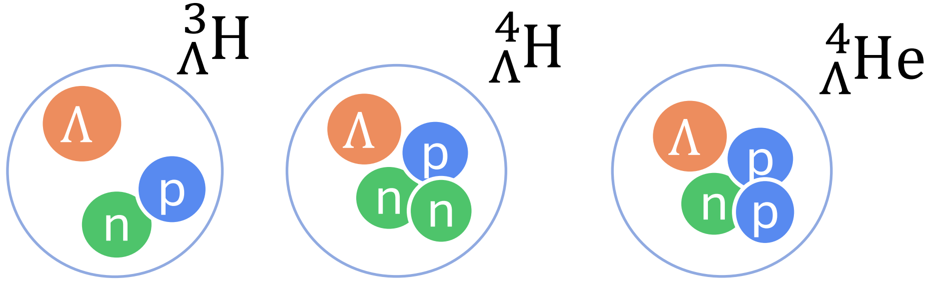

Energy Dependence of ${}^{3}_{\Lambda}\mathrm{H}$ Production

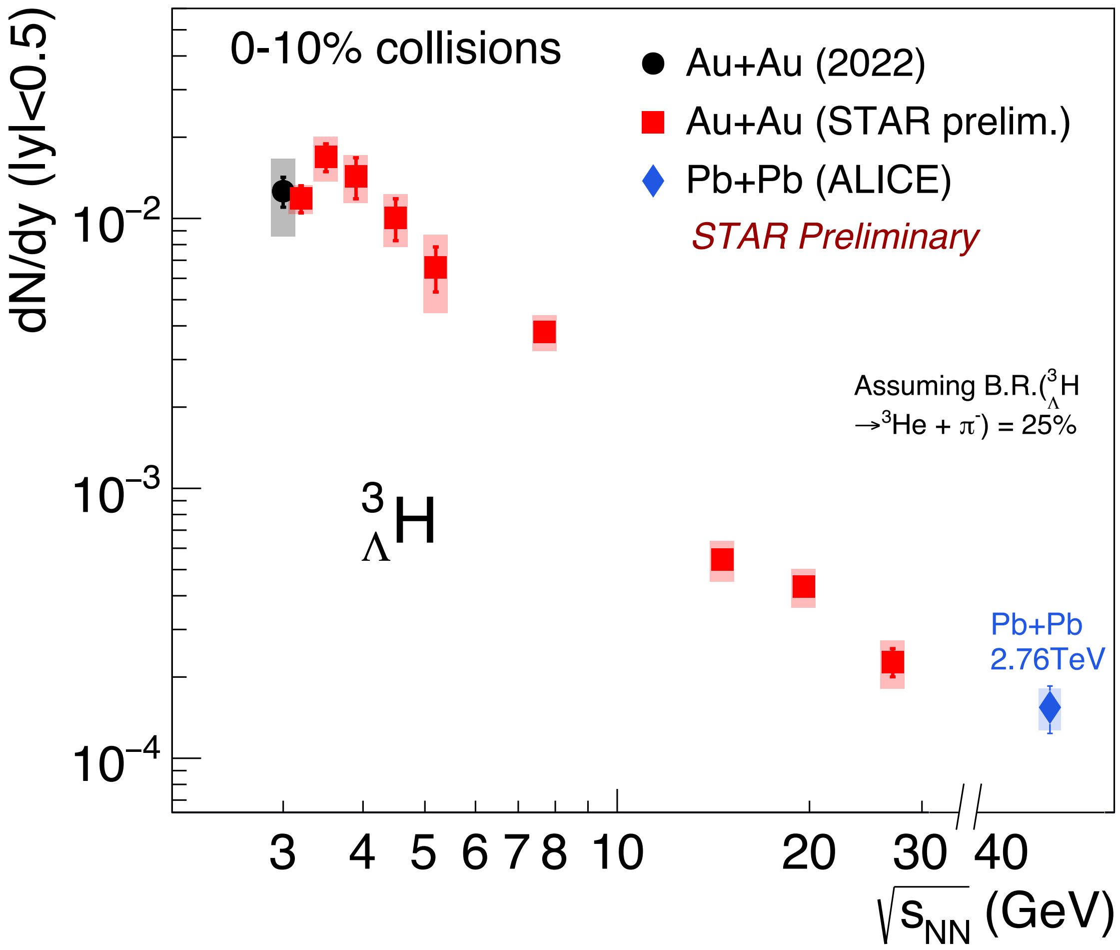

${}^{3}_{\Lambda}\mathrm{H}$ production yields reaches peak at around 3-4 GeV.

- Increase steeply from 27 to 3 GeV as $\sqrt{s_{NN}}$ goes lower
- Interplay between:
  - $\sqrt{s_{NN}}$ ↓, baryon density ↑, yields ↑
  - Hyperon production

Thermal-FIST, Coal.+UrQMD: T. Reichert et al, PRC 107, 014912 (2023)
Pb+Pb: ALICE, PLB 754, 360 (2016)
Au+Au: STAR, PRL 128, 202301 (2022)

Energy Dependence of ${}^{3}_{\Lambda}\mathrm{H}$ Production

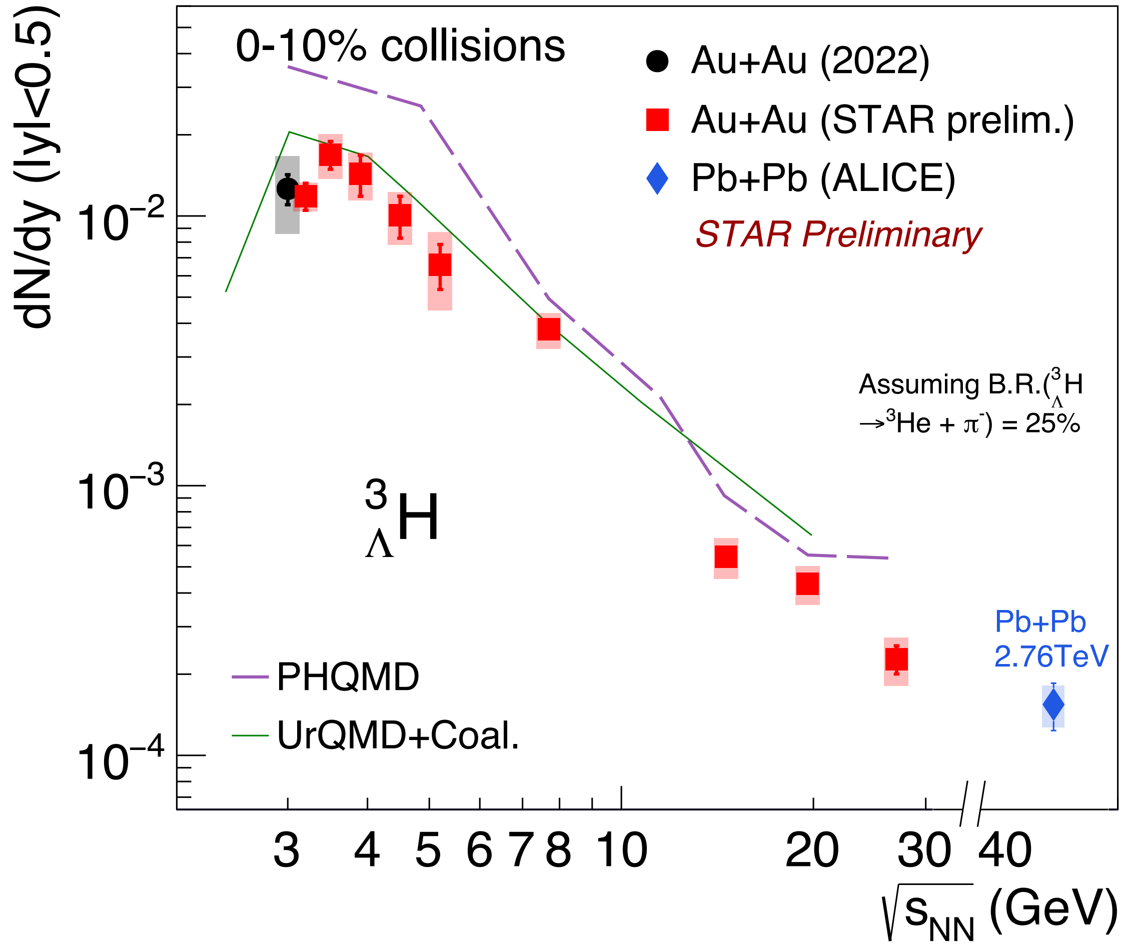

Coal. (UrQMD): T. Reichert et al. PRC 107 (2023) 1, 014912
PHQMD: S. Gläßel et al. PRC 105, 014908 (2022),
V. Kireyeu et al. arXiv:1911.09496
Pb+Pb: ALICE, PLB 754, 360 (2016)
STAR at 3 GeV: PRL 128, 202301 (2022)

UrQMD + Instant coal.

- Describe data from 3-10 GeV
- Instant coalescence after hadron kinetic freeze-out
- Coalescence condition:
  - $|\vec{p_1} - \vec{p_2}| < \Delta P, |\vec{r_1} - \vec{r_2}| < \Delta R$

PHQMD

- Transport model + dynamical cluster formation.
- Cluster can be formed before hadron kinetic freeze out.
- Future developments
  - Momentum dependent EoS
  - Y-N potential

Details see: Elena Bratkovskaya SQM2024

Energy Dependence of $^{3}_{\Lambda}H$ Production

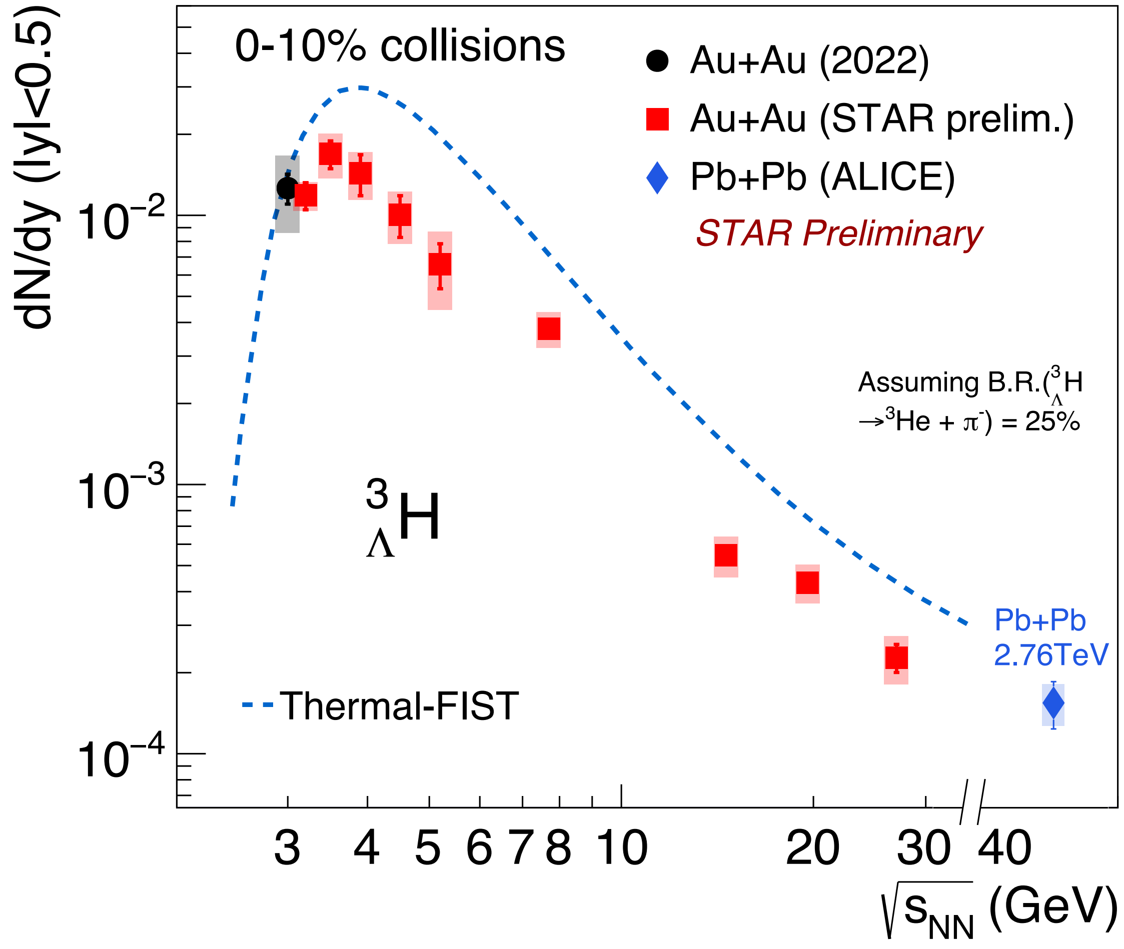

Thermal-FIST: T. Reichert et al, PRC 107, 014912 (2023)
Pb+Pb: ALICE, PLB 754, 360 (2016)
Au+Au: STAR, PRL 128, 202301 (2022)

Thermal-FIST model

- Hadron chemical freeze-out T and μ_B
  - $\frac{dN}{d^3 p} \sim \exp(-\frac{E-\mu_B}{T})$
- Strangeness canonical ensemble in low energies
- ~ 2 times larger than the data

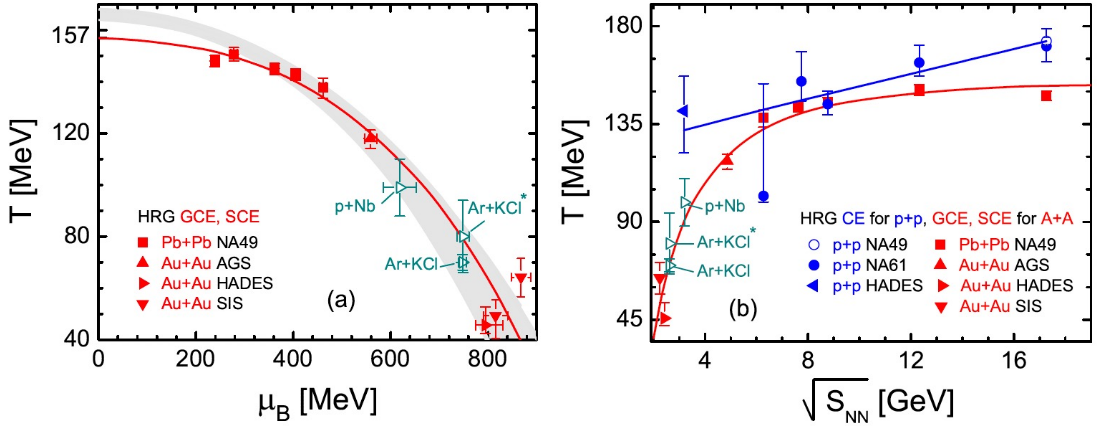

Phys. Rev. C 93, 064906 (2016)

${}^{3}_{\Lambda}H/\Lambda$ Compared to Thermal Model

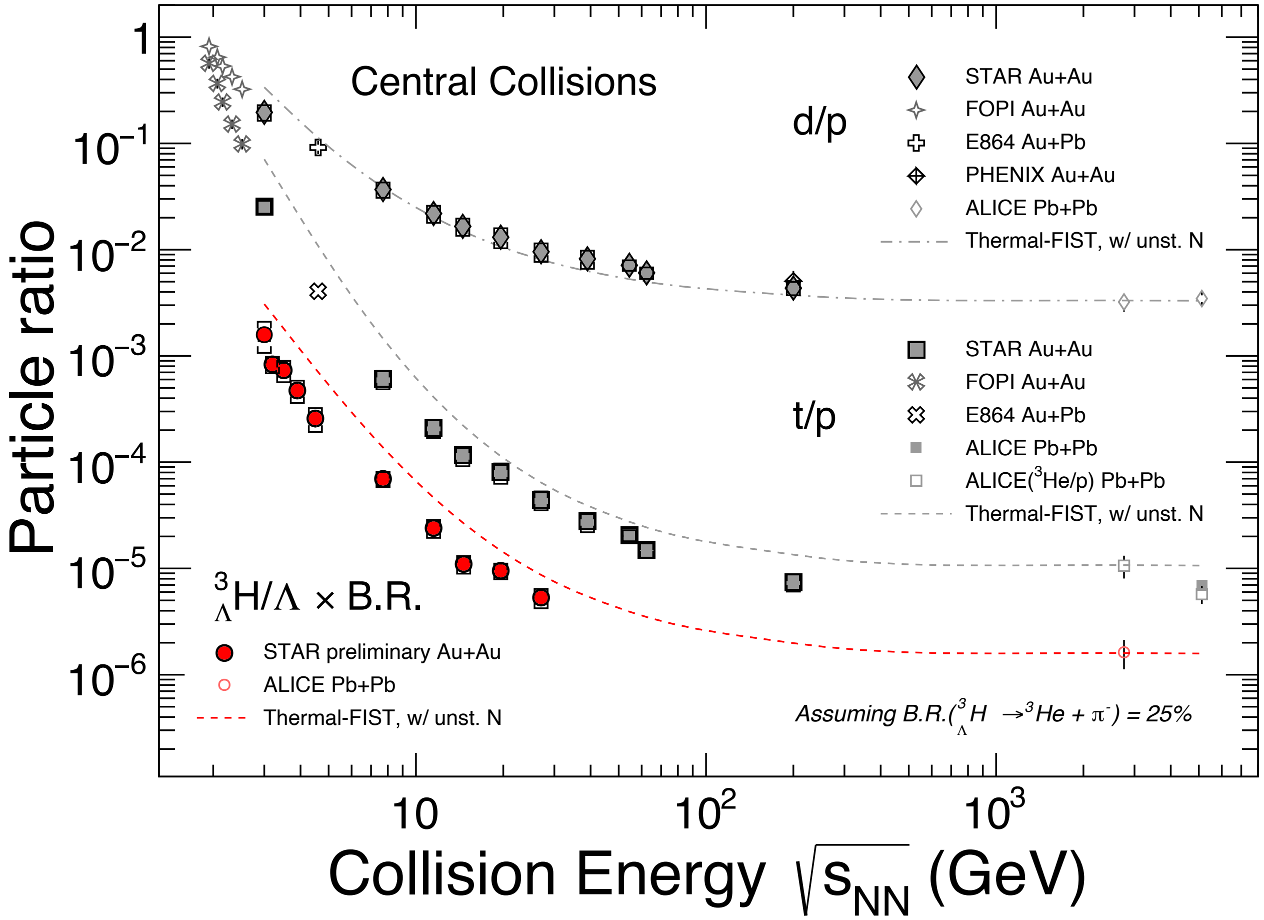

Thermal-FIST:

- Hadron chemical freeze-out T and μ_B.

T. Reichert et al, PRC 107 , 014912 (2023)

${}^{3}_{\Lambda}H/\Lambda$: Cancel strangeness canonical suppression and volume size

Thermal model at RHIC energies:
A=2 (d): Overall consistent
A=3 (t and ${}^{3}_{\Lambda}H$): ~2x higher than data

- ${}^{3}_{\Lambda}H$ (and t) maybe not in equilibrium at hadron chemical freeze out.

What happened if we decrease the temperature

- t and ${}^{3}_{\Lambda}\mathrm{H}$ -> default μ_B and 0.96*T
- Proton and Λ -> default T and μ_B
- The tuned Thermal-FIST with 0.96*T seems able to describe the data

- Note that:
  - The t and ${}^{3}_{\Lambda}\mathrm{H}$ yields modifies dramatically with the changes of temperature:

    yields ~ C*exp[-1*$(\mathrm{m_T} - \mu_B)$/T]

    m_T ~ 3 GeV for t and ${}^{3}_{\Lambda}\mathrm{H}$

    μ_B ~ 0.7 – 0.14 GeV (from 3-27 GeV)

    T ~ 0.085 – 0.155 GeV (from 3-27 GeV)

  - Because triton and ${}^{3}_{\Lambda}\mathrm{H}$ are heavy, so the impact from μ_B become less significant

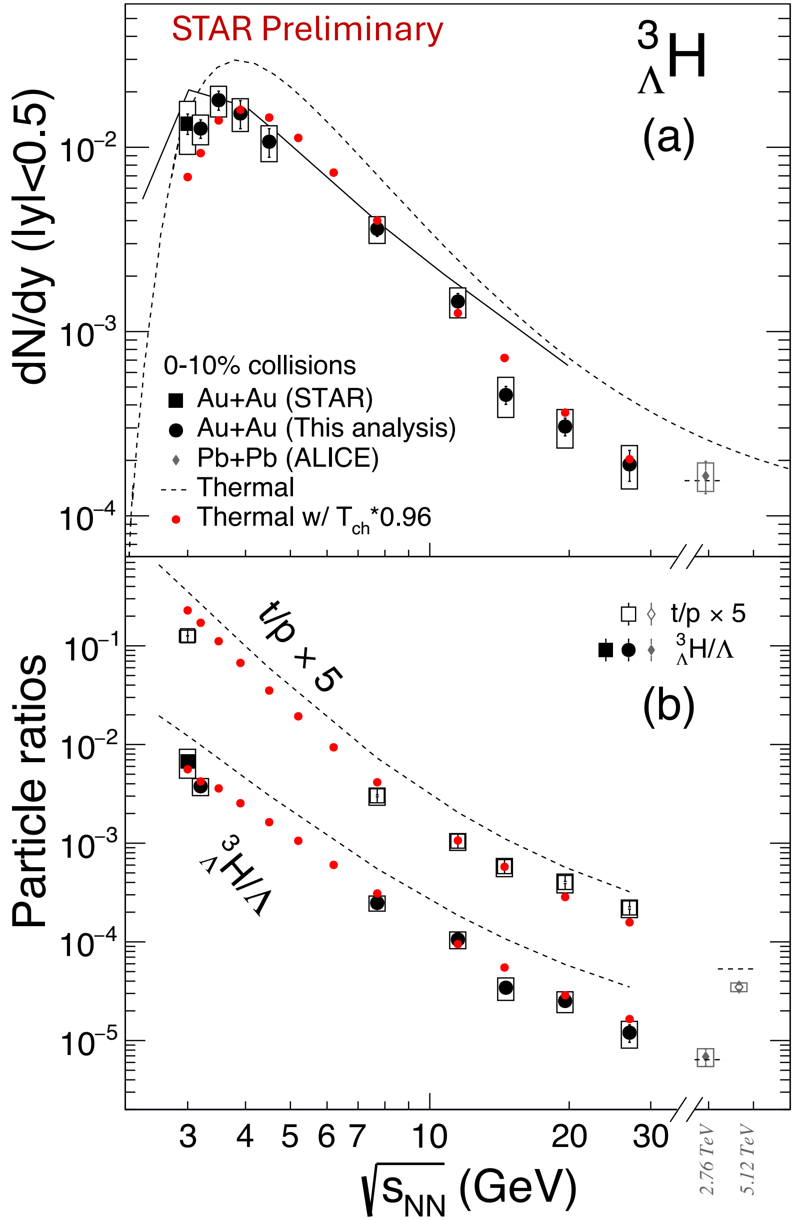

Other possible model: kinetic approch

- Relativistic kinetic equation (RKE) to include hadronic re-scattering processes.
  - Close connection to Coal. via final state interaction close to kinetic freeze-out.

P. Danielewicz et al. NPA 533 (1991) 712-748
Kaijia Sun et al, Nature Commun. 15 (2024) 1, 1074

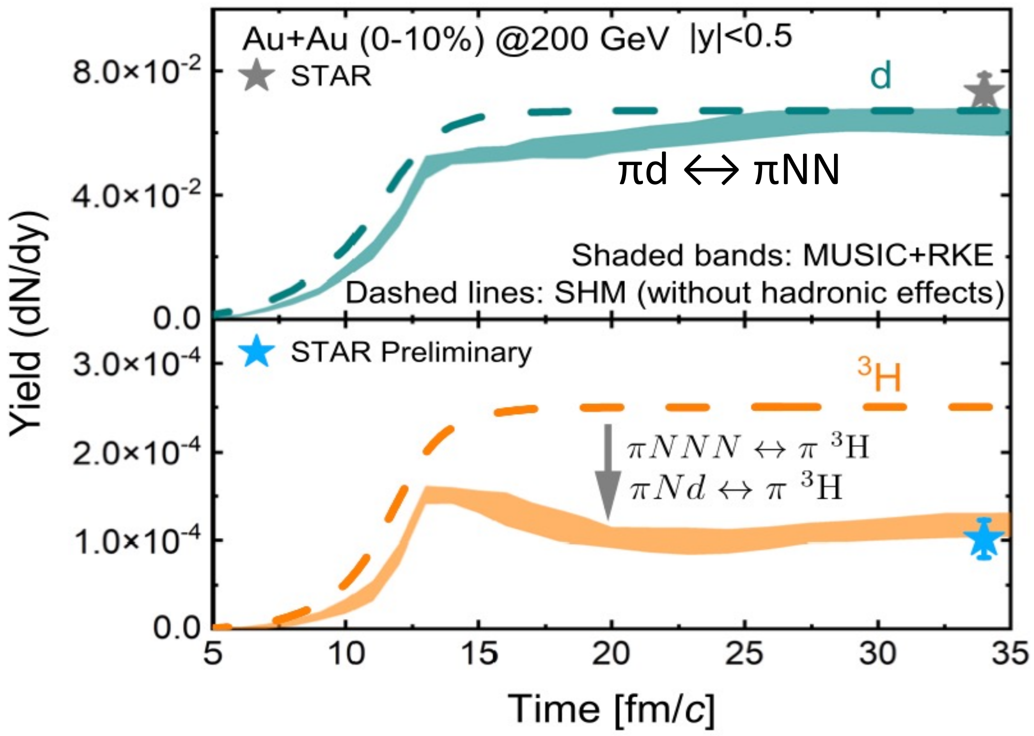

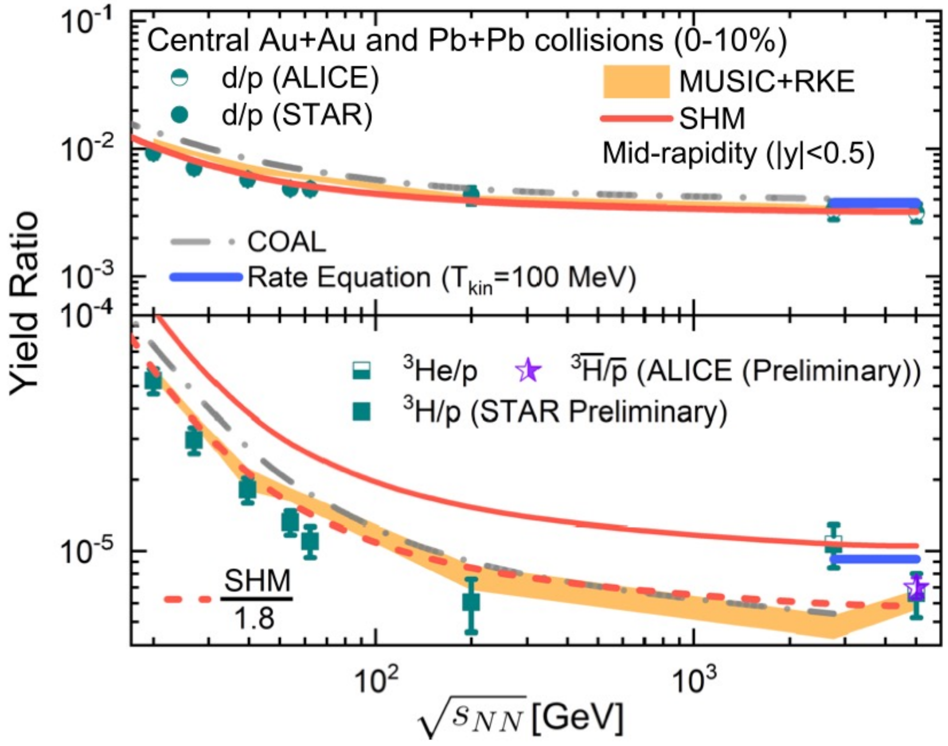

Production of ${}^{4}_{\Lambda}$H and ${}^{4}_{\Lambda}$He

${}^{4}_{\Lambda}$He: *Chenlu Hu, SQM2024*

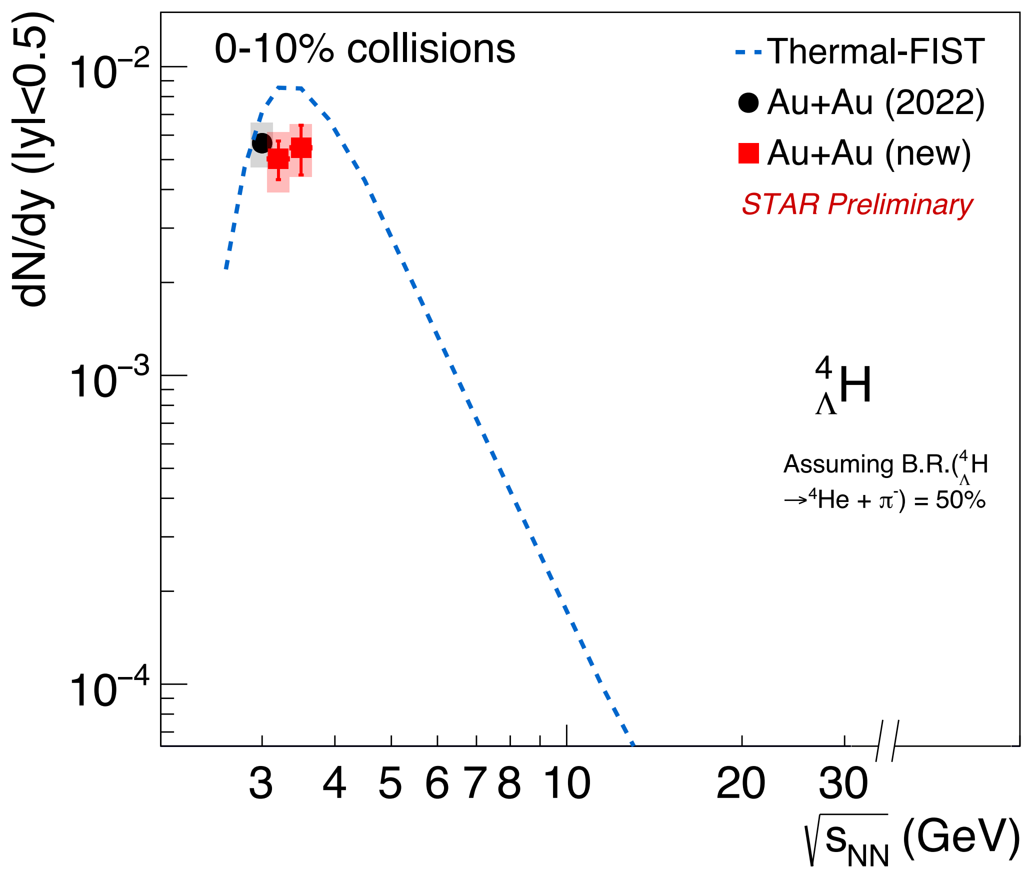

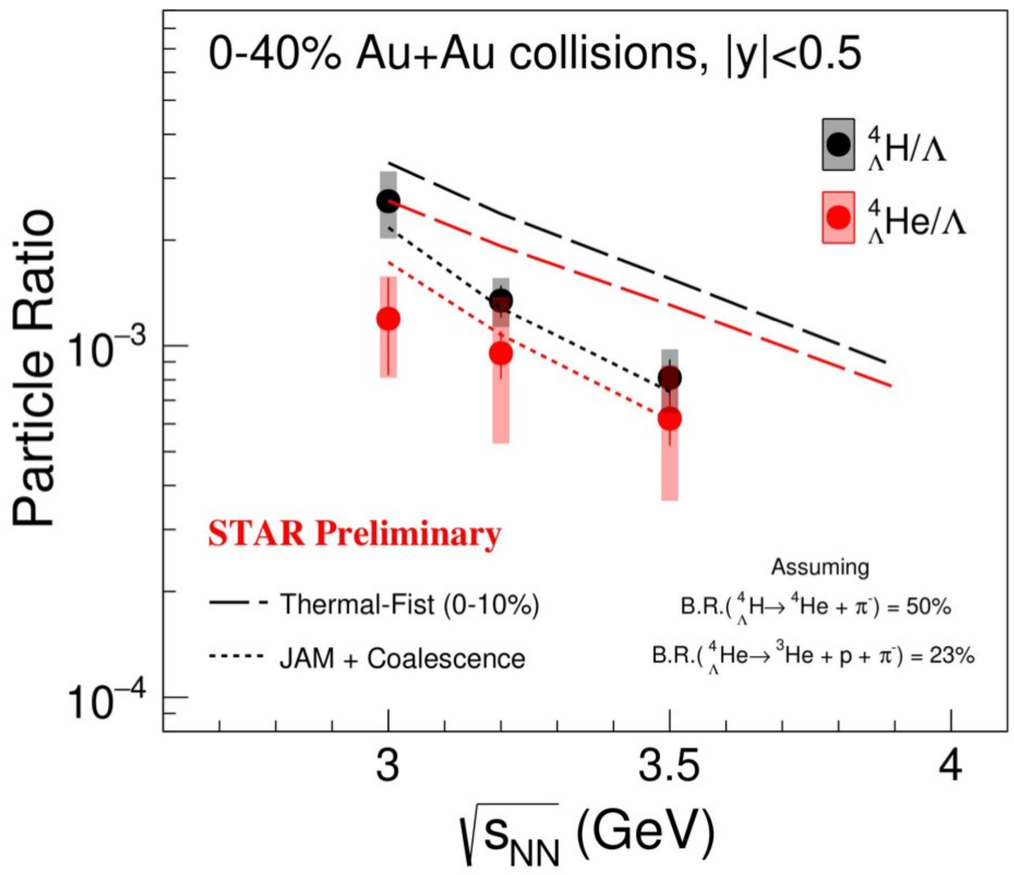

- Thermal model also over-predict ${}^{4}_{\Lambda}$H and ${}^{4}_{\Lambda}$He yields while JAM+coal. describes the data.

Thermal-FIST: T. Reichert et al, PRC 107 , 014912 (2023)

Production of ${}^4_\Lambda$H and ${}^4_\Lambda$He

Thermal expectation: $\frac{dN}{dy} \sim \exp(-\frac{m}{T})$

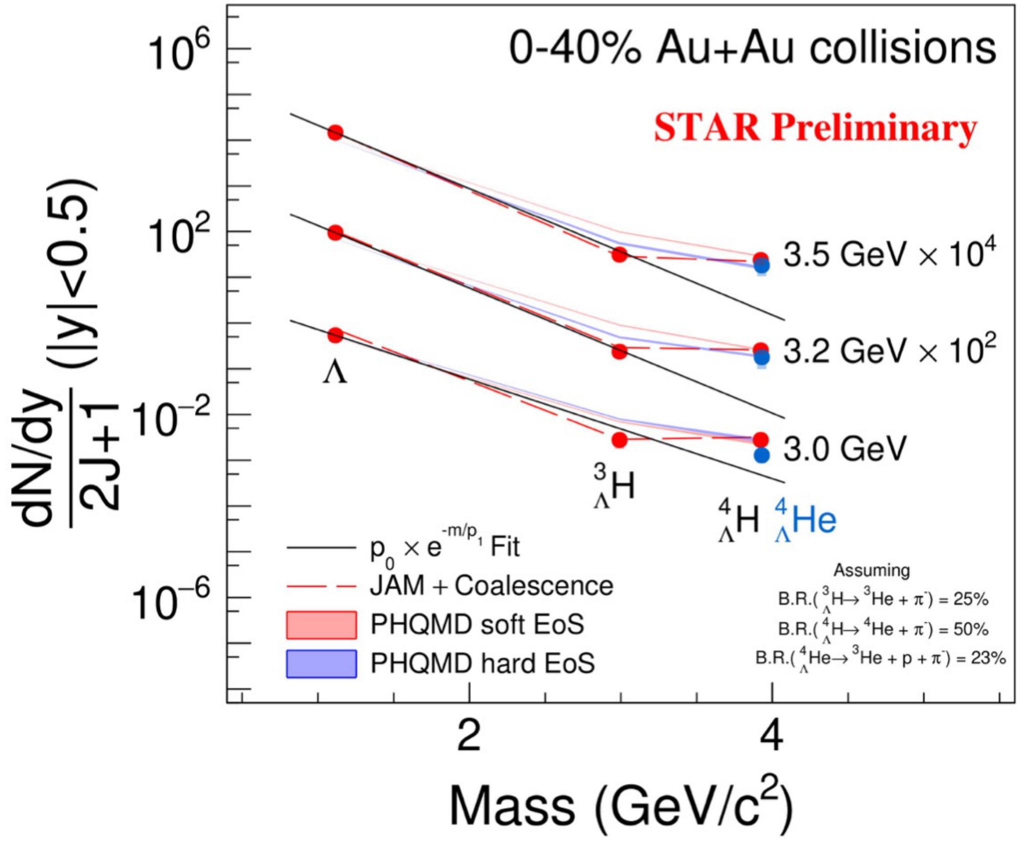

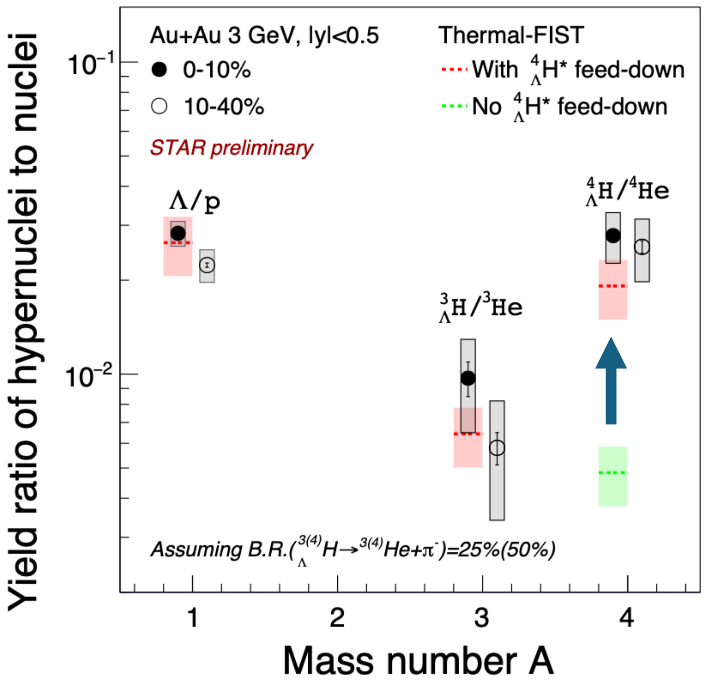

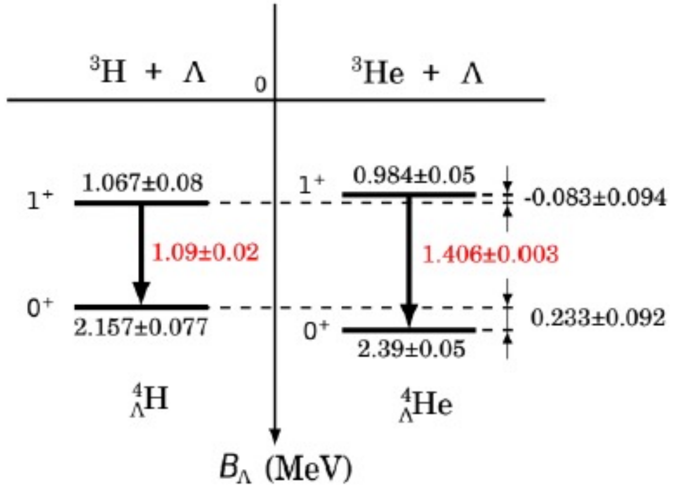

${}^4_\Lambda\mathrm{H}^*(J^+ = 1) \rightarrow {}^4_\Lambda\mathrm{H}(J^+ = 0) + \gamma$

PHQMD: S. Gläßel et al. PRC 105, 014908 (2022)

- Evidence of the formation of ${}^4_\Lambda$H and ${}^4_\Lambda$He excited states in 3-4 GeV collisions.

Energy Dependence of ${}^{3}_{\Lambda}\mathrm{H}\ \langle p_T \rangle$

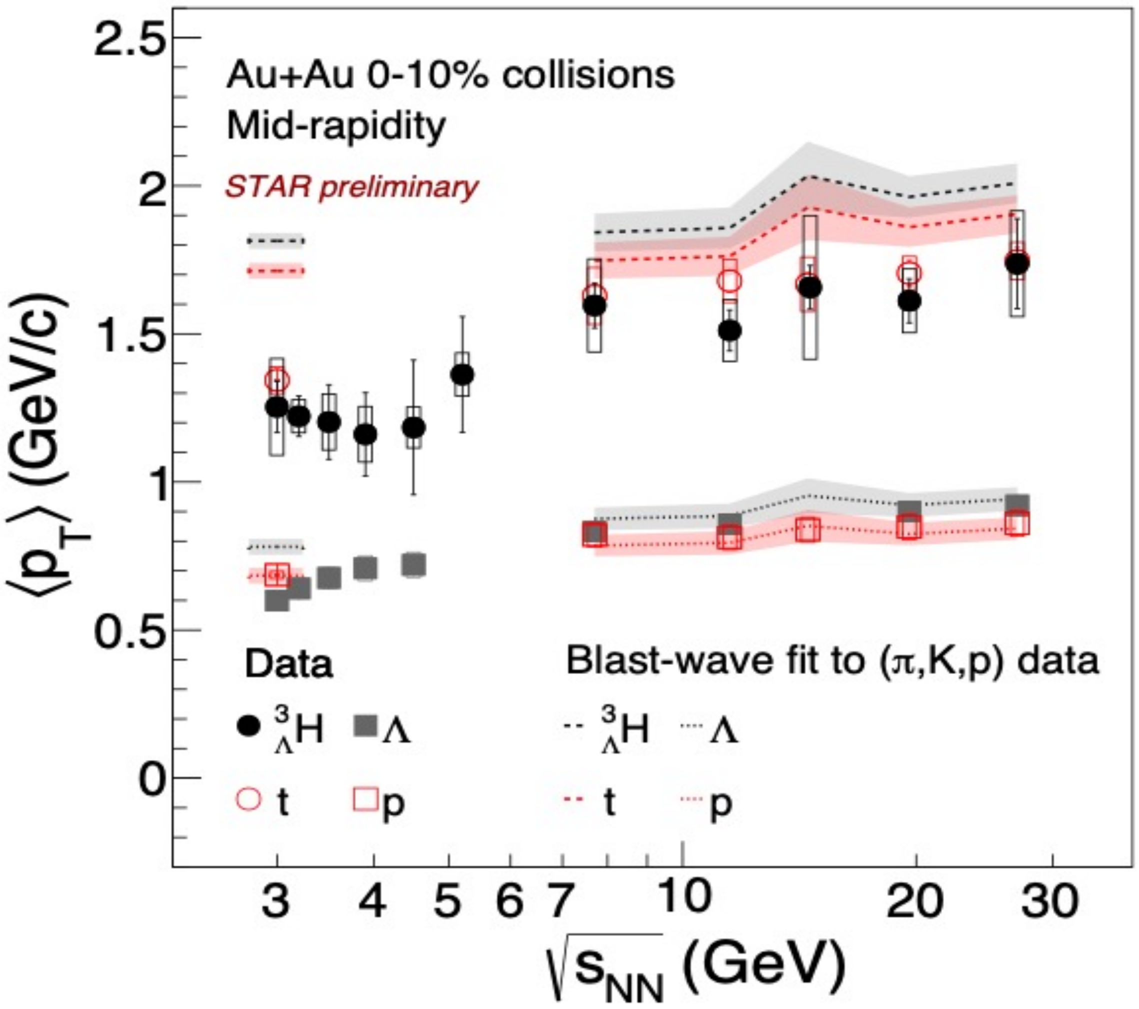

- ${}^{3}_{\Lambda}\mathrm{H}$ and t $\langle p_T \rangle < \langle p_T \rangle^{BW}$ at 3 GeV
- Hint of ${}^{3}_{\Lambda}\mathrm{H}$ and t $\langle p_T \rangle < \langle p_T \rangle^{BW}$ > 7.7 GeV
  - $\langle p_T \rangle^{BW}$: Blast-wave (BW) expectation calculated using kinetic freeze-out parameters from measured light hadron (π, K, p) spectra.

Blastwave function:

$$\frac{1}{2\pi p_T}\frac{d^2N}{dp_T dy} \propto \int_0^R r dr m_T I_0\left(\frac{p_T \sinh\rho(r)}{T_{kin}}\right) \times K_1\left(\frac{m_T \cosh\rho(r)}{T_{kin}}\right)$$

${}^{3}_{\Lambda}\mathrm{H}$ and t might do not follow the same collective expansion as light hadrons.

STAR, Phys. Rev. C 102 (2020) 34909; Phys. Rev. C 96 (2017) 44904

Hypernuclei Collectivity versus Mass

$\langle p_T \rangle$ -> Radial flow contributions

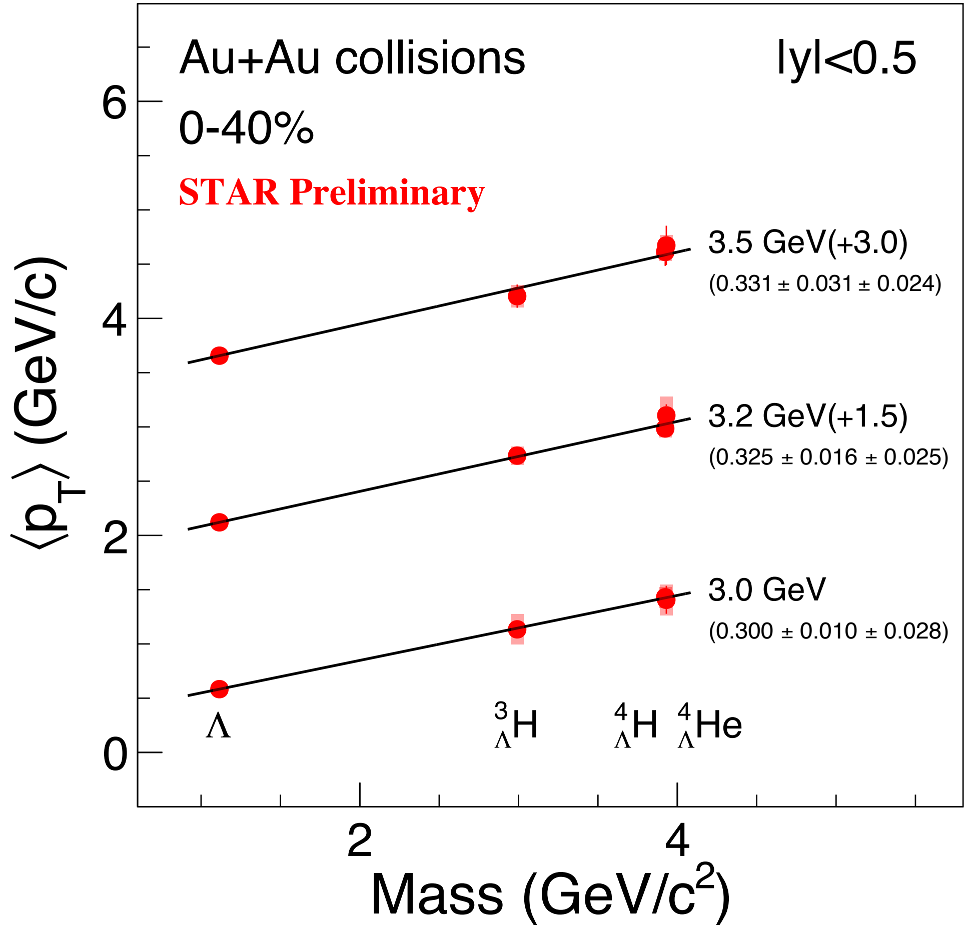

v_1 -> Directed flow

$$E\frac{d^3N}{dp^3} = \frac{1}{2\pi}\frac{d^2N}{p_T dp_T dy}\left(1 + \sum_1^{\infty} 2v_n \cos\left[n\left(\phi - \psi_{RP}\right)\right]\right)$$

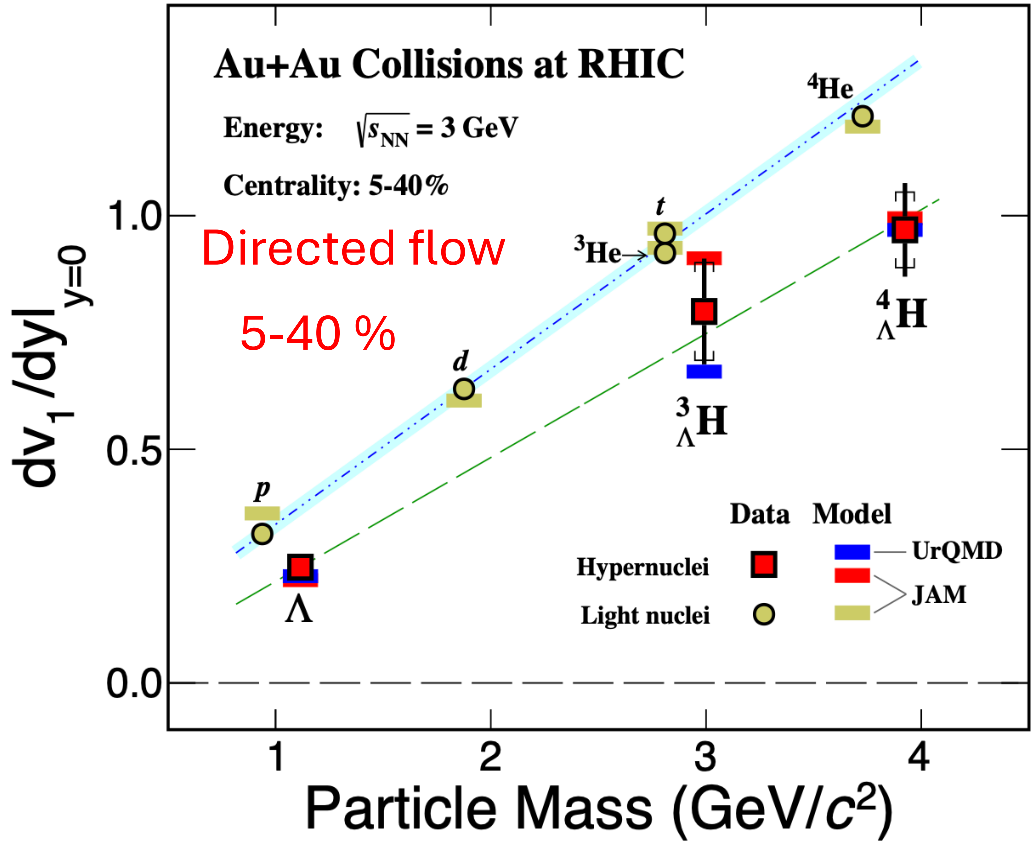

STAR, PRL 130 (2023) 212301

- Hypernuclei $\langle p_T \rangle$ (and v_1) show linear mass scaling from 3 to 3.5 GeV in mid-rapidity.
  - Consistent with coalescence formation picture.

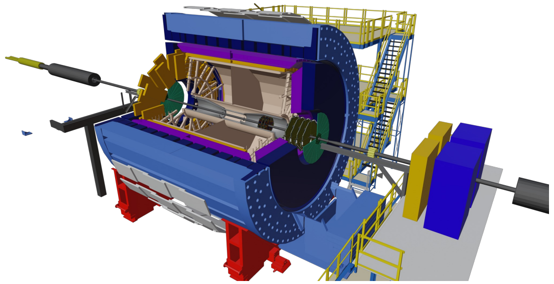

Multiplicity Dependence of Hypernuclei Production

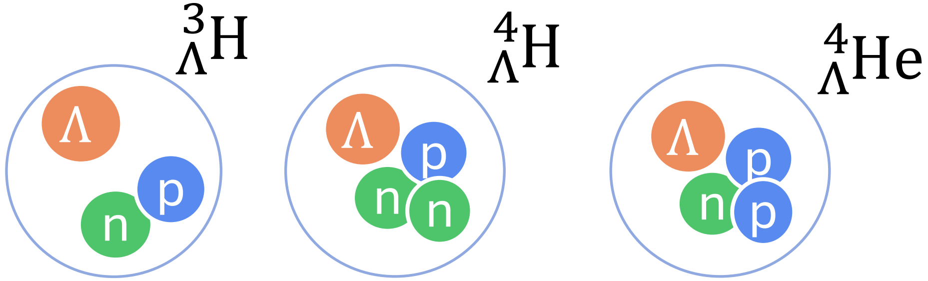

Strangeness Population Factor (S_A)

$$S_A = \frac{{}^{A}_{\Lambda}\mathrm{H}(A \times p_T)}{{}^{A}\mathrm{He}(A \times p_T) \times \frac{\Lambda}{p}(p_T)} = \frac{B_A({}^{A}_{\Lambda}\mathrm{H})(p_T)}{B_A({}^{A}\mathrm{He})(p_T)}$$

S. Zhang et al, PLB 684, 224 (2010)

- S_A: Direct connection to coalescence parameters B_A

F. Bellini, PRC 99, 054905 (2019)

$$E_A \frac{d^3 N_A}{dp_A^3} = B_A \left(E_{p,n} \frac{d^3 N_{p,n}}{dp_{p,n}^3} \right)^A \Bigg|_{\vec{p}_p = \vec{p}_n = \frac{\vec{p}_A}{A}}$$

Under some coalescence scenarios:

$$B_A = \frac{2J_A + 1}{2^A} \frac{1}{\sqrt{A}} \frac{1}{m_T^{A-1}} \left(\frac{2\pi}{R^2 + (\frac{r_A}{2})^2} \right)^{\frac{3}{2}(A-1)}$$

Emit source size Radius

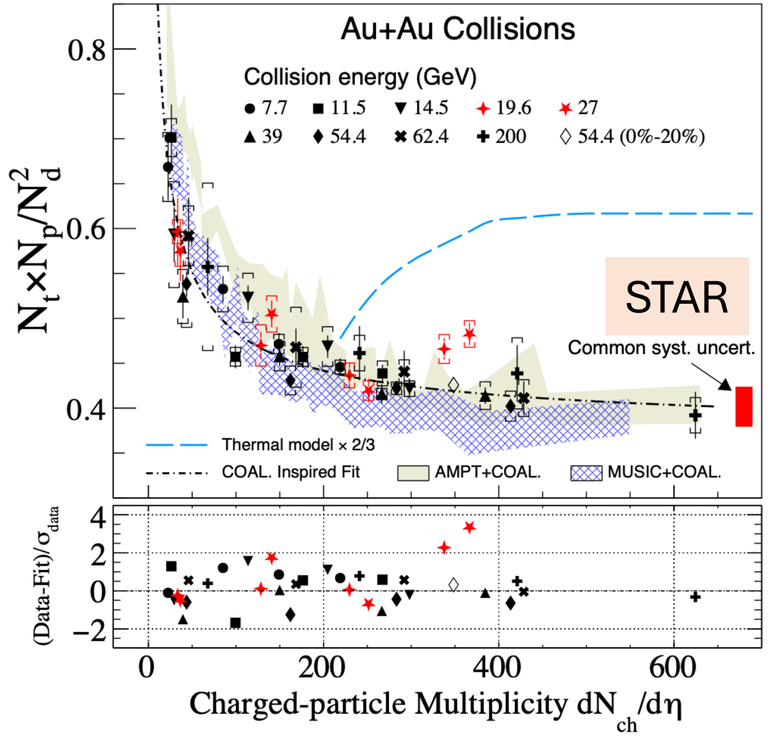

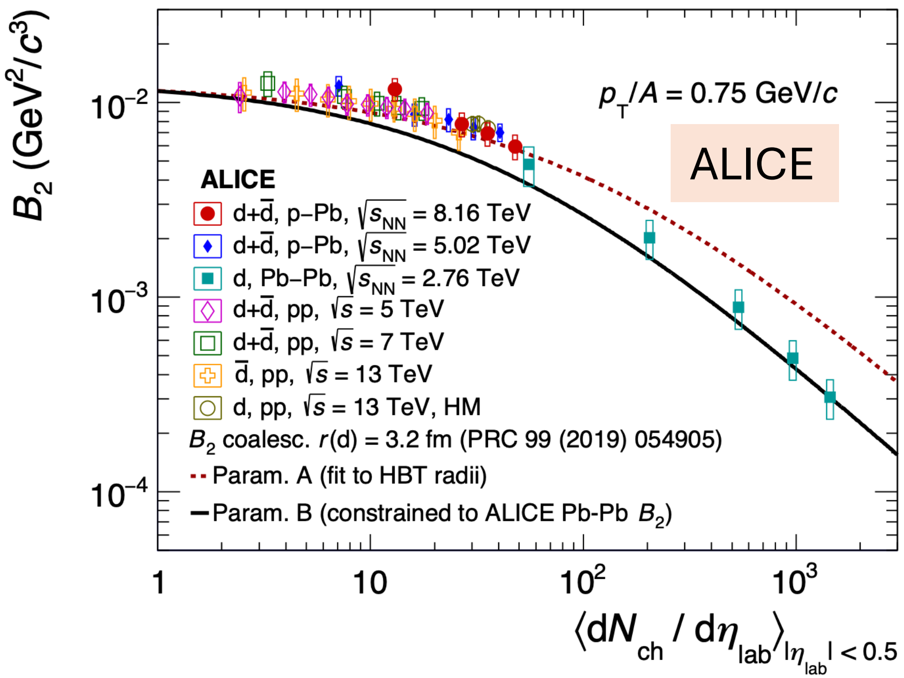

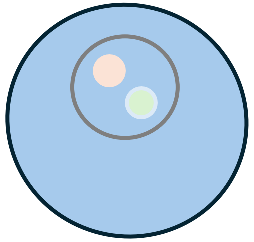

Emit source

Phys. Rev. Lett. 130, 202301 (2023)

Strangeness Population Factor (S_A)

$$S_A = \frac{{}^{A}_{\Lambda}\mathrm{H}(A \times p_T)}{{}^{A}\mathrm{He}(A \times p_T) \times \frac{\Lambda}{p}(p_T)} = \frac{B_A({}^{A}_{\Lambda}\mathrm{H})(p_T)}{B_A({}^{A}\mathrm{He})(p_T)}$$

S. Zhang et al, PLB 684, 224 (2010)

- S_A: Direct connection to coalescence parameters B_A
- S_3 vs. $dN_{ch}/d\eta$: Possible insights to ${}^{3}_{\Lambda}\mathrm{H}$ radius and coalescence mechanism

T. Reichert et al, PRC 107, 014912 (2023)

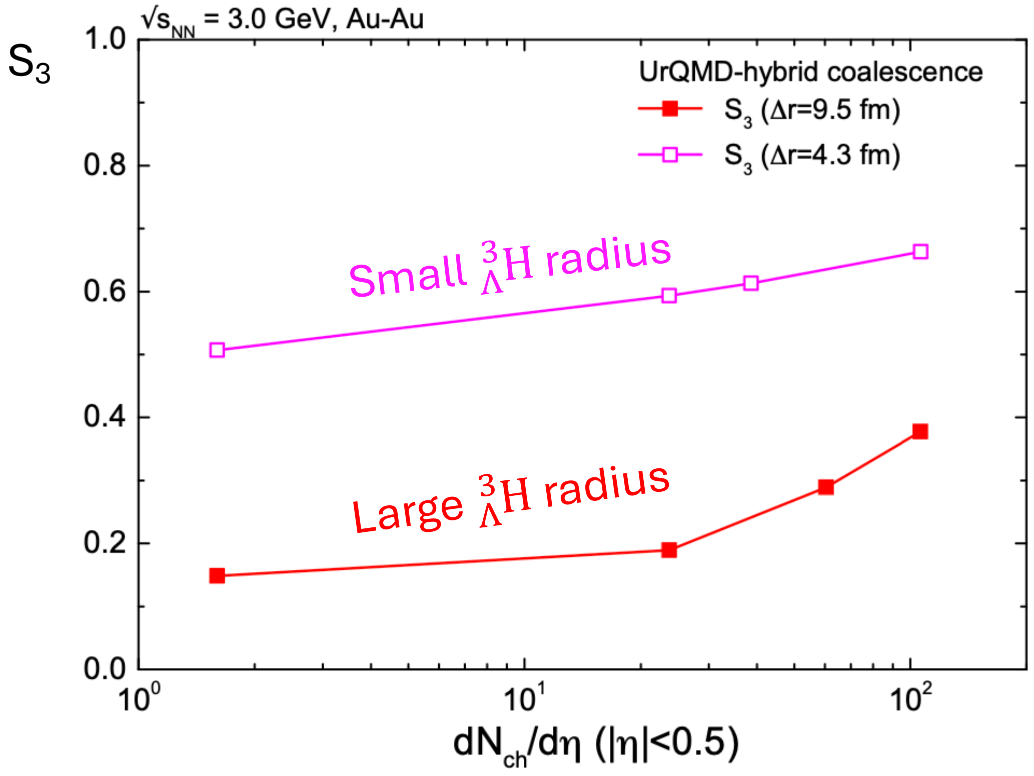

K. Jia. PLB 792 (2019) 132-137

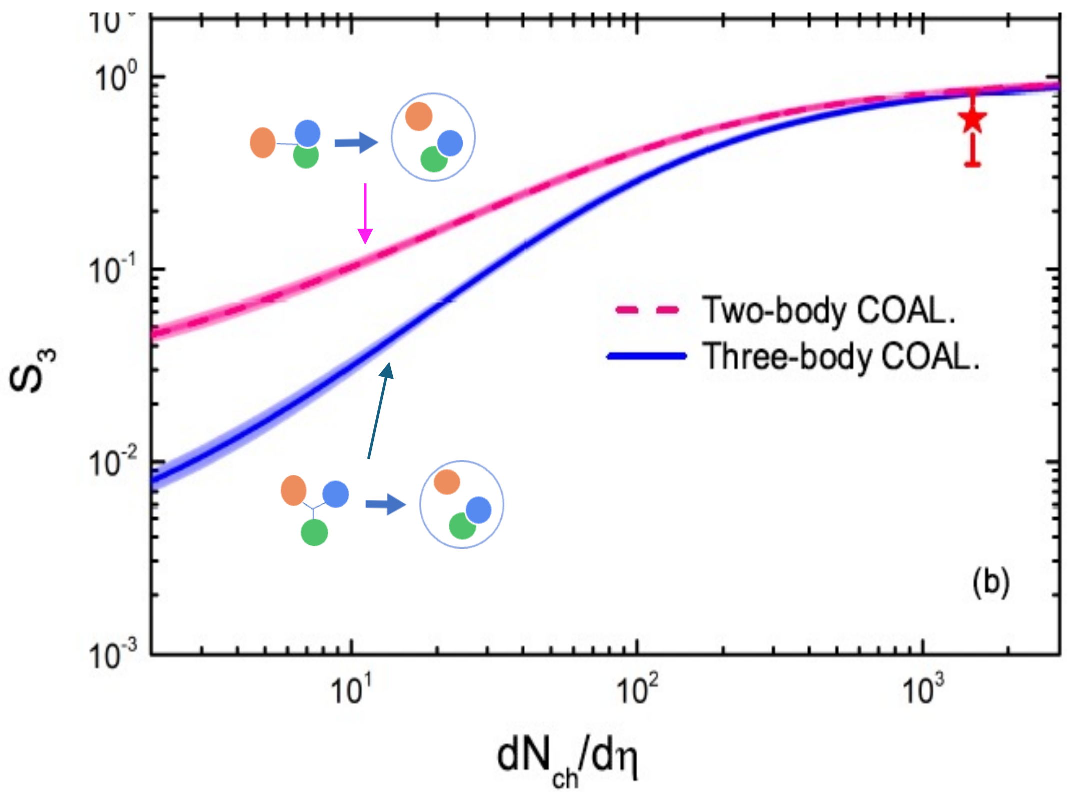

S_3 and S_4 in Au+Au 3 GeV

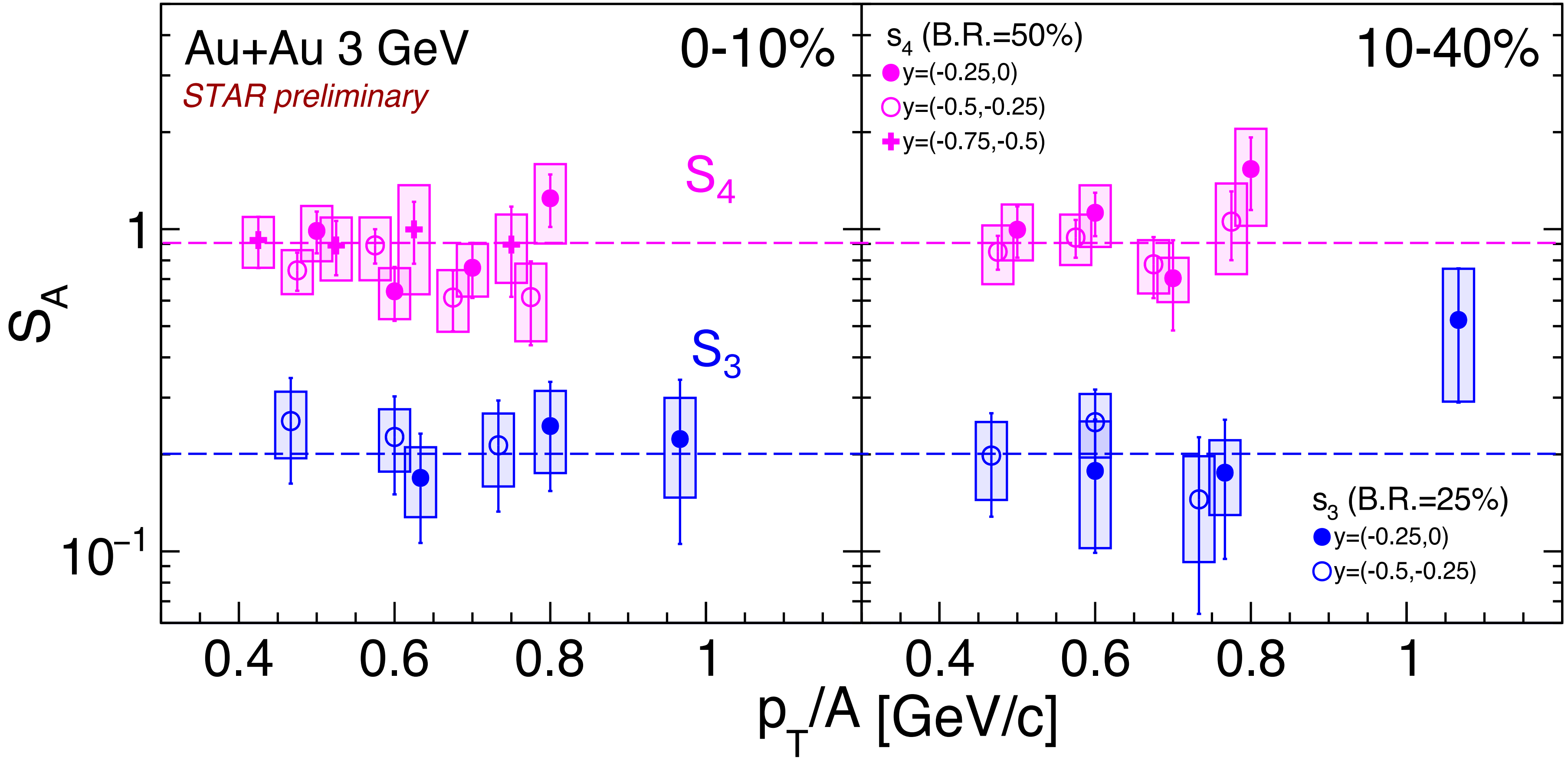

$$S_A = \frac{{}^{A}_{\Lambda}H(A\times p_T)}{{}^{A}_{\Lambda}He(A\times p_T)\times\frac{\Lambda}{p}} = \frac{B_A({}^{A}_{\Lambda}H)(p_T)}{B_A({}^{A}He)(p_T)}$$

- No obvious p_T, rapidity and centrality dependence of S_A observed at 3 GeV
  - Evidence that B_A of light and hyper nuclei follow similar tendency versus p_T, rapidity and centrality

System Size Dependence of S_3

STAR COL data: Yue Hang Leung, CPOD2024

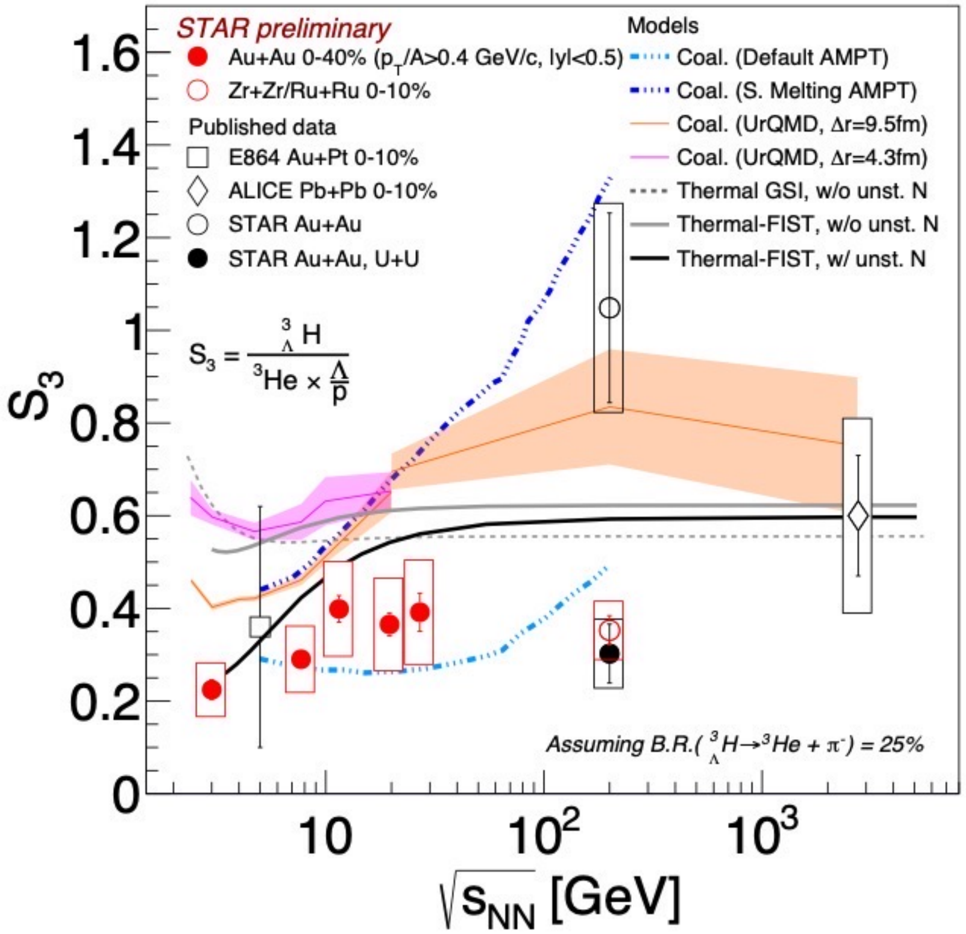

$$S_A = \frac{{}^{A}_{\Lambda}\mathrm{H}(A \times p_T)}{{}^{A}\mathrm{He}(A \times p_T) \times \frac{\Lambda}{p}(p_T)}$$

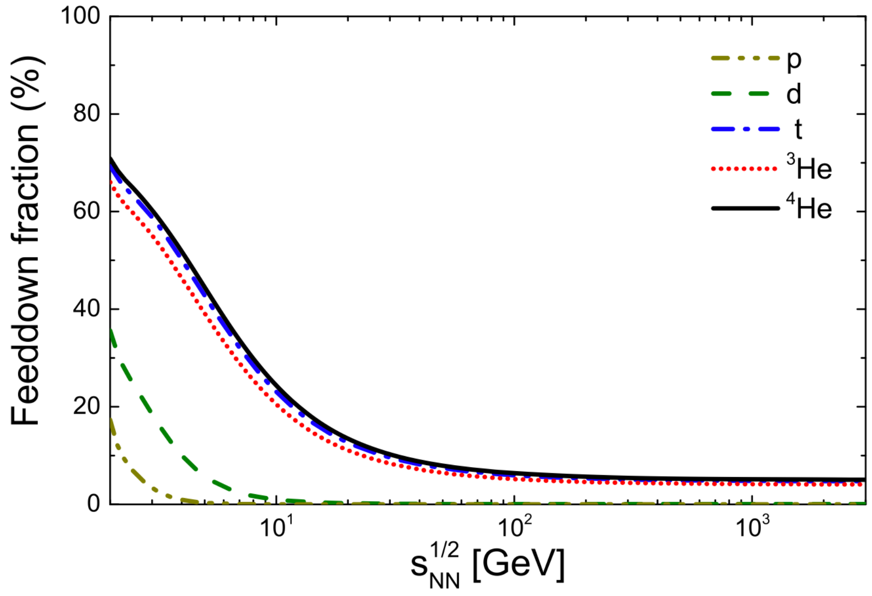

V. Vovchenko, PLB (2020) 135746

- Increasing trend observed in S_3 vs collisions energy.
  - Possibly due to stronger feed down contribution in lower energies.

System Size Dependence of S_3

STAR COL data: Yue Hang Leung, CPOD2024

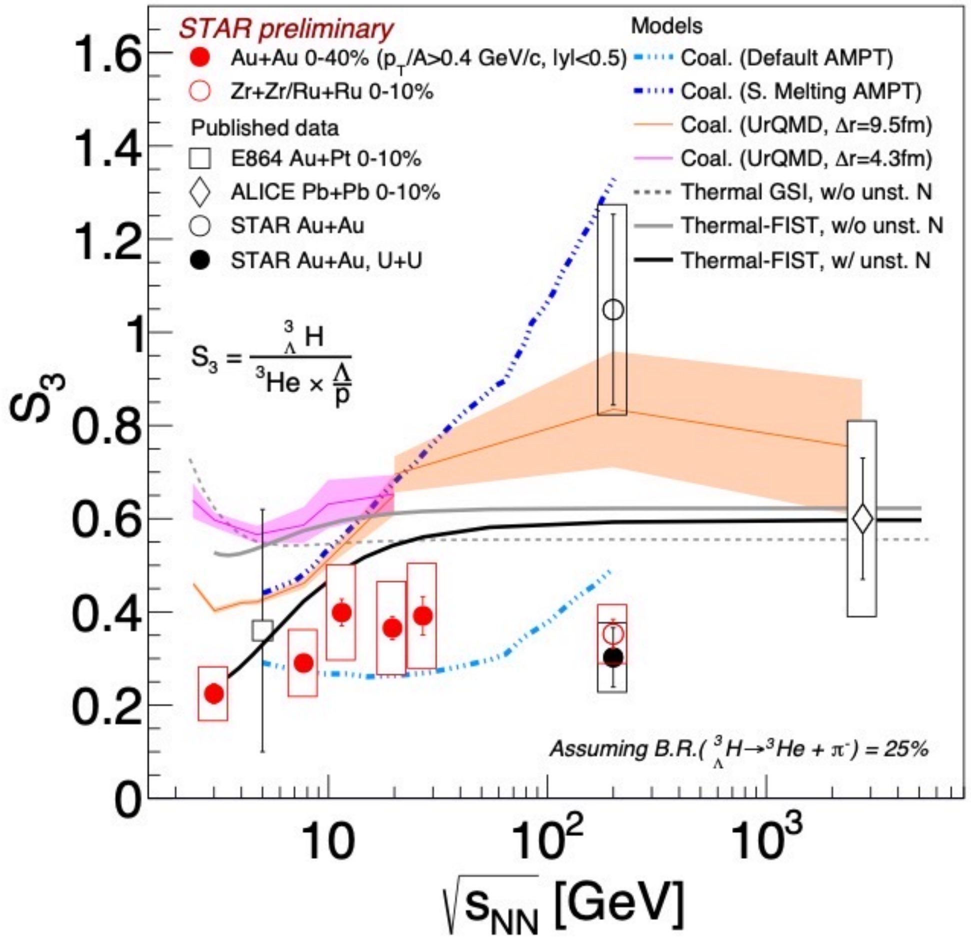

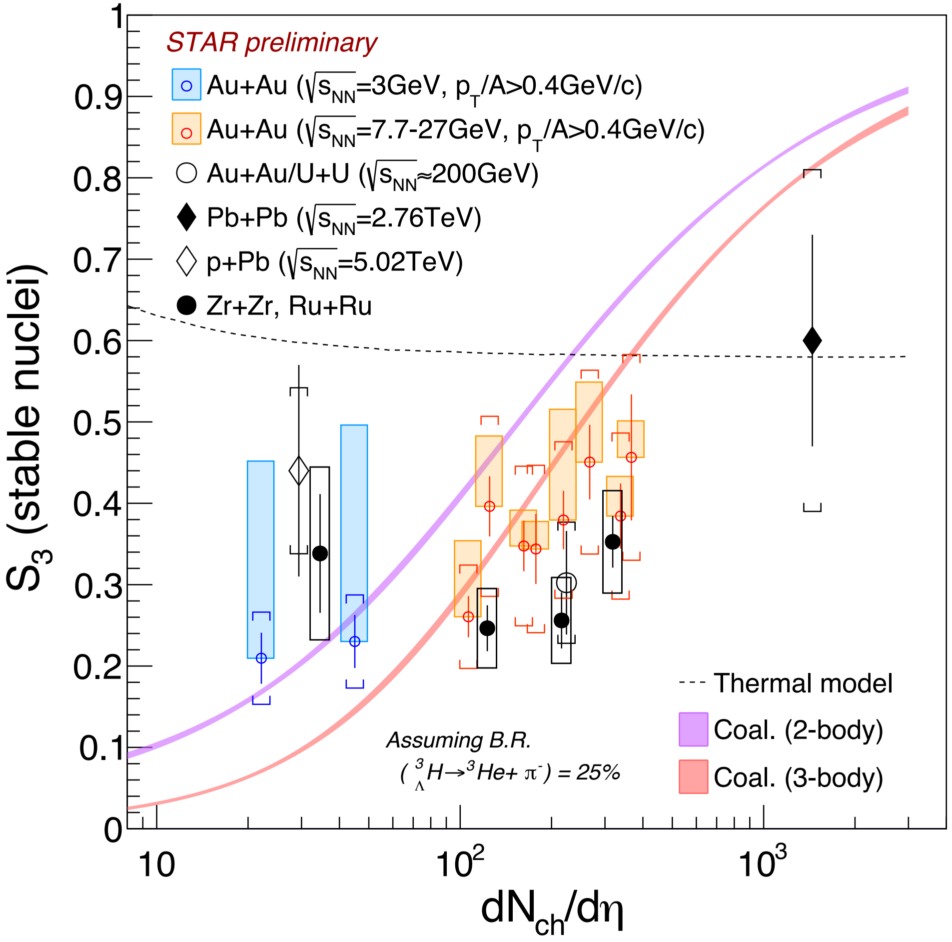

- Increasing trend observed in S_3 vs collisions energy.
  - Possibly due to stronger feed down contribution in lower energies.
- S_3 vs. $dN_{ch}/d\eta$: coalescence model describes the data within uncertainties.

V. Vovchenko, PLB (2020) 135746

Summary

New experimental data on:

- ${}^{3}_{\Lambda}\mathrm{H}$ in 3.0 – 27 GeV Au+Au collisions
- ${}^{4}_{\Lambda}\mathrm{H}$, ${}^{4}_{\Lambda}\mathrm{He}$ in 3.0 – 3.5 GeV Au+Au collisions
- ${}^{3}_{\Lambda}\mathrm{H}$ in 200 GeV Zr+Zr/Ru+Ru collisions

- Experimental data support **coalescence is a dominate mechanism** of hypernuclei formation at mid-rapidity in heavy-ion collisions at RHIC.
- Hypernuclei **are not in equilibrium** at hadron chemical freeze-out at RHIC energies.

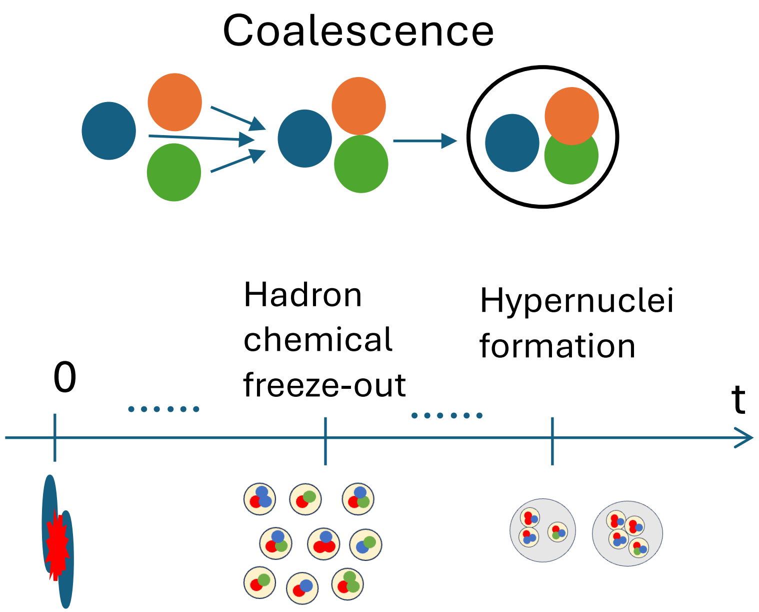

What's Next at RHIC?

Huge datasets from BES-II and 200 GeV Au+Au collisions at RHIC.
- Enable measurements on both high μ_B and $\mu_B \to 0$ region.

BES II datasets

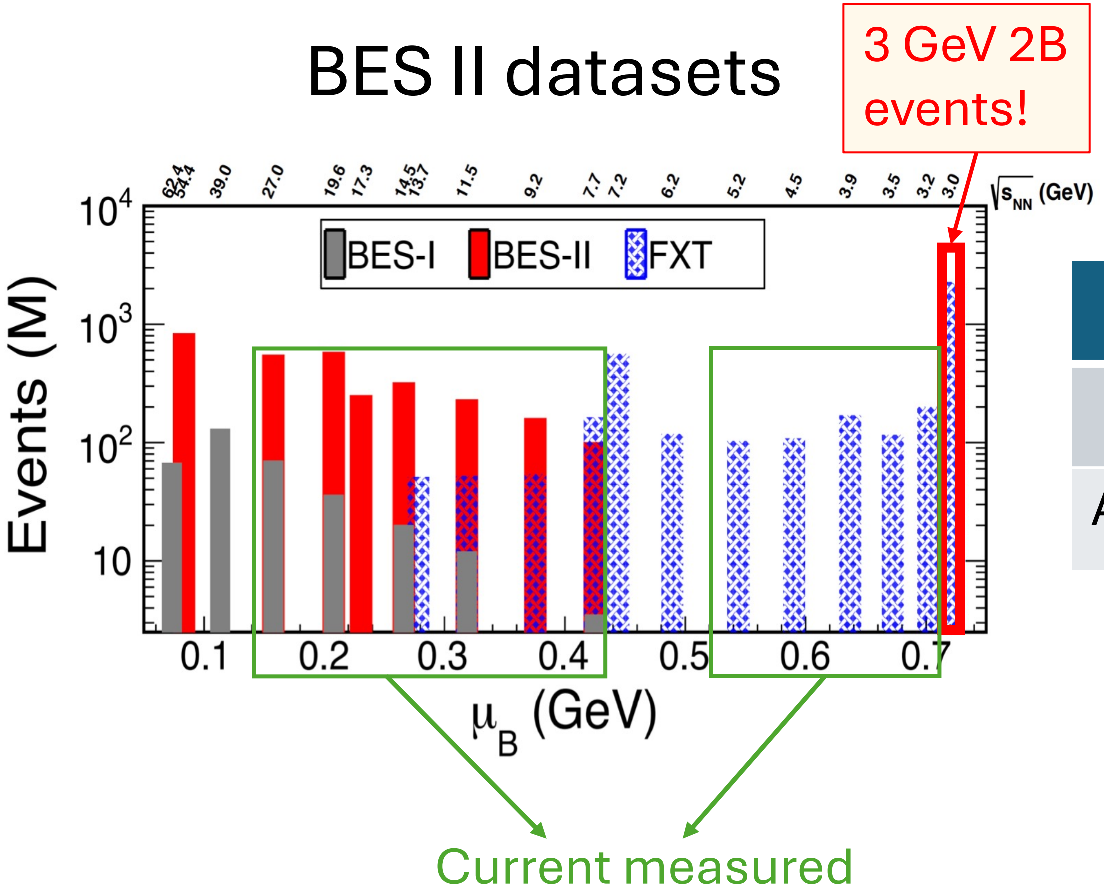

High energy runs in 2023-2025

System	Run year	No. events/Luminosity
p+p 200 GeV	2024	235 pb^{-1}
Au+Au 200 GeV	2023+2025	20B / 40 nb^{-1}

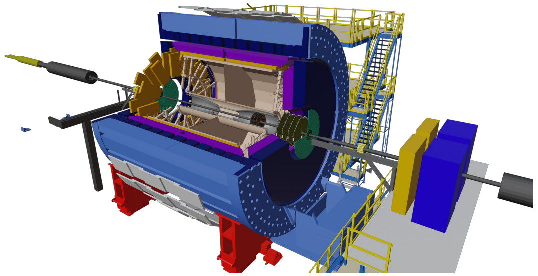

STAR

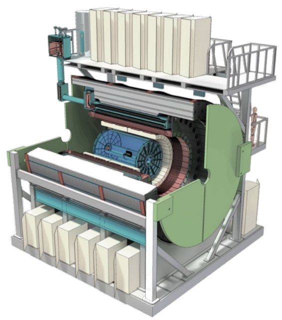

sPHENIX

What's Next at RHIC?

Huge datasets from BES-II and 200 GeV Au+Au collisions at RHIC.
- Enable measurements on both high μ_B and $\mu_B \rightarrow 0$ region.

BES II datasets

3 GeV 2B events!

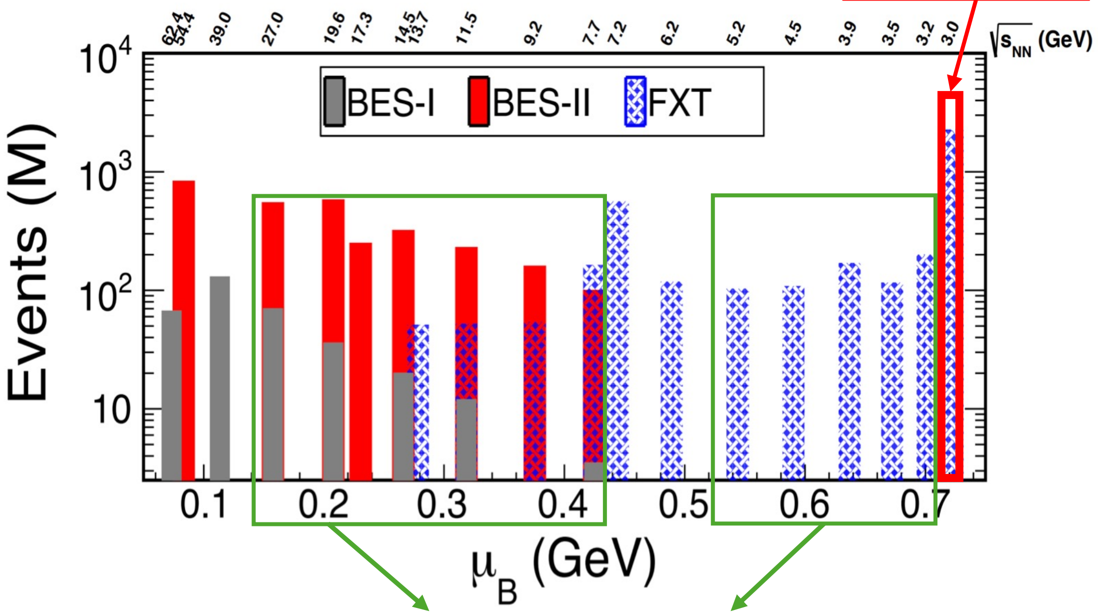

Current measured

Expected total significance from BES-II:

${}^{4}_{\Lambda}$H : 60σ; ${}^{4}_{\Lambda}$He: 40σ; ${}^{5}_{\Lambda}$He: 10σ

- ${}^{3}_{\Lambda}\mathrm{H}\ R_3$

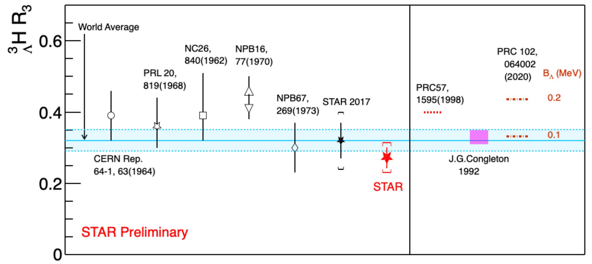

- Global polarization arXiv:2405.12015

Spin structures

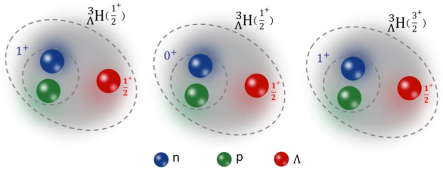

- Kenimatics

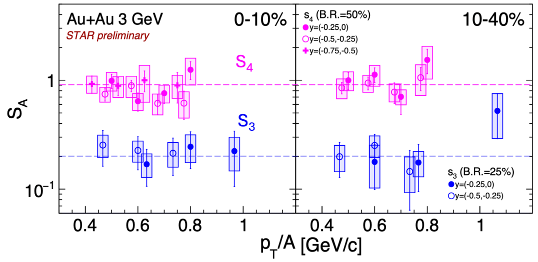

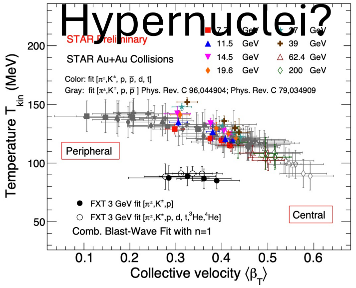

- Ξ^- and double-Λ hypernuclei

Future Perspective

Great potential for discovering unobserved hypernuclei in heavy ion collisions.

- A>=5 and Ξ hypernuclei
- Anti-hypernuclei
- Exotic strangeness states and double Λ hypernuclei
- etc

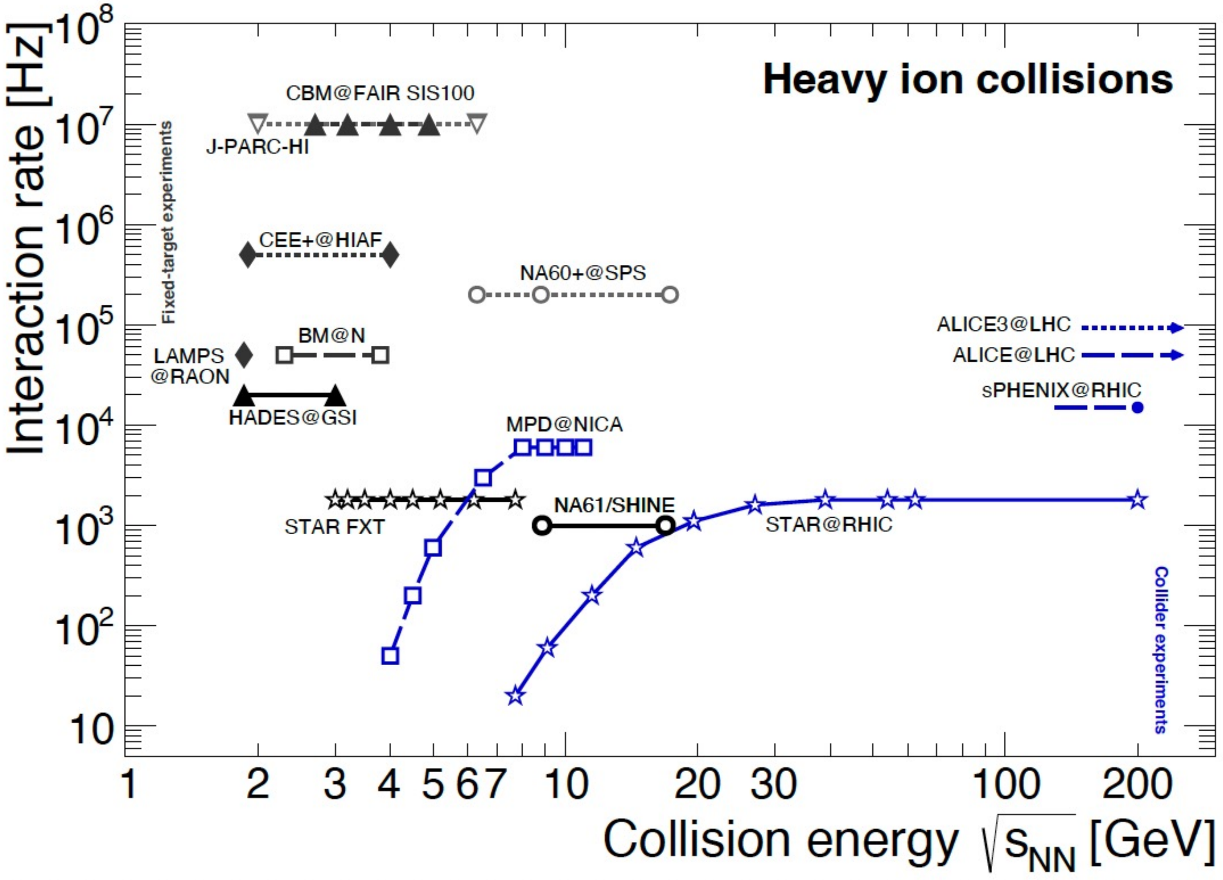

T. Galatyuk, NPA 982 (2019)

Thermal prediction

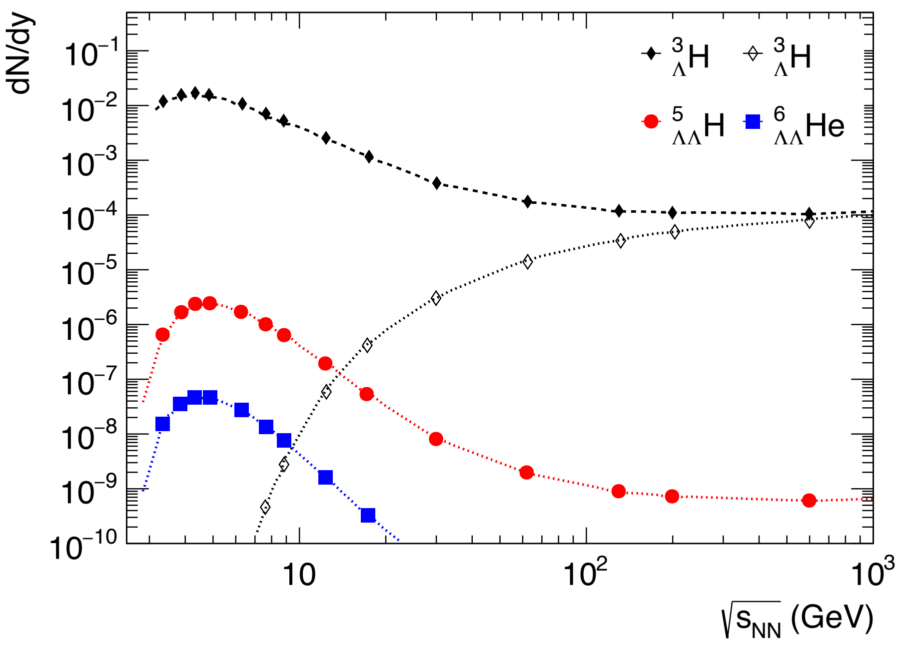

Thermal model: B. Dönigus, Eur. Phys. J. A 56:280 (2020)
A. Andronic et al, PLB 697, 203 (2011)

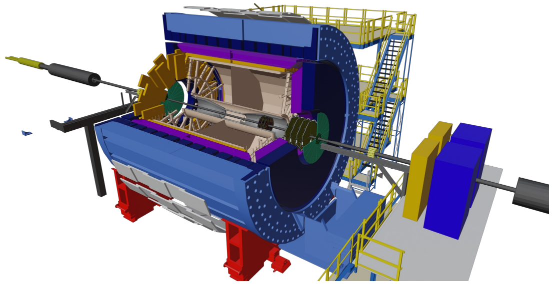

Thank you!

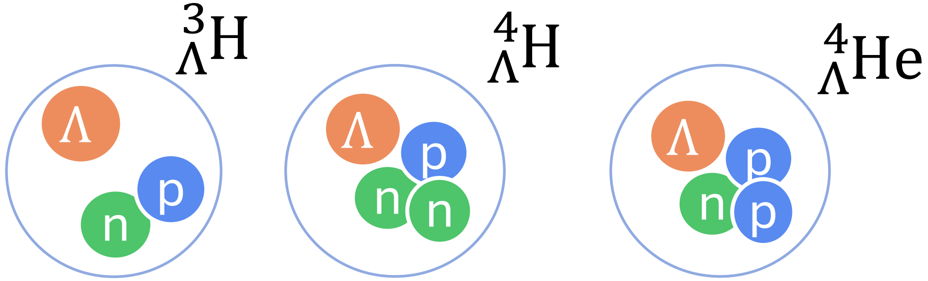

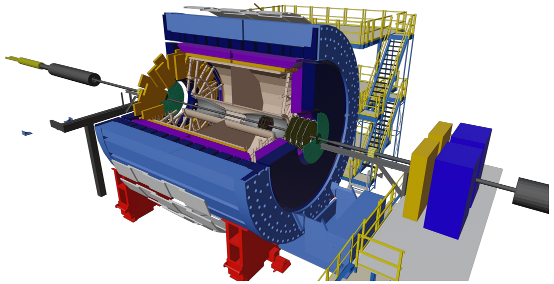

Back ups

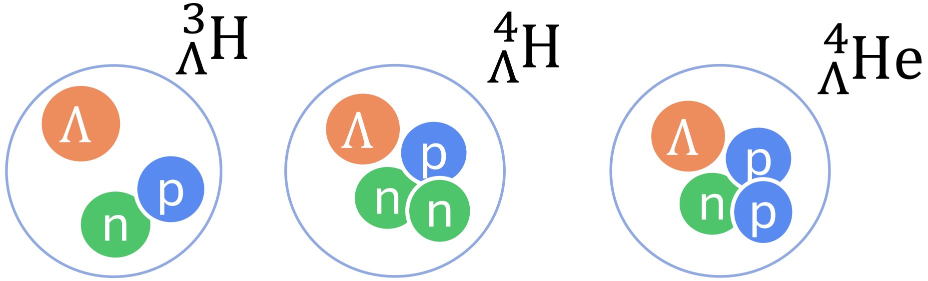

$^{3}_{\Lambda}H$ reconstruction

- Decay channel:
  $^{3}_{\Lambda}H \rightarrow {}^{3}He\,\pi^{-}$ ~ B.R. 20-25%,
  $^{3}_{\Lambda}H \rightarrow dp\pi^{-}$ ~B.R. ~ 40-50%,
- Backgrounds reconstructed by rotation of ^{3}He.

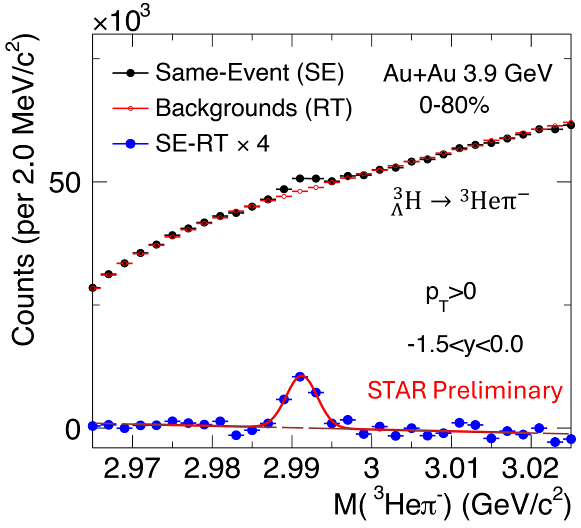

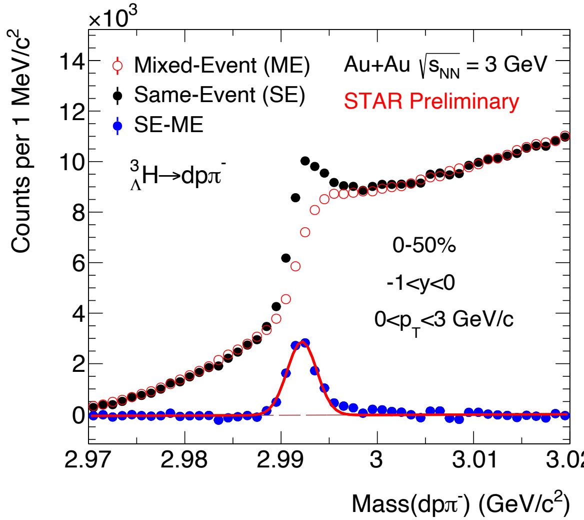

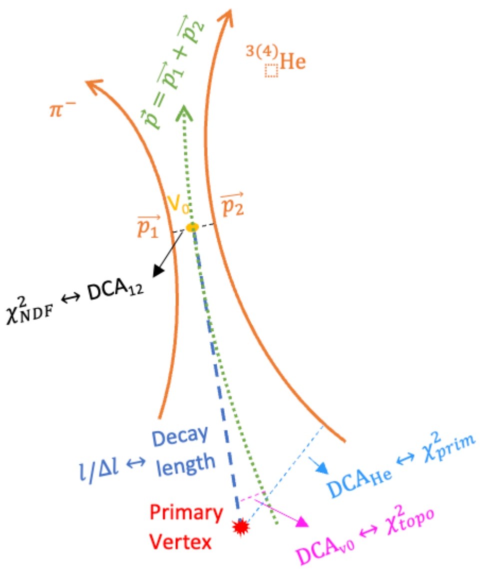

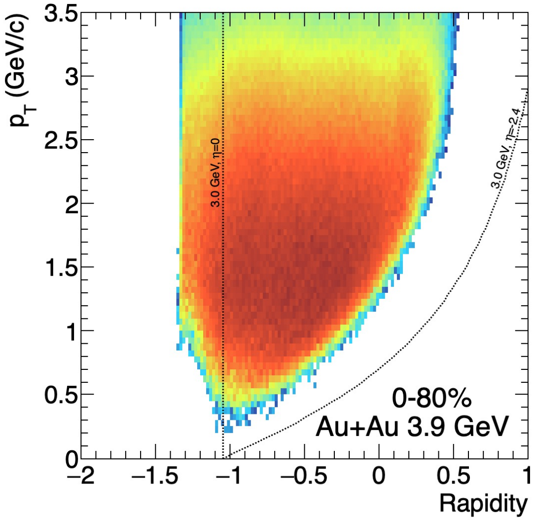

2-body decay phase space

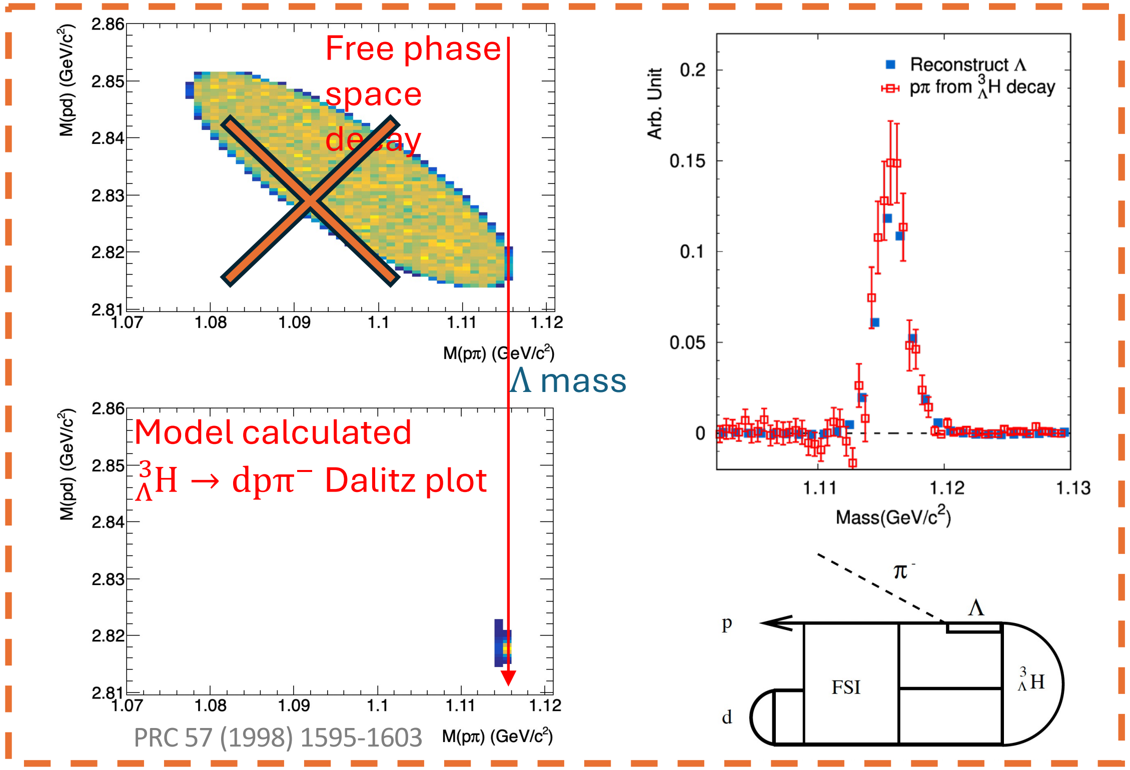

Hypernuclei reconstruction at STAR

- Signals are reconstructed by **KFParticle package.**
  - Based on Kalman Filter method.
  - All particles are described by
    - State vectors
    - Covariance matrix.
  - Benefit from:
    - Secondary vertex reconstruction
    - Reconstructing multiple particles at the same time.

X. Ju et al. Nucl. Sci. Tech. 34, 10, 158 (2023)

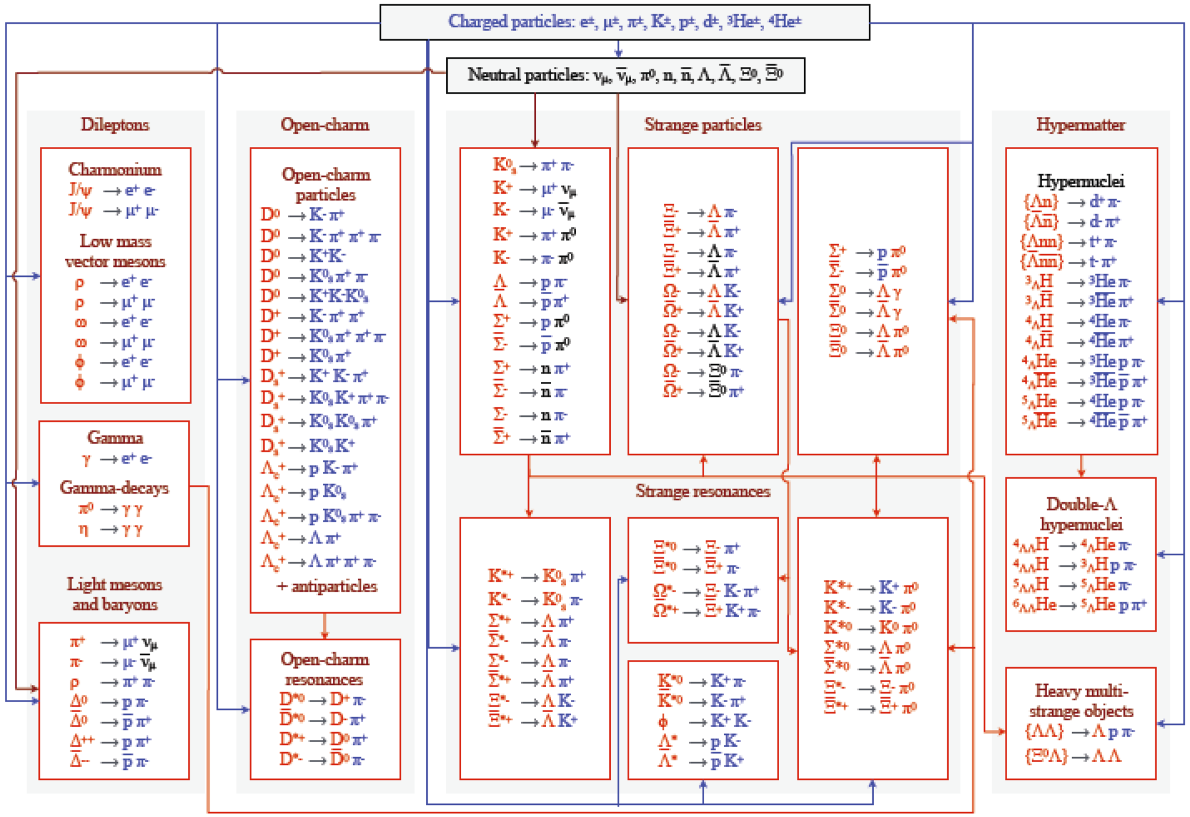

Encode tracking and detector performance

$$r = \{x, y, z, p_x, p_y, p_z, E\}$$

State vector position Four momentum

Momentum dependent potential → EoS in PHQMD

PHQMD

2) Momentum dependent potential :

$$V(\mathbf{r}_1, \mathbf{r}_2, \mathbf{p}_{01}, \mathbf{p}_{02}) = (a\Delta p + b\Delta p^2)\ exp[-c\sqrt{\Delta p}]\ \delta(\mathbf{r}_1 - \mathbf{r}_2)$$

$$\Delta p = \sqrt{(\mathbf{p}_{01} - \mathbf{p}_{02})^2}$$

Parameters a, b, c are fitted to the "optical" potential (Schrödinger equivalent potential U_{SEP}) extracted from elastic scattering data in pA: $U_{SEQ}(p) = \frac{\int^{p_F} V(\mathbf{p} - \mathbf{p}_1) dp_1^3}{\frac{4}{3}\pi p_F^3}$

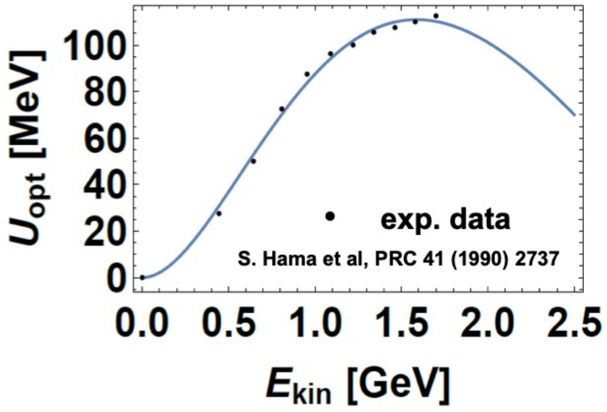

❖ **In infinite matter a potential corresponds to the EoS:**

$$E/A(\rho) = \frac{3}{5}E_F + V_{Skyrme\ stat}(\rho) + V_{mom}(\rho)$$

$$V_{Skyrme} = \alpha\frac{\rho}{\rho_0} + \beta\frac{\rho}{\rho_0}^{\gamma}$$

compression modulus K of nuclear matter:

$$K = -V\frac{dP}{dV} = 9\rho^2\frac{\partial^2(E/A(\rho))}{(\partial\rho)^2}|_{\rho=\rho_0}.$$

E.o.S.	$\alpha[MeV]$	$\beta[MeV]$	γ	K [MeV]
S	-383.5	329.5	1.15	200
H	-125.3	71.0	2.0	380
SM	-478.87	413.76	1.10	200
	a $[MeV^{-1}]$	b$[MeV^{-2}]$	c$[MeV^{-1}]$	
	236.326	-20.73	0.901	

EoS for infinite cold nuclear matter at rest

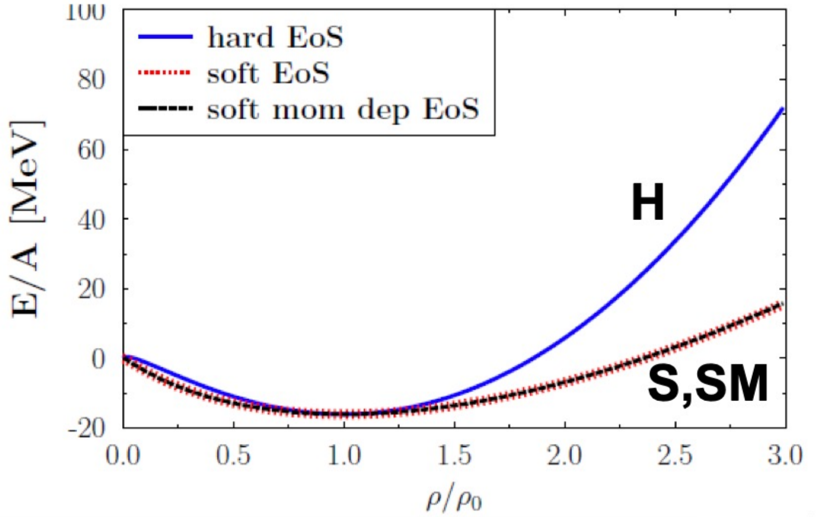

6

Other possible model: kinetic approch

- Relativistic kinetic equation (RKE) to include hadronic re-scattering processes.
  - Close connection to Coal. via final state interaction close to kinetic freeze-out.

P. Danielewicz et al. NPA 533 (1991) 712-748
Kaijia Sun et al, Nature Commun. 15 (2024) 1, 1074

- Evolution of QGP: MUSIC
- Hadron and light nuclei yields at QGP hadronization: SHM
- The evolution of the hadronic matter (besides the nonlocal many-body scatterings for d / t): AMPT

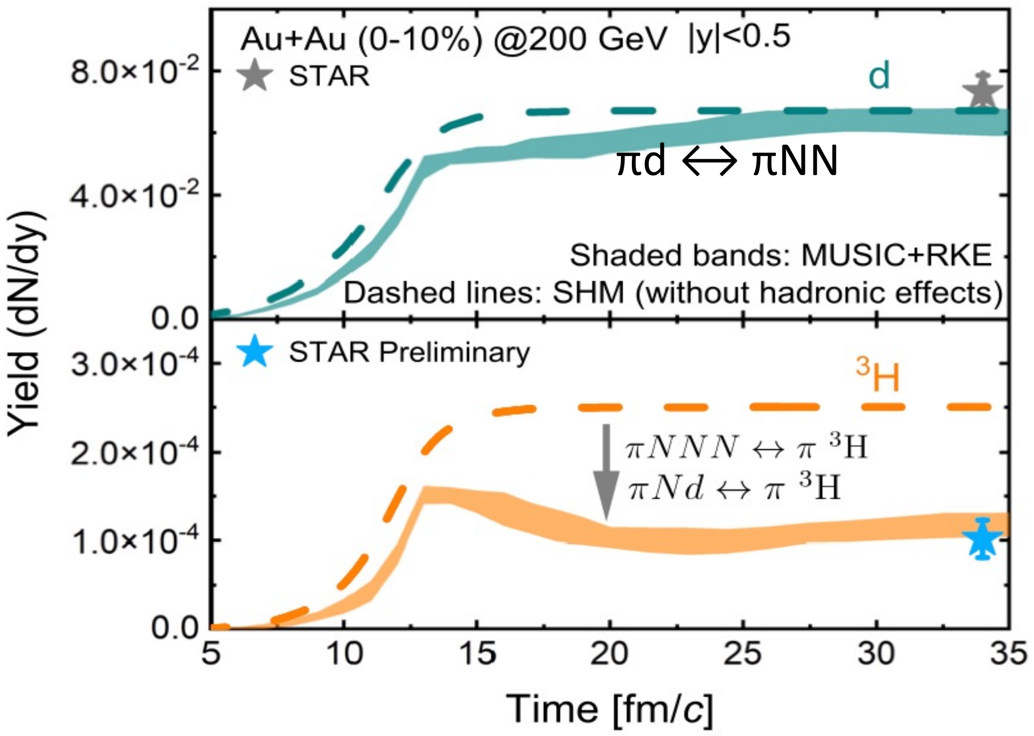

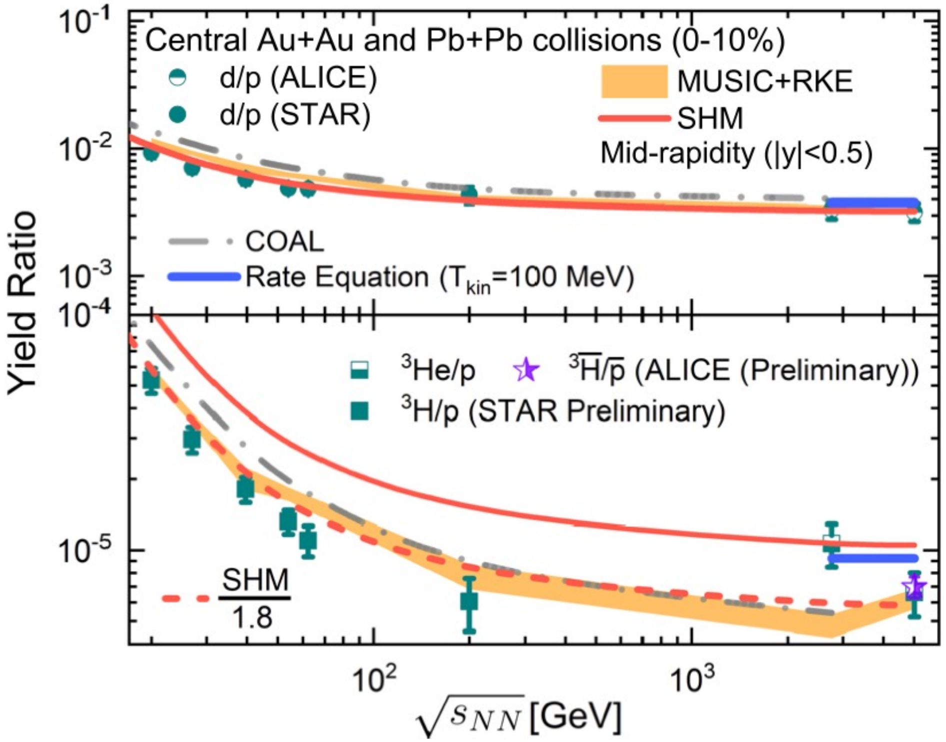

Triton yields with tuned T

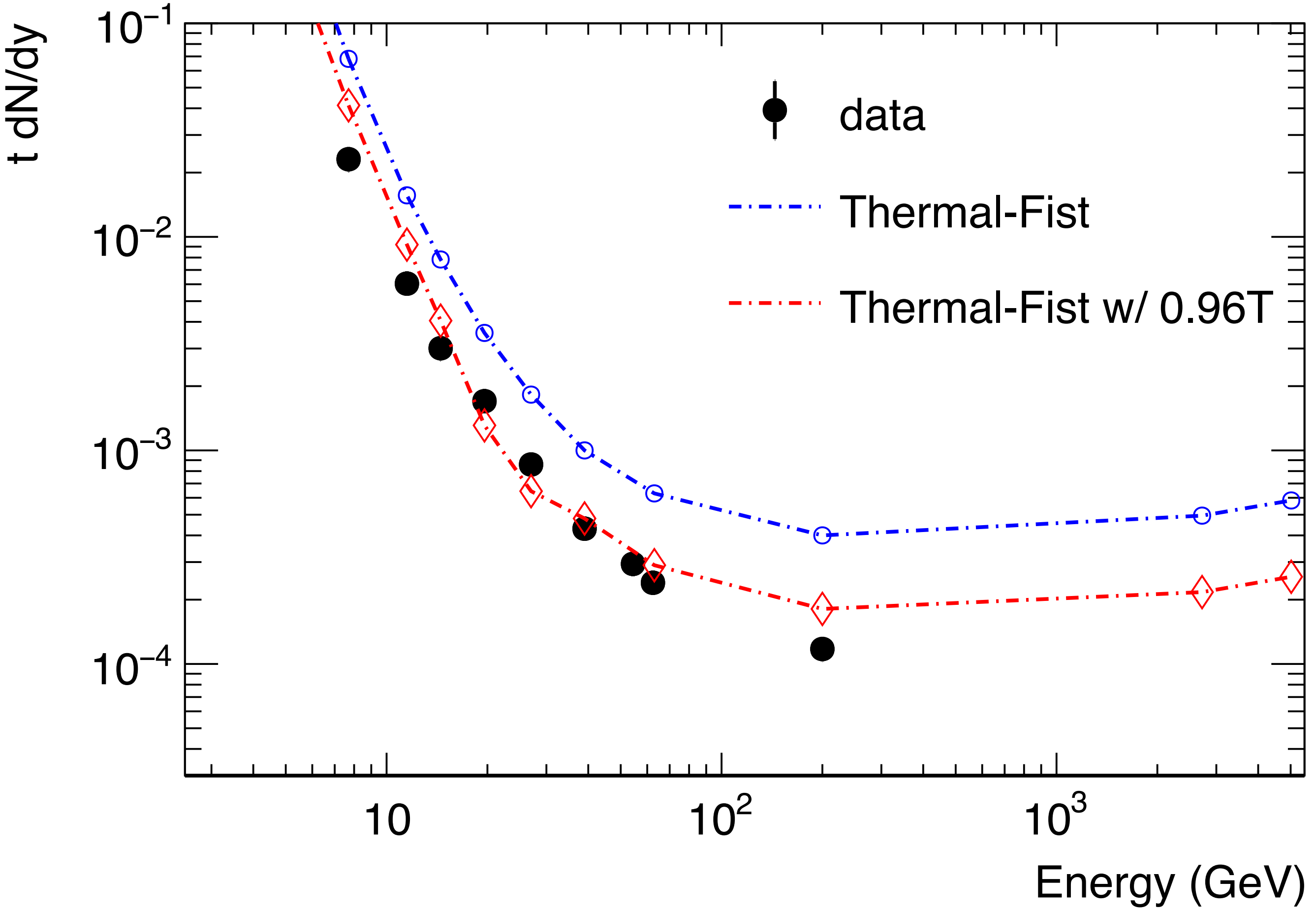

- Triton yields are closer to the data compared with default Thermal.

Hypernuclei Production in HIC

Other proposed mechanism

Nuclear fragmentation of hypercluster

- Dominates at beam rapidity.
  Dominate for heavy hypernuclei formation.

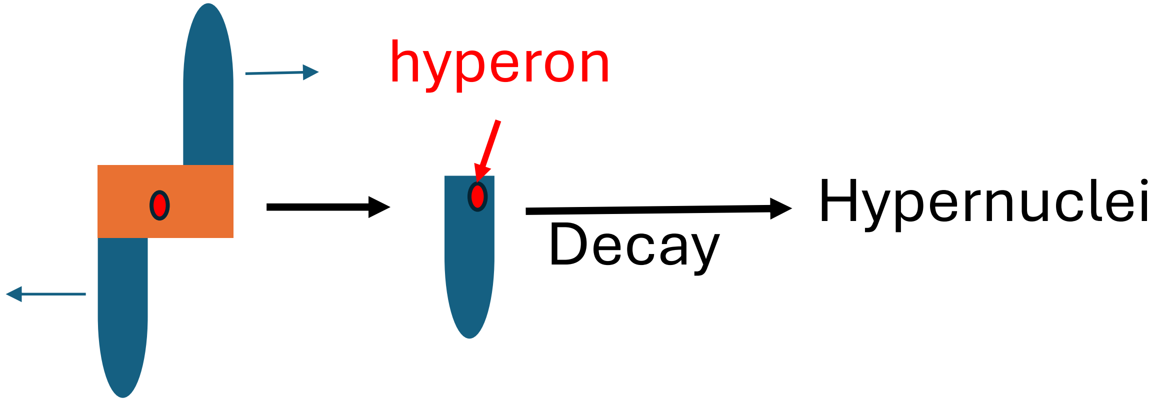

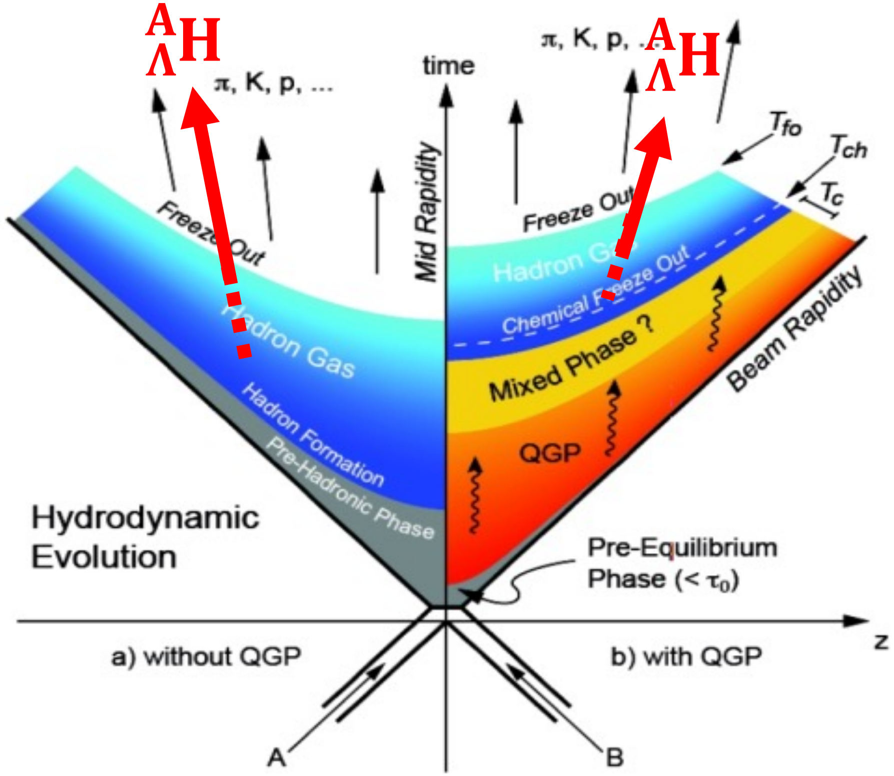

M. Wakai et al. PRC 38, 748 (1988)
A.S. Botvina et al. PLB 742, 7-14 (2015)

^{3}He/p and d/p from BES II

SQM 2024, Yixuan Jin, 05/06

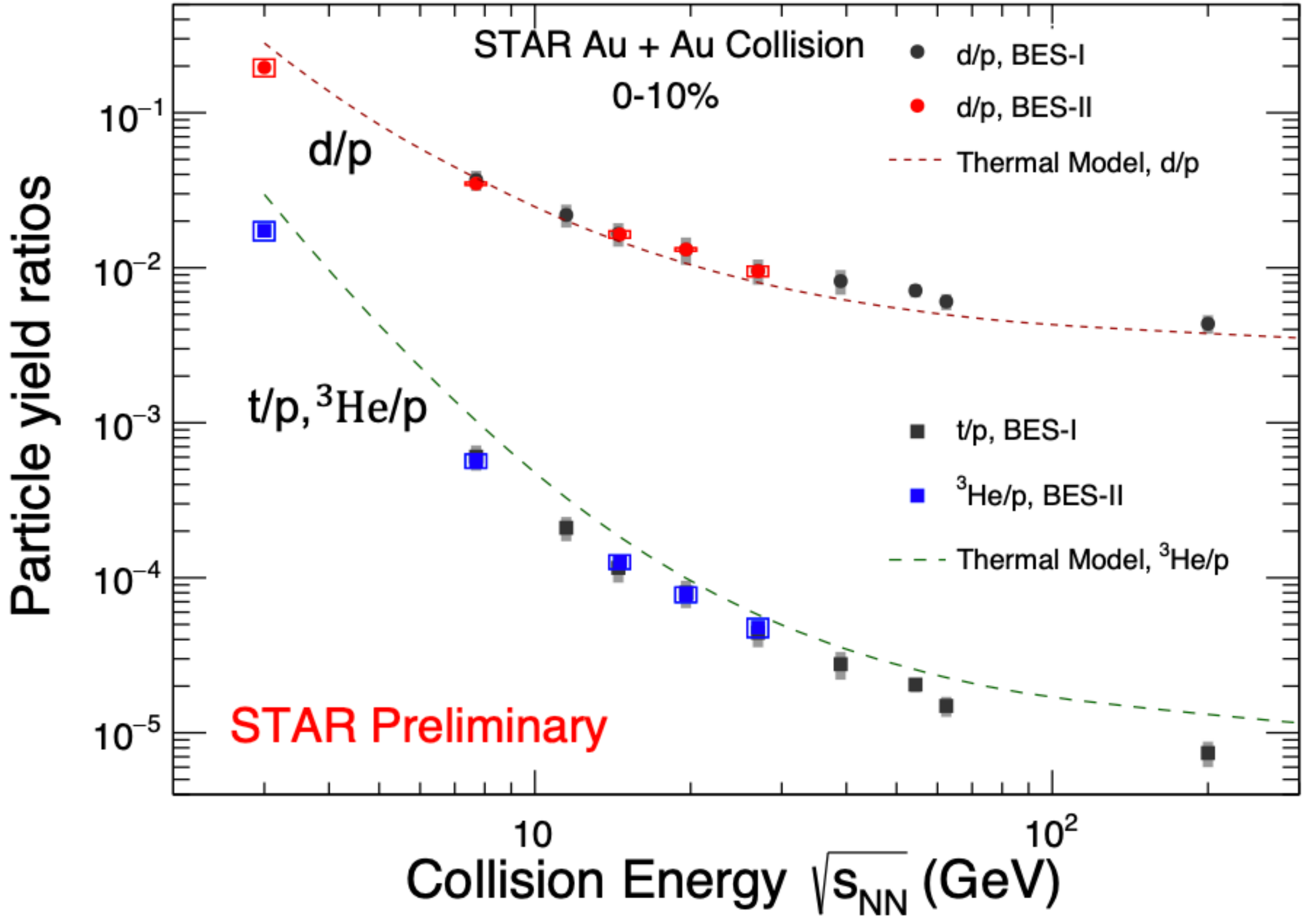

STAR, Phys. Rev. Lett. 130, 202301 (2023)

Shadow box:

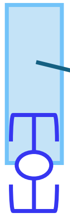

Feed down from excited nuclei.

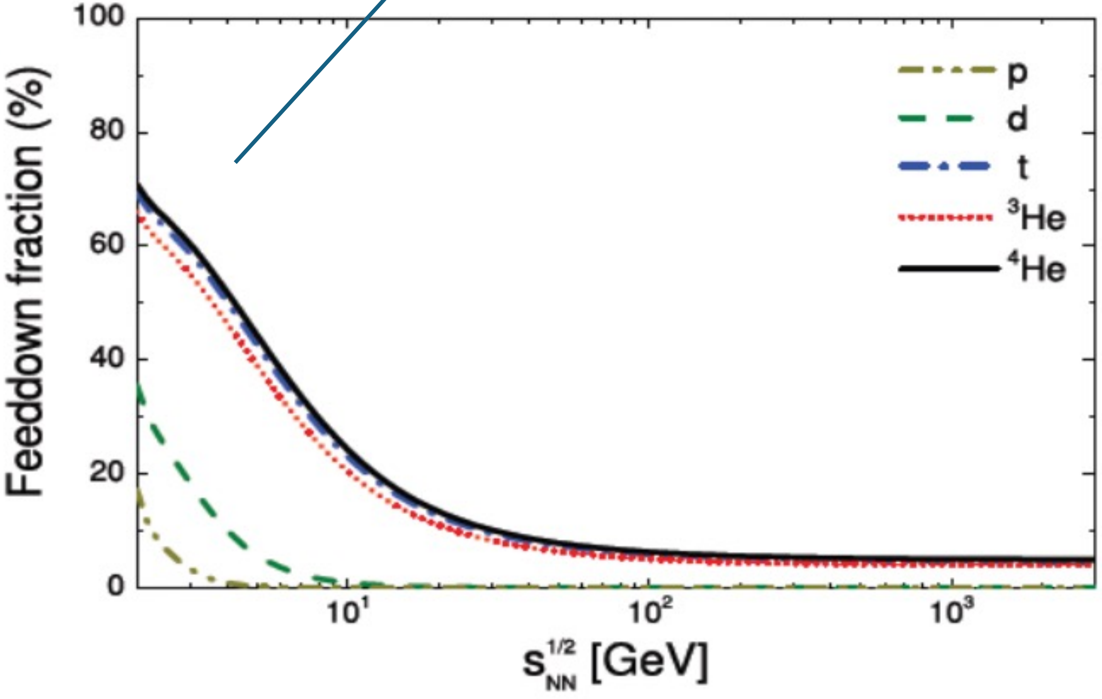

V. Vovchenko, PLB (2020) 135746

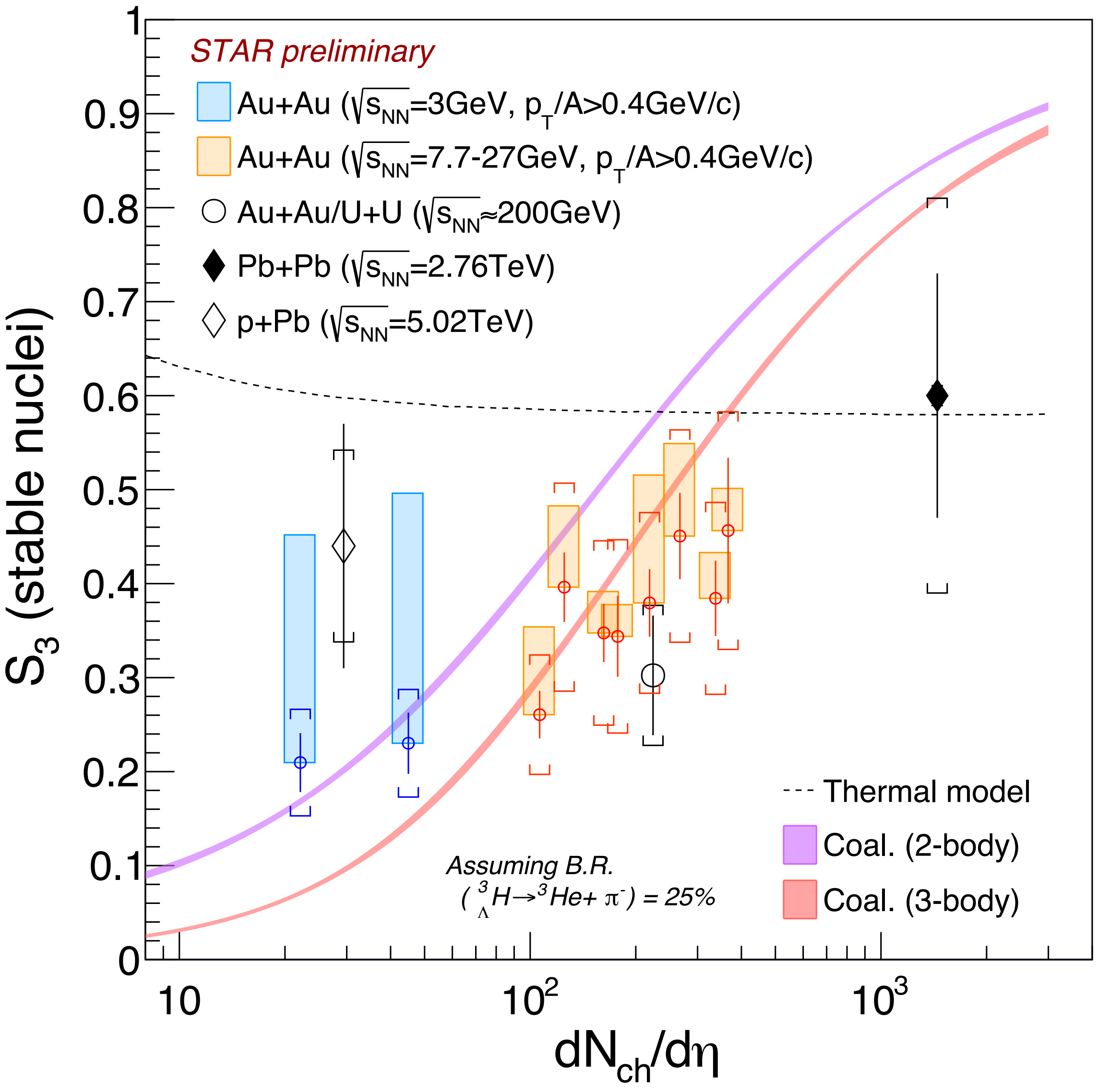

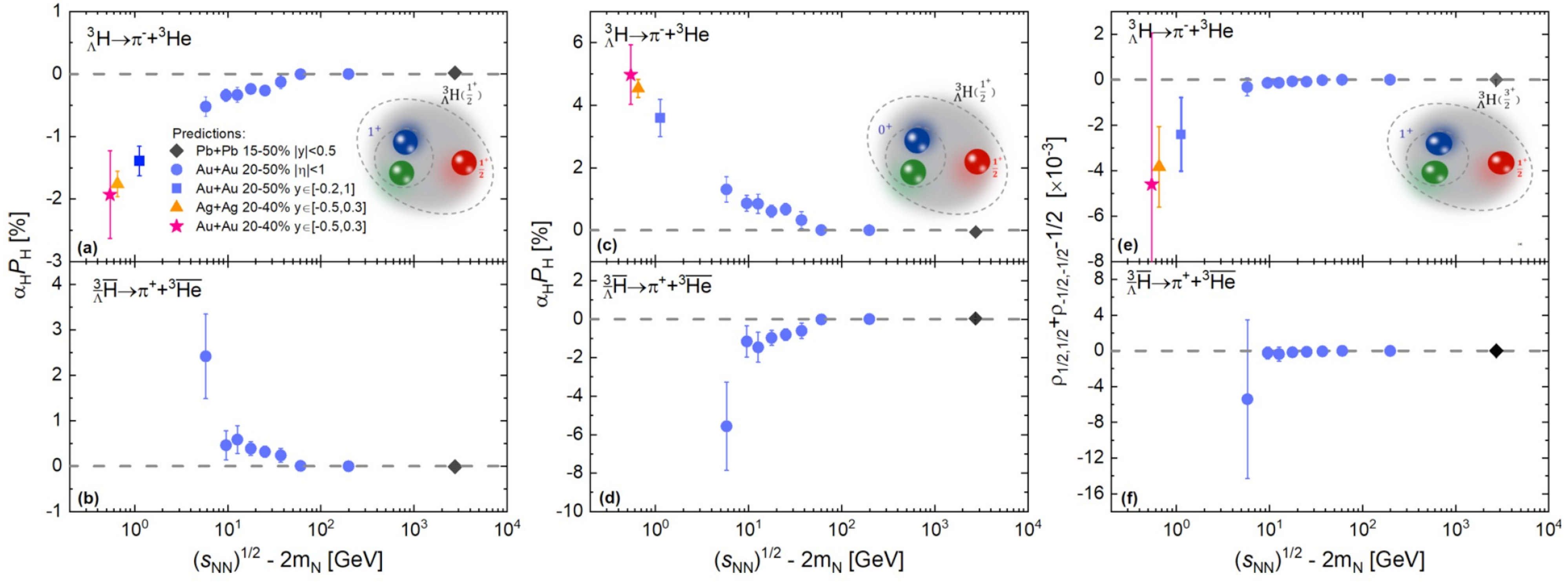

FIG. 2. Collision energy dependence of (anti-)hypertriton polarization predicted from the decay channel ${}^3_\Lambda\mathrm{H} \to \pi^- + {}^3\mathrm{He}$ (upper panels) and ${}^3_\Lambda\overline{\mathrm{H}} \to \pi^+ + {}^3\overline{\mathrm{He}}$ (lower panels) based on the Λ polarization data from the STAR [51], ALICE [52], and HADES [53] Collaborations. Panels (a) and (b) depict results for ${}^3_\Lambda\mathrm{H}\,(\frac{1}{2}^+)$ and ${}^3_\Lambda\overline{\mathrm{H}}\,(\frac{1}{2}^-)$, respectively, assuming the two nucleons inside the (anti-)hypertriton are in a spin-triplet state, while results shown in panels (c) and (d) are for the case that the two nucleons are in a spin-singlet state. Panels (e) and (f) depict results for the combined spin density matrix element $\hat{\rho}_{\frac{1}{2},\frac{1}{2}} + \hat{\rho}_{-\frac{1}{2},-\frac{1}{2}} - \frac{1}{2}$ for ${}^3_\Lambda\mathrm{H}\,(\frac{3}{2}^+)$ and ${}^3_\Lambda\overline{\mathrm{H}}\,(\frac{3}{2}^-)$, respectively.

Multiplicity Dependence of S_3 at $\mu_B \rightarrow 0$

Dongsheng Li, SQM 2024

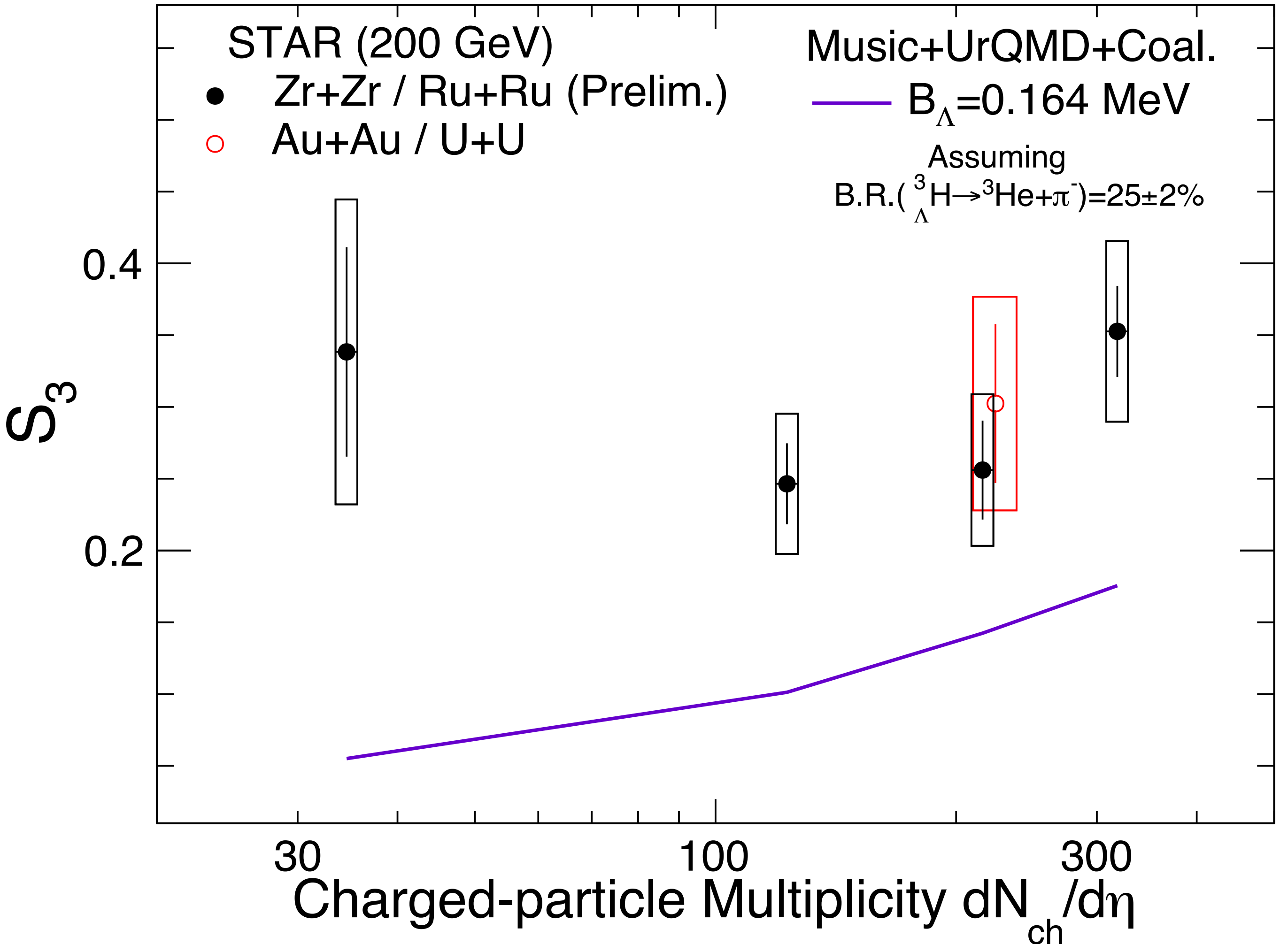

- No obvious multiplicity dependence within uncertainties
- Within uncertainties, coalescence calculations are consistent with the measured data
  - More precise data needed

STAR: arXiv:2310.12674; Science 328, 58-62 (2010)
MUSIC + UrQMD + Coal.: arXiv:2404.02701

Multiplicity Dependence of S_3 at $\mu_B \to 0$

Dongsheng Li, SQM 2024

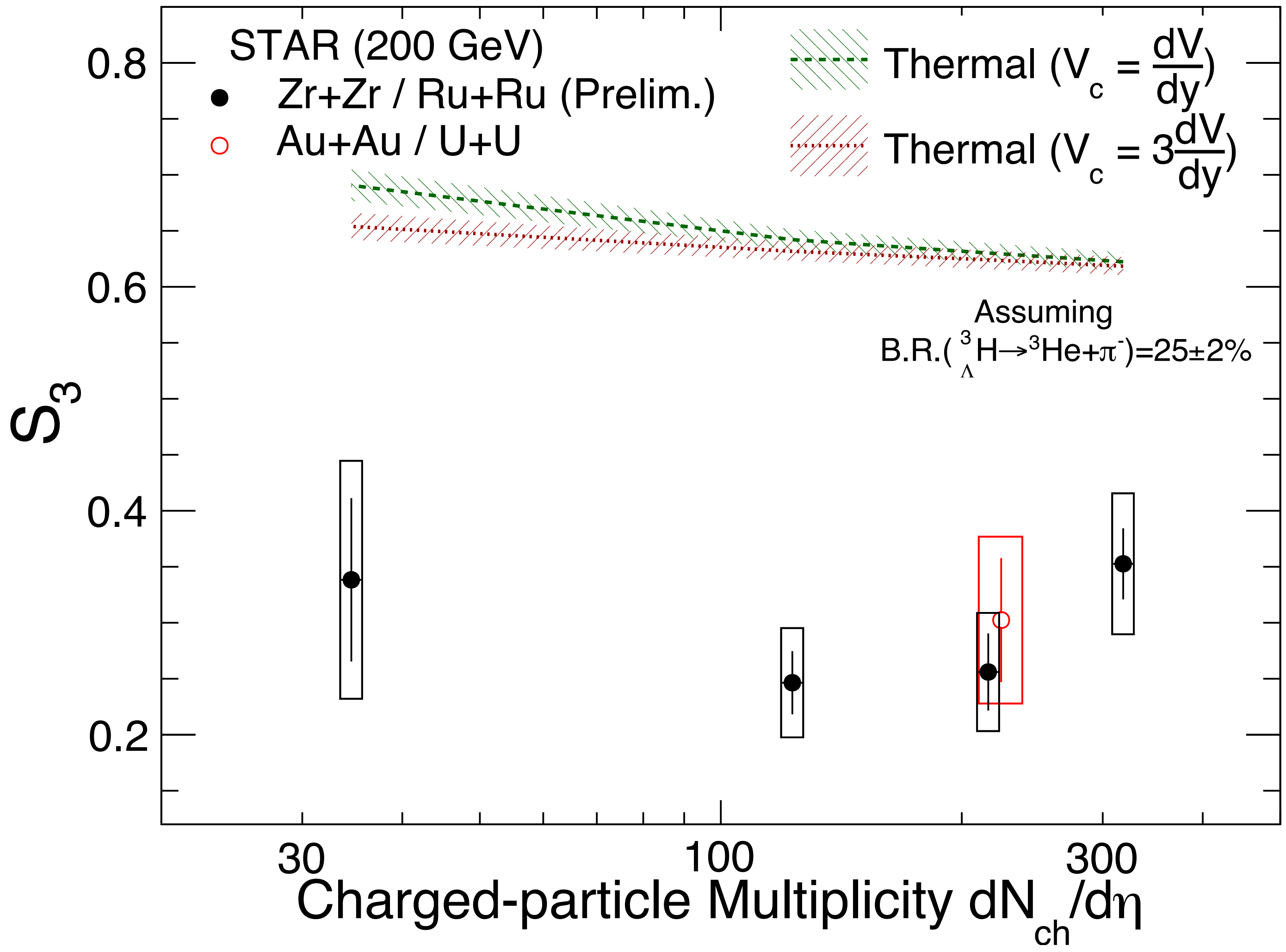

- Thermal-FIST with canonical ensemble fails to describe the data trend
  - Ratios have already canceled volume size and strangeness suppression factor

STAR: arXiv:2310.12674; Science 328, 58-62 (2010)
Thermal-FIST: Com. Phys. Comm. 244, 295 (2019)
PLB 785, 171 (2018)

T and μ_B from π/K/p spectra